

SUPPLEMENTAL MATERIAL

CRISPR-Cas9 Screen Reveals a *MYCN*-amplified Neuroblastoma Dependency on *EZH2*

Liyang Chen, Gabriela Alexe, Neekesh V. Dharia, Linda Ross, Amanda Balboni Iniguez, Amy Saur Conway, Emily Jue Wang, Veronica Veschi, Norris Lam, Jun Qi, W. Clay Gustafson, Nicole Nasholm, Francisca Vazquez, Barbara A. Weir, Glenn S. Cowley, Levi D. Ali, Sasha Pantel, Guozhi Jiang, William F. Harrington, Yenarae Lee, Amy Goodale, Rakela Lubonja, John M. Krill-Burger, Robin M. Meyers, Aviad Tsherniak, David E. Root, James E. Bradner, Todd R. Golub, Charles W. M. Roberts, William C. Hahn, William A. Weiss, Carol J. Thiele, and Kimberly Stegmaier

SUPPLEMENTAL METHODS

Cell Lines

SIMA and MHH-NB-11 were maintained in RPMI (Cellgro) supplemented with 10% fetal bovine serum (Sigma-Aldrich) and 1% penicillin-streptomycin with glutamine (Cellgro). All other neuroblastoma cell lines were maintained in DMEM (Cellgro) supplemented with 10% fetal bovine serum (Sigma-Aldrich) and 1% penicillin-streptomycin with glutamine (Cellgro). All cell lines were cultured at 37°C in a humidified atmosphere containing 5% CO₂.

Determination of cell viability

Cell viability was assessed using the CellTiter-Glo Luminescent Cell Viability Assay (Promega). Luminescent readings were obtained using the FLUOstar Omega microplate reader (BMG Labtech). Cells were treated across a range of concentrations and area under curve was calculated from ATP luminescence measurements after 5 days of treatment using log-transformed, normalized data in GraphPad Prism 6.0 (GraphPad Software, Inc.). Cell viability was also determined following pLKO.1 lentiviral shRNA-mediated knockdown or CRISPR-Cas9-mediated knockout of *EZH2*. ATP content was measured at multiple time points after transduction.

Flow Cytometry

Apoptosis was measured using the Annexin V: APC Apoptosis Detection Kit as per the manufacturer's protocol (BD Pharmingen). Cell cycle was determined by measuring DNA content using propidium iodide staining.

In Vivo Studies

Inducible shRNA experiment: The human neuroblastoma cell line NGP was stably transduced with a TET-inducible *EZH2* shRNA to generate an NGP-sh*EZH2* cell line. Tumor xenografts were established by injecting 2×10^6 NGP-sh*EZH2* cells in the left flank of 5-week-old female athymic nude mice (Taconic). When tumors reached 75-150 mm³, animals were stratified into cohorts that received doxycycline-chow or regular chow ($n=10$ per group). Tumor growth was monitored with a caliper 3 times a week. In each group, 5 tumors were collected and protein lysate analyzed for *EZH2* expression and target inhibition on Day 20 after starting treatment. Statistical significance of survival curves was determined by a log-rank (Mantel-Cox) test and variance of the tumor volume between doxycycline and control was determined by two-way ANOVA. All xenograft studies were approved by the Animal Care and Use Committee of the National Cancer Institute, and all mice treatments, including their housing, were in accordance with the institutional guidelines (PB-023).

Drug treatment experiment with JQEZ5: Tumor xenografts were established in NOD/SCID/gamma female mice using 2×10^6 Kelly cells resuspended in 30% matrigel and injected into the flank. After cell implantation, mice were randomized into cohorts to be treated with 100 mg/kg JQEZ5 ($n=10$) or vehicle (10% HP- β -CD/90% water) ($n=10$) delivered by daily IP injection for 7 days, followed by a 5-day holiday and subsequently treated with 75 mg/kg JQEZ5 or vehicle for 9 days. Tumor volume was measured by caliper twice weekly and animals were sacrificed when tumor volumes exceeded 2,000 mm³. All animal studies were conducted under the auspices of protocols approved by the Dana-Farber Cancer Institute Animal Care and Use Committee.

Drug treatment experiment with GSK126: Tumor xenografts were established in NOD/SCID/gamma female mice using 2×10^6 human neuroblastoma cell CHP-212, SK-N-BE(2), or SH-SY-5Y, resuspended in 30% matrigel and injected into the flank. After cell implantation, mice were randomized into cohorts to be treated with 150 mg/kg GSK126 or vehicle (20% Captisol pH4.5) delivered by daily IP injection. Tumor volume was measured by caliper twice weekly and animals were sacrificed when tumor volumes exceeded 2,000 mm³. All animal studies were conducted under the auspices of protocols approved by the Dana-Farber Cancer Institute Animal Care and Use Committee.

CRISPR-Cas9 Screening

The CRISPR-Cas9 screen was performed using the Avana library containing 73,372 guides and an average of 4 guides per gene. The library contains approximately 1,000 guides that do not target any location in the reference genome as negative controls.

The version of Avana data is available on the Achilles Portal with the recent publication of the CERES algorithm (1). This dataset contains 341 cell lines, including 11 neuroblastoma lines: CHP-212, IMR-32, Kelly, KP-N-YN, MHH-NB-11, NB1, SK-N-BE(2), SK-N-AS, SK-N-DZ, SK-N-FI, and SIMA. Initially, cancer cell lines were transduced with Cas9 using a lentiviral system. Cell lines that met criteria, including acceptable Cas9 activity measuring ability to knockout transduced GFP, appropriate growth properties and other parameters, were then screened with the Avana library. A pool of guides was transduced into a population of cells. The cells were cultured for 21 days in vitro, and at the end of the assay, barcodes for each guide were sequenced for each cell line in replicate.

The sgRNA read count data were deconvoluted from sequence reads by using PoolQ. A series of quality control pre-processing steps was performed to remove samples with poor replicate reproducibility, as well as guides that have low representation in the initial plasmid pool. The replicates that failed fingerprinting and the replicates with less than 15 million reads were removed and then the replicate read counts were scaled to 1 million total reads per replicate. The replicate pairs with Pearson correlation coefficients < 0.7 and the sgRNAs with low representation in the pDNA reference library were filtered out. Next, the log fold-change (logFC) from pDNA reference was calculated and the replicates with logFC SSMD between positive and negative control sgRNAs > -0.5 were removed. The replicate logFC data were Z-MAD normalized and the gene scores were inferred by running the computational tool CERES (1) and then normalized with lists of core cell-essential and non-essential genes. CERES was developed to computationally correct the copy-number effect and to infer true underlying effect of gene-knockout as described in (1). CERES models the observed normalized log-fold change for each sgRNA and cell line as the linear combination of gene-knockout and copy-number effects with coefficients giving the guide activities. Copy-number effects are fit with a linear piece-wise model in each cell line. Once all parameters have been fit, the inferred gene scores and guide activity scores are extracted and reported.

Independent Component Analysis

Independent Component Analysis (ICA) (2, 3) was applied to the CERES CRISPR-Cas9 gene-level data to identify the dependencies significantly associated with the neuroblastoma lineage. ICA is a machine learning data decomposition technique for revealing hidden non-Gaussian independent factors that are able to accurately deconvolve the data signal.

ICA models the CERES CRISPR-Cas9 gene dependency scores as a weighted sum of independent component signals, each component capturing a different biological process associated with the tumor lineage dependencies. The genes having the largest projection onto a component (estimated based on the cut-off ICA Z-score ≥ 2.5) are representative for the biological process associated with the component and are assigned as the “leading edge” gene set for the component.

Prior to performing ICA, the CERES gene scores were rank normalized per sample, i.e., the gene level dependency scores were replaced with their rank within each sample. A robust set of 100 independent components was identified from the CERES CRISPR-Cas9 screening rank normalized data by averaging 500 runs of the FastICA v1.2.1 procedure (4) implemented in R v3.2 (<https://cran.r-project.org/web/packages/fastICA>).

The comparative marker selection method implemented in GenePattern v3.9.10 was applied for ranking the independent components based on the Signal to Noise Ratio (SNR) scores that differentiate the neuroblastoma cell lines from all other cell lines. The top 3 independent components that were identified as significantly associated with depletion in neuroblastoma cells vs. other cell lines (SNR ≤ -0.5 , permutation $P \leq 0.05$, False Discovery Rate (FDR) ≤ 0.05) were labeled IC1, IC2 and IC3 and used to project the CERES dependency data (Figure 1A).

The k -nearest neighbor classification model implemented in the R v3.2 package rminer, (<http://cran.r-project.org/package=rminer>) was trained for $k = 3$ on the CERES data projected on the independent components IC1, IC2 and IC3, which are associated with neuroblastoma depletion. This model was shown to accurately separate the neuroblastoma cells from the other cell lines (mean error for 10-fold cross validation 0.026).

The top 100 leading edge genes associated with the components IC1, IC2 and IC3 are presented in Supplementary Table S1A. The PRC2 complex genes *EZH2*, *EED*, *SUZ12* were included in

the leading edge gene set for the component IC3. Gene set enrichment analysis (GSEA) vs. the MSigDB c2.all v5.1 collection (Broad Institute) was performed for the leading edge genes of the independent components IC1, IC2 and IC3 and revealed that each of the leading gene sets were enriched in “PRC2 targets” gene set signatures.

Single-sample Gene Set Enrichment Analysis for Neuroblastoma Dependencies

A single-sample GSEA (ssGSEA) analysis (5-7) on the CERES dependency data across the Mammalian Protein Complexes in the CORUM Database available from the ConsensusPathDB platform (8, 9) was performed to further validate the functional association of the PRC2 complex with neuroblastoma dependencies in the CRISPR-Cas9 screening data.

Single-sample GSEA (ssGSEA) is a variant of the GSEA method that assigns to each individual sample, represented as a ranked list of genes, an Enrichment Score (ES) with respect to each gene set in a given collection of pathways. The ssGSEA ES is calculated as a running sum statistic by walking down across the ranked list of genes, increasing the sum when encountering genes in the gene set and decreasing it when encountering genes not in the gene set. The significance of the ES is estimated based on a permutation *P*-value and adjusted for multiple hypotheses testing through FDR. A positive ES denotes a significant overlap of the signature gene set with groups of genes at the top of the ranked list, while a negative ES denotes a significant overlap of the signature gene set with groups of genes at the bottom of the ranked list. For each sample, the ES was further transformed into a *Z*-score by subtracting the average of the ES's assigned to all other samples and by dividing the result to their standard deviation.

While GSEA generates a gene set's enrichment score with respect to phenotypic differences across a collection of samples within a dataset, ssGSEA calculates a separate enrichment score for each pairing of sample and gene set, independent of phenotype labeling. In this manner, ssGSEA transforms a single sample's gene expression profile to a gene set enrichment profile. A gene set's enrichment score represents the activity level of the biological process in which the gene set's members are coordinately up- or down-regulated. The gene set representation has an unsupervised biological interpretability and can be further analyzed with statistical and machine learning methods.

The ssGSEA Z-scores for a gene set vs. a tumor cell line in the CRISPR-Cas9 screening data describe the level of dependency of the gene set vs. the cell line, based on the significance cut-off Z-score for depletion ≤ -1 .

The EED_EZH2 protein complex (gene members *EED*, *EZH2*, *SUZ12*, *RBBP4*, *AEBP2*) showed a significant dependency associated with the neuroblastoma cell lines vs. all other cell lines ($P = 0.006$, Mann-Whitney non-parametric t-test) and scored as most depleted in the neuroblastoma lineage (average Z-score = -1.48 across the neuroblastoma lineage, average Z-score = 0.05 across all other lineages). The distribution of the ssGSEA Z-scores for the EED_EZH2 protein complex across the lineages showed a significant variability across the lineages in the CERES data (1-way ANOVA F score = 3.05, $P < 0.0001$).

ChIP-seq and ChIP-qPCR

Crosslinking was performed in fresh cell culture medium containing 1% formaldehyde with gentle rotation for 5 mins in room temperature. Fixation was stopped by the addition of glycine (125 mM final concentration). Fixed cells were trypsinized, washed twice in ice-cold PBS, and then resuspended in 3×10^6 cells/130 μ l SDS lysis buffer (1% SDS, 10 mM EDTA, 50 mM Tris-HCl, pH 8.1, supplemented with fresh Complete mini-protease inhibitor cocktail (Roche, Indianapolis, IN)). Chromatin was sheared to about 200bp fragments by Covaris ultrasonication. Centrifugation was used to remove debris at 4°C for 10 mins at top speed. The supernatant was diluted 1:10 using ice-cold ChIP dilution buffer (0.01% SDS, 1.1% Triton-X100, 1.2 mM EDTA, 16.7 mM Tris-HCl, 167 mM NaCl pH 8.1, supplemented with fresh Complete mini-protease inhibitor cocktail). Five percent of the diluted sample was saved as input controls and the remainder of the diluted sample was used for immunoprecipitation with antibodies overnight at 4°C. Precipitates were washed sequentially with ice cold low salt wash (0.1% SDS, 1% Triton-X-100, 2 mM EDTA, 20 mM Tris-HCl, pH 8.1, 150 mM NaCl), high salt wash (0.1% SDS, 1% Triton-X-100, 2 mM EDTA, 20 mM Tris-HCl, pH 8.1, 500 mM NaCl), LiCl wash (0.25 M LiCl, 1% IGEPALCA-630, 1% deoxycholic acid, 1 mM EDTA, 10 mM Tris-HCl, pH 8.1) and then twice with TE (1 mM EDTA, 10 mM Tris-HCl, pH 8.1). They were then eluted and reverse cross-linked in elution/reverse cross-linking buffer (1% SDS, 0.1 M NaHCO₃, 0.2 M NaCl) for 5 hours. Eluted DNA fragments were purified with Qiagen PCR purification kit and analyzed by qPCR, or barcoded with a NEBNext DNA library preparation kit (NEB, Ipswich, MA) and subjected to sequencing on Illumina HiSeq 2000 platform.

Antibodies used in ChIP experiments are: anti-EZH2 (Cell Signaling 5246S); anti-MYCN (Santa Cruz sc-53993); anti-H3K27me3 (Millipore 07-449); anti-H3K4me3 (Abcam ab8580).

Primer sequences for ChIP-qPCR: *MCM7* forward: GCGGGAGGTGAAGAAGGCC; *MCM7* reverse: CTGTGGCCGGCCAACCG; *ZIC3* forward: CGGTGTGTAATTCGGGAAGTG; *ZIC3* reverse: GCCAAGCGTTGACCCTTTAG; *EZH2* (TSS-300bp) forward: CTGCACACCGCCTTCCT; *EZH2* (TSS-300bp) reverse: CCGCCGTCTCTTTGTTCTT; *EZH2* (TSS-200bp) forward: CCAGTGGCGTCCCTTACAG; *EZH2* (TSS-200bp) reverse: TGCGCTCAGGGCTCGT; *EZH2* (TSS) forward: AAAAGCGATGGCGATTGG; *EZH2* (TSS) reverse: GGCTCCACTGCCTTCTGAGT.

ChIP-seq Data Analysis

All of the ChIP-seq data sets were aligned using Bowtie v2.2.3 (10, 11) to the build version NCBI37/hg19 of the human genome. Quality control tests were performed based on the FastQC v.0.11.2 software (Babraham Bioinformatics, <http://www.bioinformatics.babraham.ac.uk/projects/fastqc/>) and by using the ChIPQC library available from Bioconductor v3.2 (12).

The ChIP-seq peaks for EZH2 and H3K4me3 were identified using MACS v1.4.3, and the ChIP-seq broad peaks for H3K27me3 were identified using MACS v.2.0.10 (13) with the cut-off 1e-05 for the *P*-value. The peaks were annotated by using the Annotate Peaks function available in the Homer v4.7 package (14).

The relative ChIP occupancy signal in the gene promoter regions expressed in units of reads per million mapped reads per bp (rpm/bp) was computed for each mark by using the DeepTools v2.2.3 software (15) as the ratio between the area under curve (AUC) of the mark normalized signal vs. the AUC of the background input signal. Gene promoters were defined as the +/- 5 kb regions around the gene transcription start site (TSS). The gene targets for EZH2 and H3K27me3 were identified separately for each of the Kelly and LAN-1 cells as the genes with high relative occupancy of EZH2 or H3K27me3, respectively, ChIP signal in the promoter. The “high” level for the relative occupancy signal in the promoter regions was estimated based on the cut-off 1.5 for the ratio of the AUC signal of the mark vs. the AUC signal of the input. In addition, “core” lists of gene targets for EZH2 and H3K27me3 were defined by intersecting the target gene sets for Kelly and LAN-1 cell lines. The lists of gene targets for EZH2 and H3K27me3 are provided in

Supplemental Table 3. The correlation between the relative promoter signal for H3K27me3 and the relative promoter signal for EZH2 across the hg19 genes was tested for significance by using the `rcorr` function available in the `Hmisc R v3.4` library.

Actively transcribed genes were assessed based on the existence of significantly enriched regions of H3K4me3 within ± 5 kb of the TSS, combined with the Z-score of genome-wide expression > 1 . In order to verify that these genes were not bivalently marked or repressed, we assayed the repressive histone mark H3K27me3 and required that no significantly enriched region for H3K27me3 overlapped within ± 5 kb of the TSS gene promoter region.

The ChIP-seq data for this study is available for download from the Gene Expression Omnibus (GEO) repository (GSE85432) upon manuscript publication.

Metagene Representation of Gene Promoter Occupancy

The metagene representations of global genome-wide average ChIP-seq signal promoter occupancy for EZH2, H3K27me3 and H3K4me3 were performed as described in (16) based on the expression data for cells cultured in baseline growth conditions, available for the Kelly cells in the CCLE database (17) and for the LAN-1 cells in the Gene Expression Omnibus GSE56552 data (18). The genes for each data set were grouped into three categories: highly expressed (Z-score for genome-wide log₂ RMA expression ≥ 1.5), medium expressed (absolute Z-score for genome-wide log₂ RMA expression ≤ 0.5) and poorly expressed (Z-score for genome-wide log₂ RMA expression ≤ -1.5). The metagenes for the EZH2, H3K27me3 and H3K4me3 relative ChIP signal occupancy at promoters were created for 500 randomly selected genes from each of the three categories. The ChIP-seq signal was mapped to the ± 10 kb regions flanking TSS. The TSS ± 10 kb regions were aligned and split into 50 bp bins. The normalized ChIP-seq signal occupancy with background input subtracted was then computed as the “Area under the Curve” density signal in rpm/bp units in the flanked regions. Finally, the meta-representations were derived based on the average normalized ChIP signal across the 500 genes selected from the highly expressed, medium expressed and poorly expressed categories.

GSEA for EZH2 and H3K27me3 Target Genes

The GSEA v2.2.0 software (6, 7) was utilized to identify gene sets that have a significant overlap with the genes marked by EZH2 and by H3K27me3. First the hg19 genes were ranked based on the H3K27me3, respectively based on the EZH2 relative ChIP-seq occupancy signal in the

promoter. The goal of GSEA was to identify the gene sets that are distributed at the top or at the bottom of the ranked list of genes. For this purpose, the Pre-Rank GSEA module was run across the comprehensive collection c2 of 4,726 curated canonical pathways and gene sets, available in the MSigDB v5.1 database <http://www.broadinstitute.org/gsea/msigdb/index.jsp> (6). Gene sets with a nominal $P \leq 0.05$ and an FDR ≤ 0.25 for the Kolmogorov-Smirnov enrichment test were considered significant hits. The gene sets identified as significantly enriched in gene targets for EZH2 and H3K27me3 were further tested for association with the PRC2 complex by applying the two-tailed Fisher exact test. Of the 4,726 gene sets available in the c2 collection of MSigDB, 83 were manually annotated as related to the PRC2 complex.

In addition, the lists of core gene targets for EZH2 (361 genes) and H3K27me3 (428 genes) were further tested for significant overlap with the MSigDB v5.1 c2 collection of 4,726 curated canonical pathways based on the “Investigate GeneSets” module available in MSigDB. The significance of the overlap was assessed based on a hypergeometric test, with the 0.05 cut-offs for the P -value and the FDR.

Genome-wide Expression Analysis

Kelly and LAN-1 cells were treated in duplicate with 2 μ M GSK126 or DMSO for 2 or 5 days. Total RNA was extracted with an RNeasy Kit (Qiagen) and profiled by RNA sequencing (HiSeq, Illumina) at the Center for Cancer Computational Biology (CCCB) at the Dana-Farber Cancer Institute.

RNA-seq Data Processing

Quality control tests for the mapped reads were performed using the FASTQC software (www.bioinformatics.babraham.ac.uk/projects/fastqc/). The reads were aligned to the GRCh37/hg19 human genes by using Tophat2 v2 (19). Quality control tests for the aligned reads and for the replicate consistency were performed by using the qualimap v2.2 (20) and the SARTools (21) pipelines. The total number of reads for individual samples ranged from 17 to 24 Mb. The average percentage of uniquely mapped reads in the aligned data was 86.50%, with a standard deviation 2.3%. The RNA-seq data for this study is available for download from the Gene Expression Omnibus (GEO) repository (GSE85432) upon manuscript publication.

Gene level reads and gene level expression estimated as $\log_2(\text{FPKM})$ scores were computed using the Feature Counts method implemented in the Bioconductor v3.2 RSubread package (22).

The genome-wide expression data were projected onto a heatmap by using the GENE-E software (<http://www.broadinstitute.org/cancer/software/GENE-E/>). The overall significance of the differential expression between the control and treatment phenotypes was estimated by using the EdgeR method available from the Bioconductor v3.2 EdgeR library (23) with the significance cut-off $P \leq 0.05$ for the posterior probability.

Comparative Marker Analysis

The 16 samples available in the data were analyzed for changes in expression induced by GSK126 vs DMSO at days 2 and 5 in individual cell lines and in both cell lines. The Comparative Marker Selection module from GenePattern v3.9.6 (24) was employed to identify individual genes that were differentially expressed between treated and vehicle conditions. The analysis was performed on the gene level expression data estimated as $\log_2(\text{FPKM})$ by applying a 2-sided signal-to-noise ratio (SNR) test followed by 1,000 permutations of the phenotype labels. The settings for the SNR parameters were log-transformed-data: yes, complete: no, balanced: no, smooth P -values: yes. Molecular signatures for genes down-regulated (respectively up-regulated) by GSK126 vs. DMSO were defined based on the cut-offs: absolute fold change for $\log_2(\text{FPKM})$ expression ≥ 1.5 (for “stringent” signatures), absolute fold change for $\log_2(\text{FPKM})$ expression ≥ 0.5 (for “relaxed” signatures), permutation $P \leq 0.05$, Benjamini-Hochberg false discovery rate (FDR) ≤ 0.05 .

The differential changes in expression induced by GSK126 were first identified separately for the Kelly and LAN-1 cells. “Core” lists of differentially upregulated and downregulated genes were defined by intersecting the lists of genes differentially upregulated or downregulated by GSK126 in each of the Kelly and LAN-1 cell lines. The GSK126 “stringent” de-repression signature at day 5 consists of 348 genes upregulated between treated samples vs. vehicle in Kelly cells 244 genes upregulated in LAN-1 cells, and 30 core genes upregulated in both cell lines. The GSK126 “relaxed” de-repression signature at day 5 consists of 1,346 genes upregulated between treated samples vs. vehicle in Kelly cells, 1,187 genes upregulated in LAN-1 cells, and 248 core genes up-regulated in both cell lines.

GSEA for the Expression Changes Induced by GSK126

GSEA v2.1.0 software (6, 7) was used to identify functional associations of the molecular phenotypes induced by GSK126 with a compendia of gene signatures: (a) the MSigDB v5.1 collection c2 of 4,726 curated pathways and experimental gene sets, (b) the MSigDB v5.1

collection c5 of 825 Gene Ontology – Biological Processes gene sets, (c) the lists of gene targets for EZH2 and H3K27me3 identified in our ChIP-seq experiments, and (d) signatures of genes repressed in *MYCN*-amplified and high-risk neuroblastoma tumors.

The signatures of genes repressed in *MYCN*-amplified or high-risk neuroblastoma tumors were derived from two primary neuroblastoma gene expression datasets: the Affymetrix U133 A GSE12460 (25) data describing 64 tumors, and the RNA-seq GSE49711 (26) data describing 498 tumors. Gene sets with less than 15 genes or more than 500 genes were excluded from the analysis. Gene sets with a nominal $P \leq 0.05$ and $FDR \leq 0.25$ were considered significant hits. The results were visualized on GSEA plots, heatmaps and networks for selected gene signatures.

The Enrichment Map v2.1.0 software (27) was employed to organize the significantly enriched gene sets into a network called an “enrichment map.” In the enrichment map, the nodes correspond to the gene sets and the edges reflect the overlap between the gene sets corresponding to the nodes according to the two-tailed Fisher exact test. The size of a node correlates with the enrichment P -value for the gene set associated to the node. The hubs correspond to collections of gene sets with a unifying functional group label.

Association of the EZH2 Target Gene and GSK126 De-repression Signatures with *MYCN*-amplified Status in Primary Neuroblastoma Tumors

The EZH2 gene signatures identified in the ChIP-seq and the RNA-seq experiments in our study were further tested for association with the *MYCN*-amplified status and the high-risk neuroblastoma phenotypes in primary tumors. The two neuroblastoma gene expression datasets: GSE12460 (25), describing 64 tumors, and GSE49711 (26), describing 498 tumors, were analyzed for this purpose.

Drug Synergy Screening and Analysis for Combinations with GSK126

The EZH2 inhibitor GSK126 was screened *in vitro* for the synergistic combination with a panel of 10 small molecules. The screening was performed on Kelly cells. The synergistic activity of the *in vitro* GSK126 combinations was assessed based on the Delta Bliss Sum Negative (DBSumNeg) score with the conservative synergy cutoff $DBSumNeg < -3$ (28). The DBSumNeg score was introduced as a new metric to quantify the synergy of the combination of two drugs across all dose combinations tested and was computed simply as the sum of the synergistic deviations from the Excess over Bliss model (29).

Chou-Talalay Combination Index for Loewe Additivity

To assess whether individual treatment combinations were synergistic, additive, or antagonistic we computed the combination index (CI) scores for Loewe Additivity based on the Chou-Talalay Median Effect model (30-32) as implemented in CalcuSyn v2.11 (<http://www.biosoft.com/w/calculusyn.htm>). The median effect model states that the effect x of a dose of a drug is described by the equation $x/(1-x) = (d/D_{IC50})^m$, where D_{IC50} is the IC_{50} dose of the drug, and m is a parameter that estimated from the dose-effect curve kinetics of the drug: $m = 1$ (hyperbolic), $m > 1$ (sigmoidal), $m < 1$ (flat sigmoidal). Loewe additivity is a dose-effect model which states that additivity occurs in a two-drug combination if the sum of the ratios of the dose vs. the median-effect for each individual drug is $d_1/D_{IC50,1} + d_2/D_{IC50,2} = 1$, where d_1, d_2 are the doses for the two drugs, and $D_{IC50,1}$ and $D_{IC50,2}$ represent the IC_{50} doses (median-effect) for the two drugs, respectively. Chou and Talalay (30) showed that Loewe equations are valid for enzyme inhibitors with similar mechanisms of action -- either competitive or non-competitive toward the substrate.

The Chou-Talalay Combination Index for Loewe Additivity model assigns a quantitative measure to any given effect x produced by the combination of dose d_1 of drug 1 and dose d_2 of drug 2: $CI = d_1/D_{x1} + d_2/D_{x2}$, where D_{x1} is the dose of drug 1 that alone produces the effect x and D_{x2} is the dose of drug 2 that alone produces the effect x , as estimated from the median effect model. For any given endpoint of the effect measurement CI estimates synergism ($CI < 0.8$), strong synergism ($CI < 0.6$), antagonism ($CI > 1.2$), strong antagonism ($CI > 1.4$) or additive effect (CI in the range 0.8-1.2). The drug combinations were analyzed based on two types of diagnostic plots:

Effect-oriented plots: the effect x of the drug combination on the X axis, and $CI = d_1/D_{x1} + d_2/D_{x2}$ on the Y axis

Dose-oriented (isobologram) plots: d_1/D_{x1} on the X axis, d_2/D_{x2} on the Y axis, along with the Loewe additivity isobole line: $d_1/D_{IC50,1} + d_2/D_{IC50,2} = 1$

SUPPLEMENTAL FIGURE LEGENDS

Supplemental Figure 1. Neuroblastoma Cell Lines Are Dependent on PRC2 Complex and EZH2. (A) EED-EZH2 Complex dependency Z-score in neuroblastoma versus all other cell lines in the CRISPR-Cas9 screen based on single sample GSEA. (B) The correlation of relative dependency on *EED* and *EZH2* (*left*), *SUZ12* and *EZH2* (*middle*), or *SUZ12* and *EED* (*right*), in each of the neuroblastoma cell lines. X-axis and Y-axis show the gene CERES dependency score. (C) Heat map showing *EZH2*, *EED*, and *SUZ12* dependency scores in all cell lines in the screen. (D) Immunoblot showing the effect of *EZH2* CRISPR-Cas9 knockout or *EZH2* shRNA knockdown on the H3K27me3 levels in SK-N-BE(2). (E) Immunoblot showing the *EZH2* expression before or after *EZH2* replacement with control (*GFP*), *EZH2* wildtype (*EZH2*-WT), or *EZH2* triple point-mutant (*EZH2*-TM). (F) Cell viability assay before or after *EZH2* replacement with control (*GFP*), *EZH2* wildtype (*EZH2*-WT), or *EZH2* triple point-mutant (*EZH2*-TM). Shown is a representative of two independent experiments. Mean \pm SD of eight technical replicates is shown.

Supplemental Figure 2. Pharmacological Inhibition of EZH2 in MYCN-amplified Neuroblastoma *in Vitro*. (A) Immunoblot showing dose-dependent target inhibition by JQEZ5 (*left*) or GSK126 (*right*) in neuroblastoma cell lines. Total H3 served as control for H3K27me3. (B) Mann-Whitney test of area under curve response to *EZH2* inhibitors comparing *MYCN*-amplified and *MYCN*-nonamplified neuroblastoma. (C) Flow cytometry analysis for Annexin V and PI staining in neuroblastoma cell lines treated with 3 μ M JQEZ5, GSK126 or DMSO control for 8-10 days.

Supplemental Figure 3. Genome-wide EZH2 Binding Pattern in MYCN-amplified Neuroblastoma LAN-1 cells. (A) Metagene analysis showing the average ChIP-seq binding signals of *EZH2*, H3K27me3 or H3K4me3 for 500 randomly selected genes in each of three categories based on the gene expression level (highly expressed, medium expressed and poorly expressed). X-axis shows the distance in kb to transcription start site (TSS). (B) Scatter plot showing correlation between *EZH2* relative binding signal and H3K27me3 relative binding signal in the promoter region. (C) Gene track showing high binding signal for *EZH2* and H3K27me3 and low binding signal for H3K4me3 in two published, validated *EZH2* targets. (D) Box plots of expression values for (*top*) *EZH2* target genes versus non-*EZH2* target genes and (*bottom*) H3K27me3 target genes versus non-H3K27me3 target genes in LAN-1 cells. (E) GSEA volcano

plot showing enrichment of published PRC2 target signatures from MSigDB v5.1 among genes with (*top*) high EZH2 binding signal or (*bottom*) high H3K27me3 binding signal in LAN-1 cells. (F) Enrichment of Benporath PRC2 target signature among genes with (*top*) high EZH2 promoter binding signal or (*bottom*) high H3K27me3 promoter binding signal in LAN-1 cells.

Supplemental Figure 4. Side-by-side Heatmaps of EZH2 and H3K27me3 ChIP-seq AUC Signal. The 4,536 EZH2 peaks ± 4 kb in Kelly cells are shown on the left and the 1,936 EZH2 peaks ± 4 kb in LAN-1 cells on the right. The color scale indicates average signal on a 10-base pair window.

Supplemental Figure 5. GSEA Showing the Effect of GSK126 Treatment on Neuroblastoma Cell Lines (Kelly and LAN-1) and Single Sample GSEA of Neuroblastoma Tumors. (A) GSEA showing enrichment for the previously published gene signatures after treatment with EPZ-6438 (GSE79859) in the expression profiles following GSK126 treatment. (B) GSEA showing enrichment of neurite development and axonogenesis signatures in genes upregulated by GSK126. (C) Single sample GSEA in primary neuroblastoma tumor expression datasets GSE12460 and GSE49711.

Supplemental Figure 6. Isobologram Plots Demonstrate Synergy of Panobinostat and GSK126 in Kelly, SK-N-BE(2), LAN-1 and CHP-212 on Day 6. Shown is a representative of two to three independent experiments.

SUPPLEMENTAL TABLE LEGENDS

Supplemental Table 1. (A) Top 100 leading edge genes for the top 3 independent components IC1, IC2 and IC3 that are associated with the neuroblastoma lineage in the CRISPR-Cas9 CERES dependency data. The genes are ranked based on their Z-score per component. Leading edge genes were selected based on cut-off Z-score ≥ 2.5 . PRC2 complex genes are highlighted bold. (B) Sensitivity AUC scores for the EZH2 inhibitors GSK126 (day 5), JQEZ5 (day 5) and dependency scores for EZH2, EED, and SUZ12 across the neuroblastoma cell lines in the study.

Supplemental Table 2. Top 50 GSEA significant hits for EZH2 and H3K27me3 ChIP-seq target genes in Kelly and LAN-1 cells using the MSigDB v5.1 collection c2 of 4,726 pathways and

experimental gene sets. For each significant gene set hit the table shows if the gene set is related to the PRC2 complex (1= yes, 0=no), the size of the gene set, the GSEA normalized enrichment score (NES), P and false discovery rate (FDR). The MSigDB gene sets are ranked in decreasing order based on the NES. **(A)** Top 50 GSEA hits for EZH2 ChIP-seq target genes in Kelly cells. PRC2 related gene sets are significantly over-represented in the collection of GSEA hits (odds-ratios = 9.5, $P < 0.001$, according to the two-tailed Fisher exact test). **(B)** Top 50 GSEA hits for H3K27me3 ChIP-seq target genes in Kelly cells. PRC2 related gene sets are significantly over-represented in the collection of GSEA hits (odds-ratios = 8.1, $P < 0.001$, according to the two-tailed Fisher exact test). **(C)** Top 50 GSEA hits for EZH2 ChIP-seq target genes in LAN-1 cells. PRC2 related gene sets are significantly over-represented in the collection of GSEA hits (odds-ratios = 7.9, $P < 0.001$ according to the two-tailed Fisher exact test). **(D)** Top 50 GSEA hits for H3K27me3 ChIP-seq target genes in LAN-1 cells. PRC2 related gene sets are significantly over-represented in the collection of GSEA hits (odds-ratios = 9.5, $P < 0.001$ according to the two-tailed Fisher exact test).

Supplemental Table 3. Custom neuroblastoma PRC2 signatures consisting of the top 300 EZH2 and H3K27me3 ChIP-seq target genes in Kelly and LAN-1 cell lines. Shown in table are the EZH2 and H3K27me3 promoter relative binding signal in Kelly and LAN-1 cells. Genes were ranked in decreasing order based on the promoter binding signal in the highlighted ranking score column. The high level for the relative occupancy signal in the promoter regions was estimated based on the cut-off 1.5 for the ratio of the AUC ChIP-seq signal of the mark vs. the AUC signal of the input. **(A)** Custom neuroblastoma PRC2 signature consisting of the top 300 EZH2 ChIP-seq target genes in Kelly cells. **(B)** Custom neuroblastoma PRC2 signature consisting of the top 300 H3K27me3 ChIP-seq target genes in Kelly cells. **(C)** Custom neuroblastoma PRC2 signature consisting of the top 300 EZH2 ChIP-seq target genes in LAN-1 cells. **(D)** Custom neuroblastoma PRC2 signature consisting of the top 300 H3K27me3 ChIP-seq target genes in LAN-1 cells.

Supplemental Table 4. Top 60 significant GSEA hits for EZH2 and H3K27me3 ChIP-seq target genes in Kelly and LAN-1 cells using the MSigDB v5.1 c5 collection of 25 Gene Ontology (GO) gene sets related to biological processes. For each gene set hit the table shows if the gene set is related to any of the 15 Neural Development signatures available in the MSigDB c5 collection (1= yes, 0=no), the size of the gene set, the GSEA normalized enrichment score (NES), P and false discovery rate (FDR). The significance cut-offs were 0.05 for P and 0.25 for FDR. The top 60 gene set hits are ranked in decreasing order based on the NES. **(A)** Top 60 GSEA hits for

EZH2 ChIP-seq target genes in Kelly cells. Neural Development related gene sets are significantly over-represented in the collection of GSEA hits (odds-ratios = 51.03, $P < 0.001$, according to the two-tailed Fisher exact test). **(B)** Top 60 GSEA hits for EZH2 ChIP-seq target genes in LAN-1 cells. Neural Development related gene sets are significantly over-represented in the collection of GSEA hits (odds-ratios = 39.73, $P < 0.001$, according to the two-tailed Fisher exact test).

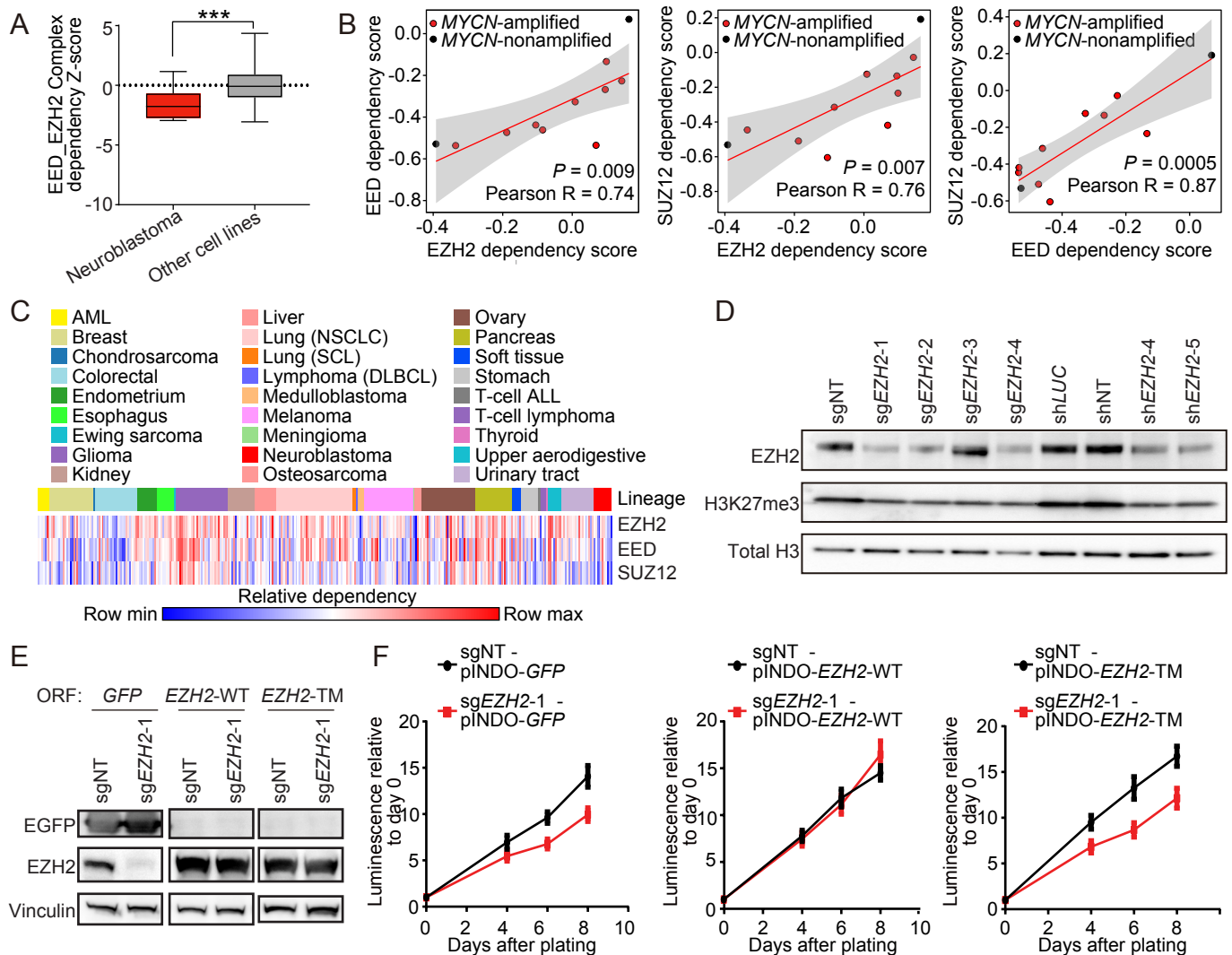
Supplemental Table 5. The shRNA sequences and the CRISPR-Cas9 sgRNA sequences targeting *MYCN* and *EZH2* that were used in this study.

REFERENCES

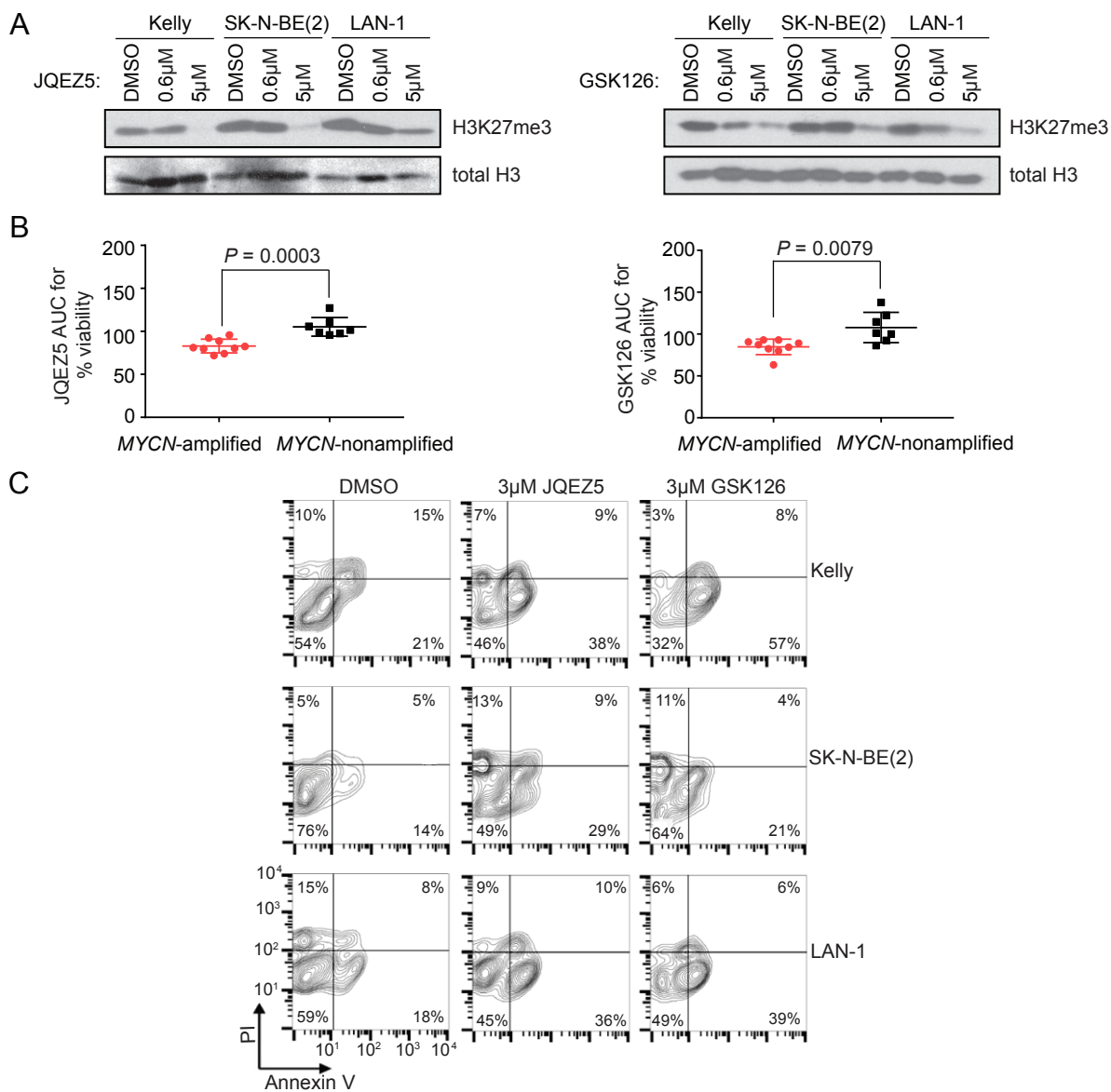
1. Meyers RM, Bryan JG, McFarland JM, Weir BA, Sizemore AE, Xu H, Dharia NV, Montgomery PG, Cowley GS, Pantel S, et al. Computational correction of copy-number effect improves specificity of CRISPR-Cas9 essentiality screens in cancer cells. *Nature Genetics*. 2017: in press.
2. Comon P. Independent component analysis, a new concept? *Signal processing*. 1994;36(3):287-314.
3. Hyvärinen A, Karhunen J, and Oja E. Independent component analysis. *Wiley, New York*. 2001.
4. Hyvärinen A. Fast and robust fixed-point algorithms for independent component analysis. *IEEE Trans Neural Netw*. 1999;10(3):626-34.
5. Barbie DA, Tamayo P, Boehm JS, Kim SY, Moody SE, Dunn IF, Schinzel AC, Sandy P, Meylan E, Scholl C, et al. Systematic RNA interference reveals that oncogenic KRAS-driven cancers require TBK1. *Nature*. 2009;462(7269):108-12.
6. Subramanian A, Tamayo P, Mootha VK, Mukherjee S, Ebert BL, Gillette MA, Paulovich A, Pomeroy SL, Golub TR, Lander ES, et al. Gene set enrichment analysis: a knowledge-based approach for interpreting genome-wide expression profiles. *Proc Natl Acad Sci U S A*. 2005;102(43):15545-50.
7. Mootha VK, Lindgren CM, Eriksson KF, Subramanian A, Sihag S, Lehar J, Puigserver P, Carlsson E, Ridderstrale M, Laurila E, et al. PGC-1alpha-responsive genes involved in oxidative phosphorylation are coordinately downregulated in human diabetes. *Nat Genet*. 2003;34(3):267-73.
8. Kamburov A, Pentchev K, Galicka H, Wierling C, Lehrach H, and Herwig R. ConsensusPathDB: toward a more complete picture of cell biology. *Nucleic Acids Res*. 2011;39(Database issue):D712-7.
9. Kamburov A, Wierling C, Lehrach H, and Herwig R. ConsensusPathDB--a database for integrating human functional interaction networks. *Nucleic Acids Res*. 2009;37(Database issue):D623-8.
10. Langmead B. Aligning short sequencing reads with Bowtie. *Curr Protoc Bioinformatics*. 2010;Chapter 11(Unit 11 7).
11. Langmead B, and Salzberg SL. Fast gapped-read alignment with Bowtie 2. *Nat Methods*. 2012;9(4):357-9.
12. Carroll TS, Liang Z, Salama R, Stark R, and de Santiago I. Impact of artifact removal on ChIP quality metrics in ChIP-seq and ChIP-exo data. *Front Genet*. 2014;5(75).
13. Feng J, Liu T, Qin B, Zhang Y, and Liu XS. Identifying ChIP-seq enrichment using MACS. *Nat Protoc*. 2012;7(9):1728-40.
14. Heinz S, Benner C, Spann N, Bertolino E, Lin YC, Laslo P, Cheng JX, Murre C, Singh H, and Glass CK. Simple combinations of lineage-determining transcription factors prime cis-regulatory elements required for macrophage and B cell identities. *Mol Cell*. 2010;38(4):576-89.
15. Ramirez F, Dundar F, Diehl S, Gruning BA, and Manke T. deepTools: a flexible platform for exploring deep-sequencing data. *Nucleic Acids Res*. 2014;42(Web Server issue):W187-91.

16. Loven J, Hoke HA, Lin CY, Lau A, Orlando DA, Vakoc CR, Bradner JE, Lee TI, and Young RA. Selective inhibition of tumor oncogenes by disruption of super-enhancers. *Cell*. 2013;153(2):320-34.
17. Barretina J, Caponigro G, Stransky N, Venkatesan K, Margolin AA, Kim S, Wilson CJ, Lehar J, Kryukov GV, Sonkin D, et al. The Cancer Cell Line Encyclopedia enables predictive modelling of anticancer drug sensitivity. *Nature*. 2012;483(7391):603-7.
18. Dassi E, Greco V, Sidarovich V, Zuccotti P, Arseni N, Scaruffi P, Tonini GP, and Quattrone A. Multi-omic profiling of MYCN-amplified neuroblastoma cell-lines. *Genom Data*. 2015;6(285-7).
19. Kim D, Pertea G, Trapnell C, Pimentel H, Kelley R, and Salzberg SL. TopHat2: accurate alignment of transcriptomes in the presence of insertions, deletions and gene fusions. *Genome Biol*. 2013;14(4):R36.
20. Garcia-Alcalde F, Okonechnikov K, Carbonell J, Cruz LM, Gotz S, Tarazona S, Dopazo J, Meyer TF, and Conesa A. Qualimap: evaluating next-generation sequencing alignment data. *Bioinformatics*. 2012;28(20):2678-9.
21. Hugo Varet J-YC, Marie-Agnès Dillies. SARTools: a DESeq2- and edgeR-based R pipeline for comprehensive differential analysis of RNA-Seq data. *bioRxiv*. 2015.
22. Liao Y, Smyth GK, and Shi W. featureCounts: an efficient general purpose program for assigning sequence reads to genomic features. *Bioinformatics*. 2014;30(7):923-30.
23. Robinson MD, McCarthy DJ, and Smyth GK. edgeR: a Bioconductor package for differential expression analysis of digital gene expression data. *Bioinformatics*. 2010;26(1):139-40.
24. Reich M, Liefeld T, Gould J, Lerner J, Tamayo P, and Mesirov JP. GenePattern 2.0. *Nat Genet*. 2006;38(5):500-1.
25. Janoueix-Lerosey I, Lequin D, Brugieres L, Ribeiro A, de Pontual L, Combaret V, Raynal V, Puisieux A, Schleiermacher G, Pierron G, et al. Somatic and germline activating mutations of the ALK kinase receptor in neuroblastoma. *Nature*. 2008;455(7215):967-70.
26. Wang C, Gong B, Bushel PR, Thierry-Mieg J, Thierry-Mieg D, Xu J, Fang H, Hong H, Shen J, Su Z, et al. The concordance between RNA-seq and microarray data depends on chemical treatment and transcript abundance. *Nat Biotechnol*. 2014;32(9):926-32.
27. Merico D, Isserlin R, Stueker O, Emili A, and Bader GD. Enrichment map: a network-based method for gene-set enrichment visualization and interpretation. *PLoS One*. 2010;5(11):e13984.
28. Mott BT, Eastman RT, Guha R, Sherlach KS, Siriwardana A, Shinn P, McKnight C, Michael S, Lacerda-Queiroz N, Patel PR, et al. High-throughput matrix screening identifies synergistic and antagonistic antimalarial drug combinations. *Sci Rep*. 2015;5(13891).
29. Bliss CI. The calculation of microbial assays. *Bacteriol Rev*. 1956;20(4):243-58.
30. Chou TC, and Talalay P. Quantitative analysis of dose-effect relationships: the combined effects of multiple drugs or enzyme inhibitors. *Adv Enzyme Regul*. 1984;22(27-55).

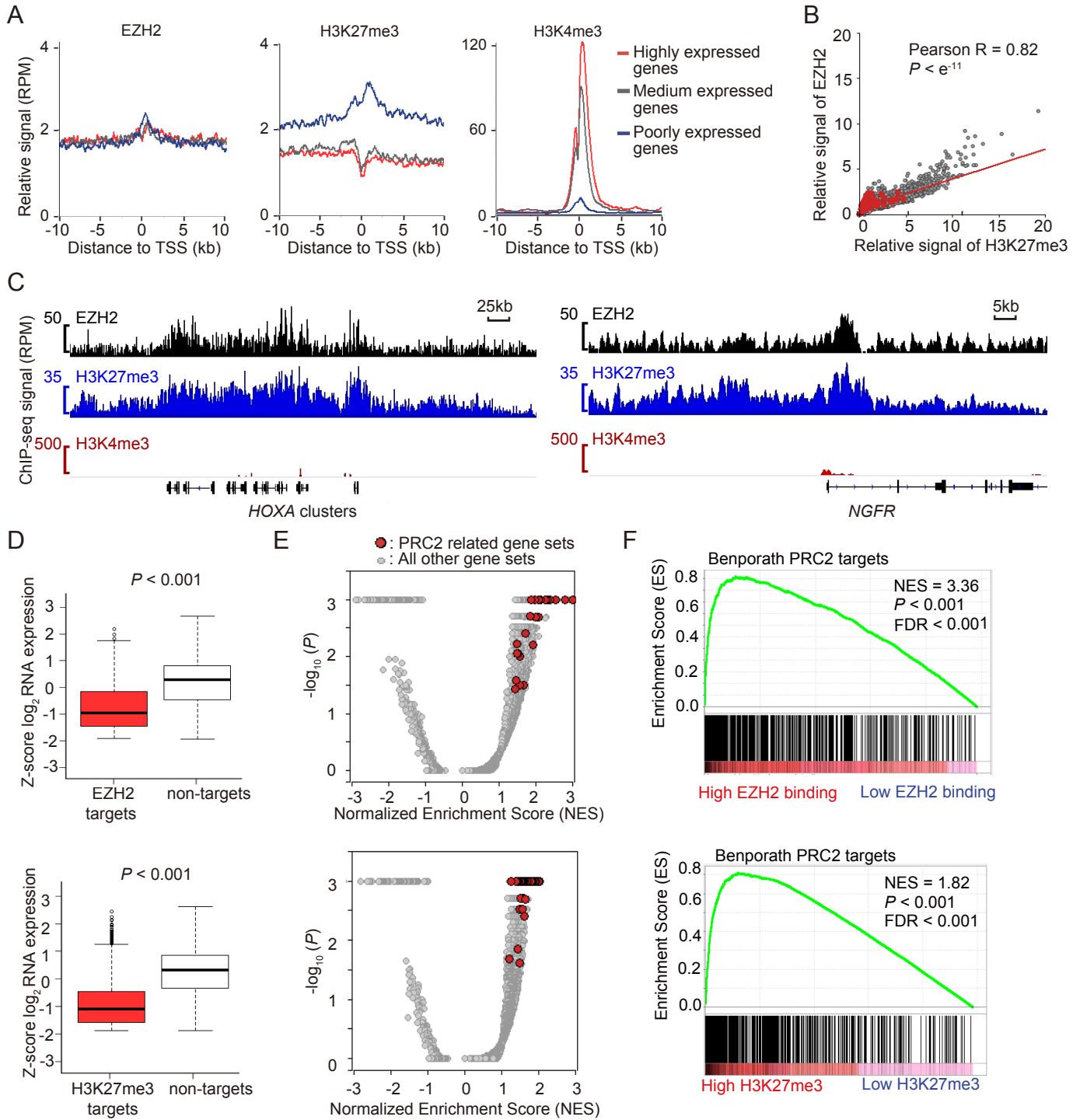
31. Chou T-C. Theoretical basis, experimental design, and computerized simulation of synergism and antagonism in drug combination studies. *Pharmacological reviews*. 2006;58(3):621-81.
32. Chou TC. Drug combination studies and their synergy quantification using the Chou-Talalay method. *Cancer Res*. 2010;70(2):440-6.



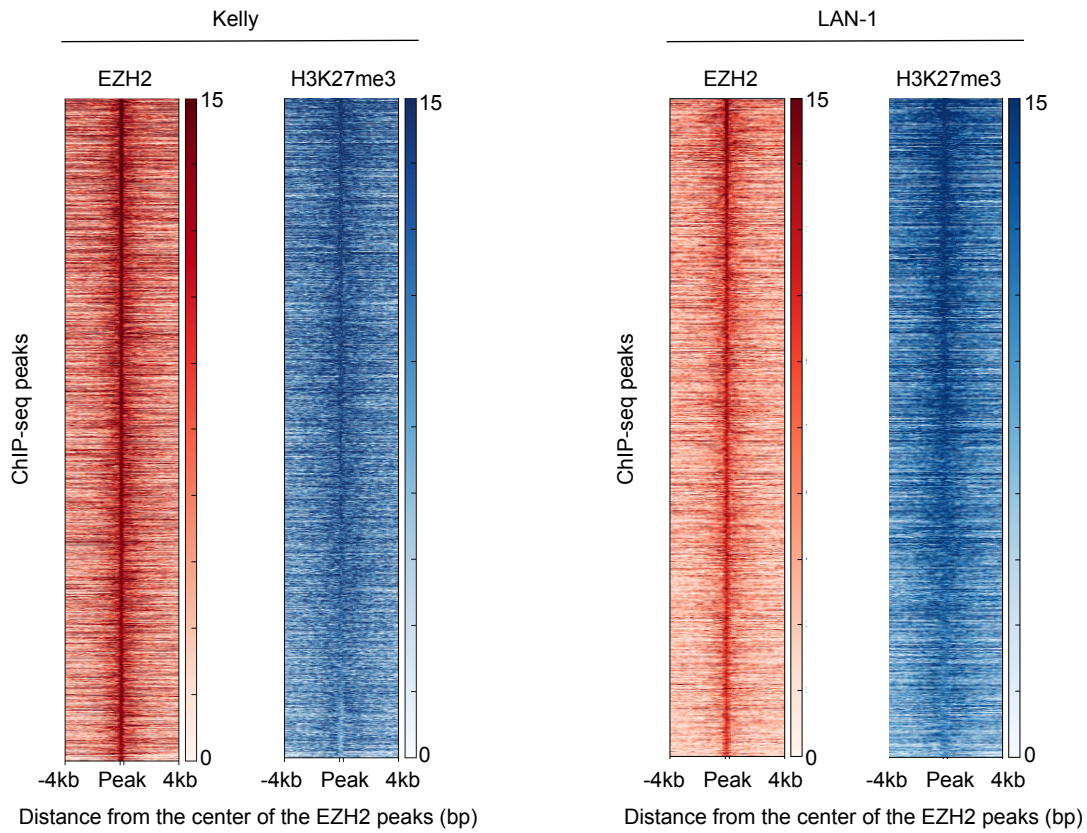
Supplemental Figure 1. Neuroblastoma Cell Lines Are Dependent on PRC2 Complex and EZH2. (A) EED-EZH2 Complex dependency Z-score in neuroblastoma versus all other cell lines in the CRISPR-Cas9 screen based on single sample GSEA. (B) The correlation of relative dependency on *EED* and *EZH2* (left), *SUZ12* and *EZH2* (middle), or *SUZ12* and *EED* (right), in each of the neuroblastoma cell lines. X-axis and Y-axis show the gene CERES dependency score. (C) Heat map showing *EZH2*, *EED* and *SUZ12* dependency scores in all cell lines in the screen. (D) Immunoblot showing the effect of *EZH2* CRISPR-Cas9 knockout or *EZH2* shRNA knockdown on the H3K27me3 levels in SK-N-BE(2). (E) Immunoblot showing the *EZH2* expression before or after *EZH2* replacement with control (*GFP*), *EZH2* wild-type (*EZH2*-WT), or *EZH2* triple point-mutant (*EZH2*-TM). (F) Cell viability assay before or after *EZH2* replacement with control (*GFP*), *EZH2* wild-type (*EZH2*-WT), or *EZH2* triple point-mutant (*EZH2*-TM). Shown is a representative of two independent experiments. Mean \pm SD of eight technical replicates is shown.



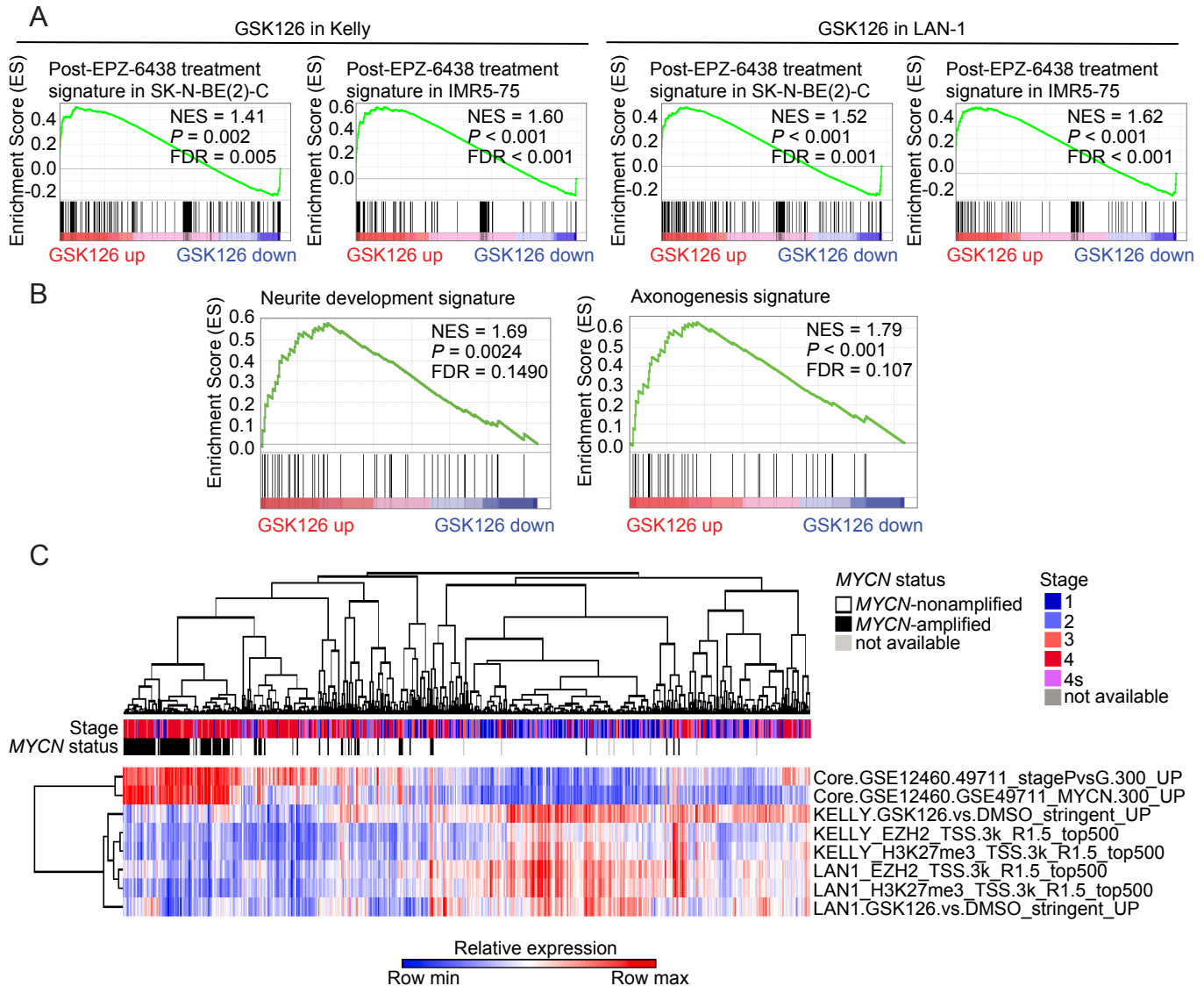
Supplemental Figure 2. Pharmacological Inhibition of EZH2 in MYCN-amplified Neuroblastoma *in Vitro*. (A) Immunoblot showing dose-dependent target inhibition by JQEZ5 (*left*) or GSK126 (*right*) in neuroblastoma cell lines. Total H3 served as control for H3K27me3. (B) Mann-Whitney test of area under curve response to EZH2 inhibitors comparing MYCN-amplified and MYCN-nonamplified neuroblastoma. (C) Flow cytometry analysis for Annexin V and PI staining in neuroblastoma cell lines treated with 3 μM JQEZ5, GSK126 or DMSO control for 8-10 days.



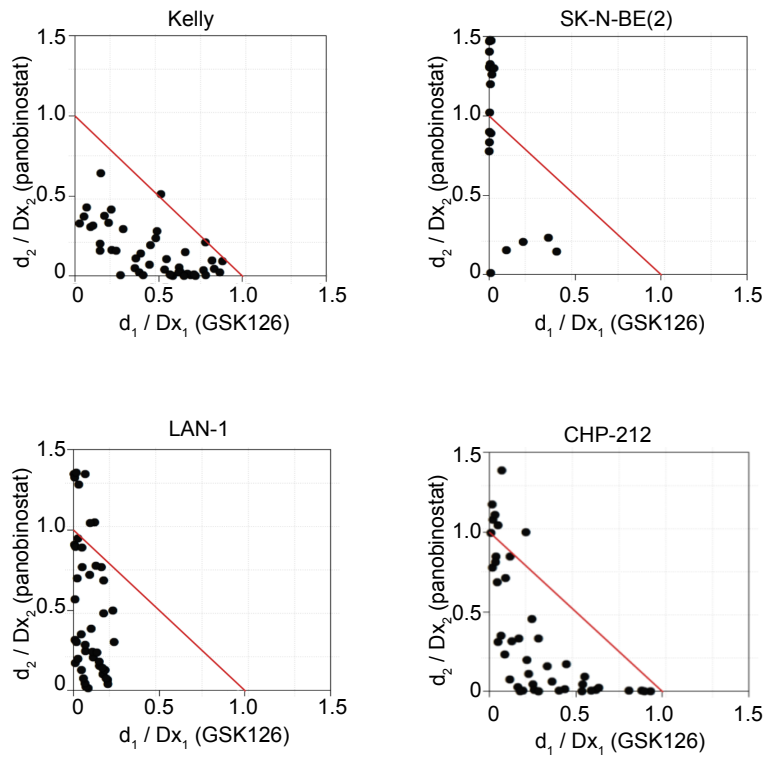
Supplemental Figure 3. Genome-wide EZH2 Binding Pattern in MYCN-amplified Neuroblastoma LAN-1 cells. (A) Metagenesis analysis showing the average ChIP-seq binding signals of EZH2, H3K27me3 or H3K4me3 for 500 randomly selected genes in each of three categories based on the gene expression level (highly expressed, medium expressed and poorly expressed). X-axis shows the distance in kb to transcription start site (TSS). (B) Scatter plot showing correlation between EZH2 relative binding signal and H3K27me3 relative binding signal in the promoter region. (C) Gene track showing high binding signal for EZH2 and H3K27me3 and low binding signal for H3K4me3 in two published, validated EZH2 targets. (D) Box plots of expression values for (top) EZH2 target genes versus non-EZH2 target genes and (bottom) H3K27me3 target genes versus non-H3K27me3 target genes in LAN-1 cells. (E) GSEA volcano plot showing enrichment of published PRC2 target signatures from MSigDB v5.1 among genes with (top) high EZH2 binding signal or (bottom) high H3K27me3 binding signal in LAN-1 cells. (F) Enrichment of Benporath PRC2 target signature among genes with (top) high EZH2 promoter binding signal or (bottom) high H3K27me3 promoter binding signal in LAN-1 cells.



Supplemental Figure 4. Side-by-side Heatmaps of EZH2 and H3K27me3 ChIP-seq AUC Signal. The 4,536 EZH2 peaks ± 4 kb in Kelly cells are shown on the left and the 1,936 EZH2 peaks ± 4 kb in LAN-1 cells on the right. The color scale indicates average signal on a 10-base pair window.



Supplemental Figure 5. GSEA Showing the Effect of GSK126 Treatment on Neuroblastoma Cell Lines (Kelly and LAN-1) and Single Sample GSEA of Neuroblastoma Tumors. (A) GSEA showing enrichment for the previously published gene signatures after treatment with EPZ-6438 (GSE79859) in the expression profiles following GSK126 treatment. **(B)** GSEA showing enrichment of neurite development and axonogenesis signatures in genes upregulated by GSK126. **(C)** Single sample GSEA in primary neuroblastoma tumor expression datasets GSE12460 and GSE49711.



Supplemental Figure 6. Isobologram Plots Demonstrate Synergy of Panobinostat and GSK126 in Kelly, SK-N-BE(2), LAN-1 and CHP-212 on Day 6. Shown is a representative of two to three independent experiments.

Supplemental Table 1. (A) Top 100 leading edge dependencies for the top 3 independent components IC1, IC2 and IC3 that are associated with the neuroblastoma lineage in the CRISPR-Cas9 CERES dependency data. The dependencies are ranked based on their Z-score per component. Leading edge dependencies were selected based on cut-off Z-score ≥ 2.5 . PRC2 complex dependencies are highlighted bold.

#	IC1 leading dependencies	IC1 component Z-score	IC2 leading dependencies	IC2 component Z-score	IC3 leading dependencies	IC3 component Z-score
1	TXK	7.20	AFMID	7.99	TAF5L	24.03
2	CWH43	6.94	TMEM105	7.93	SUPT20H	23.13
3	TLR6	6.74	ITGB4	7.64	TADA2B	22.74
4	FBXL5	6.74	SPHK1	7.32	TADA1	22.32
5	WDR19	6.52	TNRC6C	7.20	SUPT7L	16.68
6	MRFAP1L1	6.46	SSTR2	7.13	TAF6L	13.21
7	FAM114A1	6.17	P4HB	6.93	MED13	12.20
8	GRXCR1	6.01	TRIM65	6.80	KAT2A	11.20
9	CLRN2	5.95	TK1	6.76	USP22	11.15
10	CNGA1	5.91	CCDC40	6.72	MED19	10.12
11	RELL1	5.88	CD300LF	6.51	SMARCD1	8.87
12	LDB2	5.82	ST6GALNAC2	6.48	MED24	8.63
13	UBE2K	5.76	CACNG4	6.42	CCNC	8.54
14	S100P	5.72	C17orf77	6.40	MED13L	8.28
15	UCHL1	5.67	FADS6	6.37	BRD9	8.12
16	ZAR1	5.65	ABCA8	6.32	PAXIP1	7.71
17	ZCCHC4	5.65	VEZF1	6.23	MED15	7.61
18	PCDH7	5.63	PRCD	6.19	EP300	7.53
19	TMEM33	5.60	TEX19	6.09	NIPBL	7.39
20	LRPAP1	5.57	FOXK2	5.94	ATXN7	7.36
21	BLOC1S4	5.55	CBX2	5.91	MED23	7.01
22	TMEM156	5.51	CYTH1	5.85	GLTSCR1	6.77
23	DOK7	5.39	ST6GALNAC1	5.85	MED16	6.74
24	USP17L13	5.37	LOC100653515	5.76	MLLT1	6.34
25	LGI2	5.10	WBP2	5.75	PRR12	6.11
26	SEL1L3	5.09	MRC2	5.71	CCDC101	5.90
27	TBC1D1	4.97	CPSF4L	5.63	MBNL1	5.70
28	CD38	4.94	GPRC5C	5.58	CREBBP	5.22
29	KCTD8	4.93	TMEM235	5.56	ANKRD52	5.17
30	MFSD10	4.89	RNF213	5.55	DOT1L	5.00
31	ACOX3	4.65	SCAF8	5.55	EED	5.00
32	PHOX2B	4.60	SYNGR2	5.55	TCEB3	4.95
33	CHRNA9	4.60	WDR45B	5.49	KLHDC3	4.88
34	GRK4	4.59	FOXJ1	5.38	CHD2	4.85
35	ATP10D	4.59	CD79B	5.37	PTP4A1	4.80
36	DCAF4L1	4.59	TIMP2	5.33	PAGR1	4.77
37	CORIN	4.55	MIF4GD	5.32	YWHAE	4.64
38	HMX1	4.55	LLGL2	5.24	SUZ12	4.63
39	APBB2	4.48	GDPD1	5.17	TNFAIP3	4.61
40	ABLIM2	4.48	PPP1R27	5.09	RING1	4.58
41	CCKAR	4.42	FAM195B	5.08	TADA3	4.50
42	WHSC1	4.42	GGA3	5.06	EZH2	4.49
43	STIM2	4.40	SDK2	5.04	HDAC2	4.44
44	LCORL	4.40	CACNG5	4.97	C11orf30	4.42
45	SLC30A9	4.38	ACOX1	4.95	MAPKAPK2	4.41
46	ATE1	4.36	PRR29	4.95	TAF11	4.35
47	MXD4	4.32	DNAI2	4.94	KEAP1	4.30
48	RNF212	4.24	OXLD1	4.90	MAU2	4.23
49	RBKS	4.23	PRPSAP1	4.89	ATF7IP	4.19
50	SH3TC1	4.20	SEC14L1	4.80	STAG1	4.13

#	IC1 leading dependencies	IC1 component Z-score	IC2 leading dependencies	IC2 component Z-score	IC3 leading dependencies	IC3 component Z-score
51	HHAT	4.18	PRKCA	4.80	MED1	4.11
52	KCNIP4	4.16	ENDOV	4.75	PITPNB	4.01
53	HMGXB3	4.16	SLC38A10	4.72	ATXN2L	3.94
54	POLN	4.13	SECTM1	4.69	EHMT2	3.89
55	SH3BP2	4.11	PTRH2	4.65	MED25	3.88
56	TBC1D23	4.10	GPR142	4.62	SPIN1	3.86
57	CRIPAK	4.10	CD300C	4.59	ASB7	3.86
58	KLB	4.03	CEP95	4.58	TRAF3	3.78
59	HS3ST1	4.02	CARD14	4.52	FOXA2	3.70
60	KLHL5	4.01	UNK	4.50	CSRNP1	3.70
61	CPZ	4.01	BAIAP2	4.48	MORF4L1	3.67
62	GNG10	3.97	FBF1	4.48	C10orf12	3.67
63	PHLDB1	3.94	LRRRC45	4.48	PCGF1	3.61
64	MYL12B	3.91	SMIM5	4.46	SIN3B	3.59
65	FGFBP2	3.90	SGSH	4.43	BTAF1	3.57
66	GNPDA2	3.90	MAFG	4.41	FOXA1	3.48
67	FAM174B	3.89	DHX40	4.41	ACPT	3.37
68	CC2D2A	3.85	KIAA0195	4.40	KAT6A	3.32
69	CCAR2	3.84	GH1	4.40	SIRT1	3.30
70	SMIM20	3.82	CDR2L	4.37	CCNF	3.26
71	ISL1	3.81	CASKIN2	4.37	LACTB2	3.25
72	NSUN7	3.78	GALK1	4.35	APOA5	3.22
73	DCAF16	3.77	KCNJ16	4.34	MTA2	3.21
74	TLR1	3.74	NAT9	4.33	ATXN7L3	3.21
75	PPARGC1A	3.73	ENGASE	4.31	SP1	3.20
76	DEFB131	3.73	EDF1	4.30	NABP2	3.16
77	YIPF7	3.72	HID1	4.28	CLC	3.16
78	SLIT2	3.71	SMIM6	4.26	POLR2M	3.15
79	TLR10	3.69	ZNF750	4.25	PAIP1	3.14
80	LARP4B	3.63	CYGB	4.22	FBXL14	3.14
81	UBE3D	3.61	AANAT	4.15	CCNE1	3.14
82	BEND4	3.60	OTOP2	4.13	UBE2K	3.14
83	CASP7	3.59	PRR11	4.13	MTHFD1	3.10
84	FGFR3	3.59	RNF157	4.12	HEATR3	3.10
85	FZD8	3.58	MAP2K6	4.12	FAM159B	3.10
86	TNNI1	3.58	TMC6	4.09	HTT	3.09
87	ZNF292	3.57	RFNG	4.04	ZNF143	3.09
88	ADD1	3.56	CANT1	4.03	ARF6	3.09
89	NWD2	3.55	KIRREL3	4.02	THAP4	3.08
90	QDPR	3.55	EVPL	4.01	ROCK1	3.07
91	RBPJ	3.54	EFCAB3	4.01	MYCN	3.07
92	SLC34A2	3.53	KPNA2	4.00	AFF4	3.06
93	SPICE1	3.52	NOTUM	3.99	CAB39	3.06
94	LRRTM3	3.49	YPEL2	3.97	KDM1A	3.06
95	SHISA3	3.49	DUS1L	3.97	CKS1B	3.04
96	LARP7	3.49	TRAPPC13	3.97	ZNF217	3.04
97	TEC	3.47	MFSD11	3.93	ATG101	3.04
98	OCIAD1	3.46	UNC13D	3.93	SERTAD2	3.03
99	BOD1L1	3.45	PCTP	3.93	KLF5	3.03
100	SLC26A1	3.44	RNFT1	3.92	RANBP9	3.03

Supplemental Table 1. (B) Sensitivity AUC scores for the EZH2 inhibitors GSK126 (day 5), JQEZ5 (day 5) and dependency scores for EZH2, EED and SUZ12 across the neuroblastoma cell lines in the study.

#	Cell line	MYCN status	AUC score GSK126 day 5	AUC score JQEZ5 day 5	EZH2 dependency score	EED dependency score	SUZ12 dependency score
1	CHP-212	Amplified	89.150	95.720	-0.335	-0.536	-0.446
2	IMR-32	Amplified	92.850	79.670	0.098	-0.134	-0.234
3	Kelly	Amplified	87.230	80.270	-0.188	-0.474	-0.510
4	LAN-1	Amplified	92.880	92.250	na	na	na
5	MHH-NB-11	Amplified	90.510	82.370	0.095	-0.268	-0.135
6	NB-1	Amplified	82.350	71.890	0.068	-0.535	-0.419
7	NGP	Amplified	79.980	88.700	na	na	na
8	SIMA	Amplified	84.230	81.000	-0.085	-0.461	-0.315
9	SK-N-BE(2)	Amplified	63.240	74.070	-0.105	-0.438	-0.605
10	ACN	Non-amplified	122.400	110.200	na	na	na
11	CHLA-15	Non-amplified	100.100	97.660	na	na	na
12	GI-M-EN	Non-amplified	101.200	95.670	na	na	na
13	SH-SY-5Y	Non-amplified	86.250	98.660	na	na	na
14	SK-N-AS	Non-amplified	92.440	101.500	-0.392	-0.529	-0.531
15	SK-N-FI	Non-amplified	137.700	127.000	0.163	0.069	0.191
16	SK-N-SH	Non-amplified	114.500	105.700	na	na	na

Supplemental Table 2. Top 50 GSEA significant hits for EZH2 and H3K27me3 ChIP-seq target genes in Kelly and LAN-1 cells using the MSigDB v5.1 collection c2 of 4,726 pathways and experimental gene sets. For each significant gene set the table shows if the gene set is related to the PRC2 complex (1= yes, 0=no), the size of the gene set, the GSEA normalized enrichment score (NES), *P* and false discovery rate (FDR). The MSigDB gene sets are ranked in decreasing order based on the NES.

(A) Top 50 GSEA hits for EZH2 ChIP-seq target genes in Kelly cells. PRC2 related gene sets are significantly over-represented in the collection of GSEA hits (odds-ratios = 9.5, *P* < 0.001, according to the two-tailed Fisher exact test).

Rank	Gene Set	PRC2 Complex	Size	NES	<i>P</i>	FDR
1	MEISSNER_BRAIN_HCP_WITH_H3K27ME3	1	263	3.57	0.0000	0.0000
2	BENPORATH_PRC2_TARGETS	1	615	3.44	0.0000	0.0000
3	MIKKELSEN_NPC_HCP_WITH_H3K27ME3	1	332	3.30	0.0000	0.0000
4	MEISSNER_NPC_HCP_WITH_H3K4ME2_AND_H3K27ME3	1	339	3.27	0.0000	0.0000
5	MEISSNER_NPC_HCP_WITH_H3K27ME3	1	78	3.27	0.0000	0.0000
6	BENPORATH_EED_TARGETS	1	999	3.25	0.0000	0.0000
7	BENPORATH_SUZ12_TARGETS	1	984	3.24	0.0000	0.0000
8	MIKKELSEN_IPS_WITH_HCP_H3K27ME3	1	99	3.18	0.0000	0.0000
9	MIKKELSEN_MEF_HCP_WITH_H3K27ME3	1	569	3.15	0.0000	0.0000
10	MIKKELSEN_MCV6_HCP_WITH_H3K27ME3	1	418	3.13	0.0000	0.0000
11	SCHLESINGER_METHYLATED_DE_NOVO_IN_CANCER	1	85	3.03	0.0000	0.0000
12	MEISSNER_BRAIN_HCP_WITH_H3K4ME2_AND_H3K27ME3	1	56	2.86	0.0000	0.0000
13	REACTOME_REGULATION_OF_BETA_CELL_DEVELOPMENT	0	30	2.73	0.0000	0.0000
14	RORIE_TARGETS_OF_EWSR1_FLI1_FUSION_UP	0	27	2.66	0.0000	0.0000
15	MIKKELSEN_NPC_HCP_WITH_H3K4ME3_AND_H3K27ME3	1	205	2.61	0.0000	0.0000
16	KEGG_MATURITY_ONSET_DIABETES_OF_THE_YOUNG	0	25	2.61	0.0000	0.0000
17	MCGARVEY_SILENCED_BY_METHYLATION_IN_COLON_CANCER	0	40	2.55	0.0000	0.0002
18	KEGG_HEDGEHOG_SIGNALING_PATHWAY	0	56	2.55	0.0000	0.0002
19	RIZ_ERYTHROID_DIFFERENTIATION_6HR	0	40	2.52	0.0000	0.0000
20	THEODOROU_MAMMARY_TUMORIGENESIS	0	28	2.49	0.0000	0.0000
21	LI_WILMS_TUMOR	0	25	2.48	0.0000	0.0007
22	WANG_LSD1_TARGETS_UP	0	23	2.46	0.0000	0.0008
23	LIEN_BREAST_CARCINOMA_METAPLASTIC	0	35	2.45	0.0000	0.0000
24	MATZUK_IMPLANTATION_AND_UTERINE	0	22	2.43	0.0000	0.0013
25	RIZ_ERYTHROID_DIFFERENTIATION_APOBEC2	0	24	2.43	0.0000	0.0000
26	NIKOLSKY_BREAST_CANCER_5P15_AMPLICON	0	25	2.43	0.0000	0.0000
27	MARTENS_TRETINOIN_RESPONSE_UP	0	803	2.41	0.0000	0.0015
28	WONG_ENDMETRIUM_CANCER_UP	0	25	2.41	0.0000	0.0000
29	RIZ_ERYTHROID_DIFFERENTIATION_HEMGN	0	31	2.40	0.0000	0.0000
30	SCHLESINGER_H3K27ME3_IN_NORMAL_AND_METHYLATED_IN_CANCER	1	28	2.39	0.0000	0.0000
31	LEIN_CEREBELLUM_MARKERS	0	80	2.36	0.0000	0.0035
32	WANG_THOC1_TARGETS_DN	0	18	2.36	0.0000	0.0035
33	RIZ_ERYTHROID_DIFFERENTIATION_HBZ	0	41	2.35	0.0000	0.0000
34	SHIN_B_CELL_LYMPHOMA_CLUSTER_9	0	19	2.35	0.0000	0.0000
35	LIU_CDX2_TARGETS_UP	0	35	2.34	0.0000	0.0000
36	MEISSNER_NPC_HCP_WITH_H3K4ME2	1	477	2.31	0.0000	0.0070
37	KEGG_BASAL_CELL_CARCINOMA	0	55	2.31	0.0000	0.0069
38	AIGNER_ZEB1_TARGETS	0	34	2.31	0.0000	0.0001
39	REACTOME_CLASS_B_2_SECRETIN_FAMILY_RECEPTORS	0	87	2.29	0.0000	0.0001
40	KONDO_PROSTATE_CANCER_HCP_WITH_H3K27ME3	1	95	2.28	0.0000	0.0115
41	DAWSON_METHYLATED_IN_LYMPHOMA_TCL1	0	57	2.27	0.0000	0.0001
42	PEREZ_TP53_AND_TP63_TARGETS	0	194	2.26	0.0000	0.0001
43	NIKOLSKY_BREAST_CANCER_16P13_AMPLICON	0	113	2.26	0.0000	0.0001
44	WANG_MLL_TARGETS	0	280	2.25	0.0000	0.0155
45	SCHRAETS_MLL_TARGETS_DN	0	32	2.23	0.0000	0.0200
46	BEGUM_TARGETS_OF_PAX3_FOXO1_FUSION_DN	0	45	2.23	0.0000	0.0002
47	ROZANOV_MMP14_TARGETS_DN	0	33	2.23	0.0000	0.0002
48	MEISSNER_NPC_HCP_WITH_H3K4ME3_AND_H3K27ME3	1	139	2.21	0.0000	0.0242
49	YAO_TEMPORAL_RESPONSE_TO_PROGESTERONE_CLUSTER_4	0	15	2.20	0.0000	0.0286
50	MEISSNER_NPC_HCP_WITH_H3_UNMETHYLATED	1	505	2.19	0.0000	0.0301

Supplemental Table 2. (B) Top 50 GSEA hits for H3K27me3 ChIP-seq target genes in Kelly cells. PRC2 related gene sets are significantly over-represented in the collection of GSEA hits (odds-ratios = 8.1, $P < 0.001$, according to the two-tailed Fisher exact test).

Rank	Gene Set	PRC2 Complex	Size	NES	P	FDR
1	MEISSNER_NPC_HCP_WITH_H3K27ME3	1	78	1.82	0.0000	0.0000
2	MEISSNER_BRAIN_HCP_WITH_H3K27ME3	1	263	1.80	0.0000	0.0000
3	RORIE_TARGETS_OF_EWSR1_FLI1_FUSION_UP	0	27	1.69	0.0000	0.0056
4	MIKKELSEN_NPC_HCP_WITH_H3K27ME3	1	332	1.69	0.0000	0.0042
5	BENPORATH_PRC2_TARGETS	1	615	1.68	0.0000	0.0000
6	SHIN_B_CELL_LYMPHOMA_CLUSTER_9	0	19	1.67	0.0000	0.0000
7	MIKKELSEN_IPS_WITH_HCP_H3K27ME3	1	99	1.66	0.0000	0.0130
8	AIGNER_ZEB1_TARGETS	0	34	1.65	0.0000	0.0000
9	YAO_TEMPORAL_RESPONSE_TO_PROGESTERONE_CLUSTER_4	0	15	1.65	0.0000	0.0115
10	WONG_ENDMETRIUM_CANCER_UP	0	25	1.65	0.0000	0.0000
11	WANG_THOC1_TARGETS_DN	0	18	1.64	0.0010	0.0171
12	KEGG_MATURITY_ONSET_DIABETES_OF_THE_YOUNG	0	25	1.64	0.0000	0.0153
13	MEISSNER_NPC_HCP_WITH_H3K4ME2_AND_H3K27ME3	1	339	1.64	0.0000	0.0156
14	DAZARD_UV_RESPONSE_CLUSTER_G28	0	18	1.64	0.0010	0.0141
15	MATZUK_IMPLANTATION_AND_UTERINE	0	22	1.62	0.0000	0.0189
16	MIKKELSEN_MEF_HCP_WITH_H3K27ME3	1	569	1.62	0.0000	0.0189
17	MATZUK_EMBRYONIC_GERM_CELL	0	19	1.61	0.0000	0.0209
18	REACTOME_REGULATION_OF_BETA_CELL_DEVELOPMENT	0	30	1.61	0.0000	0.0206
19	BENPORATH_EED_TARGETS	1	999	1.61	0.0000	0.0001
20	YAO_HOXA10_TARGETS_VIA_PROGESTERONE_DN	0	17	1.61	0.0020	0.0212
21	BENPORATH_SUZ12_TARGETS	1	984	1.60	0.0000	0.0001
22	HE_PTEN_TARGETS_UP	0	16	1.59	0.0010	0.0002
23	SHIN_B_CELL_LYMPHOMA_CLUSTER_5	0	16	1.59	0.0000	0.0002
24	RIZ_ERYTHROID_DIFFERENTIATION_APOBEC2	0	24	1.59	0.0000	0.0002
25	MIKKELSEN_MCV6_HCP_WITH_H3K27ME3	1	418	1.59	0.0000	0.0344
26	REACTOME_OLFACTORY_SIGNALING_PATHWAY	0	298	1.56	0.0000	0.0005
27	GAURNIER_PSM4_TARGETS	0	52	1.56	0.0000	0.0664
28	LIEN_BREAST_CARCINOMA_METAPLASTIC	0	35	1.56	0.0010	0.0004
29	LI_WILMS_TUMOR	0	25	1.55	0.0010	0.0779
30	STREICHER_LSM1_TARGETS_DN	0	19	1.55	0.0010	0.0006
31	CUI_TCF21_TARGETS_DN	0	28	1.55	0.0010	0.0815
32	SCHLESINGER_H3K27ME3_IN_NORMAL_AND_METHYLATED_IN_CANCER	1	28	1.54	0.0020	0.0006
33	REACTOME_GABA_SYNTHESIS_RELEASE_REUPTAKE_AND_DEGRADATION	0	17	1.54	0.0020	0.0899
34	SCHLESINGER_METHYLATED_DE_NOVO_IN_CANCER	0	85	1.54	0.0000	0.0006
35	MEISSNER_BRAIN_HCP_WITH_H3K4ME2_AND_H3K27ME3	1	56	1.54	0.0000	0.0933
36	WANG_BARRETTS_ESOPHAGUS_AND_ESOPHAGUS_CANCER_DN	0	35	1.53	0.0000	0.0009
37	KEGG_OLFACTORY_TRANSDUCTION	0	362	1.53	0.0000	0.0932
38	SMID_BREAST_CANCER_RELAPSE_IN_PLEURA_DN	0	23	1.53	0.0030	0.0906
39	PYEON_CANCER_HEAD_AND_NECK_VS_CERVICAL_DN	0	20	1.53	0.0010	0.0879
40	HINATA_NFKB_TARGETS_KERATINOCYTE_DN	0	22	1.53	0.0010	0.0864
41	BIOCARTA_ALK_PATHWAY	0	37	1.53	0.0000	0.0885
42	CHARAFE_BREAST_CANCER_BASAL_VS_MESENCHYMAL_UP	0	114	1.53	0.0000	0.0010
43	FARMER_BREAST_CANCER_CLUSTER_1	0	41	1.52	0.0000	0.0009
44	MIKKELSEN_MCV6_LCP_WITH_H3K27ME3	1	27	1.52	0.0020	0.1006
45	LEE_NAIVE_T_LYMPHOCYTE	0	16	1.52	0.0010	0.1017
46	REACTOME_IMMUNOREGULATORY_INTERACTIONS_BETWEEN_A_LYMPHOID_	0	54	1.52	0.0000	0.0015
47	GU_PDEF_TARGETS_DN	0	37	1.51	0.0000	0.1110
48	RIZ_ERYTHROID_DIFFERENTIATION_6HR	0	40	1.51	0.0000	0.0014
49	SHIN_B_CELL_LYMPHOMA_CLUSTER_2	0	29	1.51	0.0010	0.0012
50	RIZ_ERYTHROID_DIFFERENTIATION_HBZ	0	41	1.51	0.0010	0.0014

Supplemental Table 2. (C) Top 50 GSEA hits for EZH2 ChIP-seq target genes in LAN-1 cells. PRC2 related gene sets are significantly over-represented in the collection of GSEA hits (odds-ratios = 7.9, $P < 0.001$ according to the two-tailed Fisher exact test).

Rank	Gene Set	PRC2 Complex	Size	NES	P	FDR
1	MEISSNER_BRAIN_HCP_WITH_H3K27ME3	1	262	3.74	0.0000	0.0000
2	MIKKELSEN_NPC_HCP_WITH_H3K27ME3	1	333	3.65	0.0000	0.0000
3	MEISSNER_NPC_HCP_WITH_H3K27ME3	1	79	3.57	0.0000	0.0000
4	MEISSNER_NPC_HCP_WITH_H3K4ME2_AND_H3K27ME3	1	338	3.51	0.0000	0.0000
5	MIKKELSEN_MCV6_HCP_WITH_H3K27ME3	1	419	3.44	0.0000	0.0000
6	MIKKELSEN_IPS_WITH_HCP_H3K27ME3	1	100	3.43	0.0000	0.0000
7	BENPORATH_PRC2_TARGETS	1	617	3.36	0.0000	0.0000
8	MIKKELSEN_MEF_HCP_WITH_H3K27ME3	1	568	3.25	0.0000	0.0000
9	MARTENS_TRETINOIN_RESPONSE_UP	0	804	3.01	0.0000	0.0000
10	BENPORATH_SUZ12_TARGETS	1	987	2.99	0.0000	0.0000
11	SCHLESINGER_METHYLATED_DE_NOVO_IN_CANCER	0	86	2.83	0.0000	0.0000
12	MIKKELSEN_NPC_HCP_WITH_H3K4ME3_AND_H3K27ME3	1	204	2.78	0.0000	0.0000
13	LI_WILMS_TUMOR	0	26	2.77	0.0000	0.0000
14	REACTOME_REGULATION_OF_BETA_CELL_DEVELOPMENT	0	30	2.57	0.0000	0.0000
15	KEGG_HEDGEHOG_SIGNALING_PATHWAY	0	56	2.55	0.0000	0.0001
16	MEISSNER_NPC_HCP_WITH_H3K4ME3_AND_H3K27ME3	1	139	2.52	0.0000	0.0001
17	NIKOLSKY_BREAST_CANCER_5P15_AMPLICON	0	26	2.51	0.0000	0.0000
18	NIKOLSKY_BREAST_CANCER_16P13_AMPLICON	0	114	2.46	0.0000	0.0000
19	REACTOME_CLASS_B_2_SECRETIN_FAMILY_RECEPTORS	0	87	2.44	0.0000	0.0013
20	RIZ_ERYTHROID_DIFFERENTIATION_6HR	0	40	2.42	0.0000	0.0000
21	RIZ_ERYTHROID_DIFFERENTIATION_APOBEC2	0	24	2.41	0.0000	0.0000
22	WINNEPENNINCKX_MELANOMA_METASTASIS_DN	0	41	2.40	0.0000	0.0016
23	MEISSNER_NPC_HCP_WITH_H3K4ME2	1	476	2.39	0.0000	0.0018
24	RIZ_ERYTHROID_DIFFERENTIATION_12HR	0	42	2.38	0.0000	0.0000
25	MEISSNER_BRAIN_HCP_WITH_H3K4ME2_AND_H3K27ME3	1	56	2.37	0.0000	0.0020
26	FUKUSHIMA_TNFSF11_TARGETS	0	15	2.36	0.0000	0.0021
27	KEGG_BASAL_CELL_CARCINOMA	0	55	2.31	0.0000	0.0038
28	WANG_THOC1_TARGETS_DN	0	19	2.31	0.0000	0.0000
29	REACTOME_POTASSIUM_CHANNELS	0	97	2.30	0.0000	0.0046
30	KONDO_PROSTATE_CANCER_HCP_WITH_H3K27ME3	1	95	2.29	0.0000	0.0047
31	THEODOROU_MAMMARY_TUMORIGENESIS	0	28	2.28	0.0000	0.0000
32	RORIE_TARGETS_OF_EWSR1_FLI1_FUSION_UP	0	27	2.28	0.0011	0.0050
33	CAMPS_COLON_CANCER_COPY_NUMBER_UP	0	86	2.28	0.0000	0.0049
34	PARK_TRETINOIN_RESPONSE_AND_PML_RARA_FUSION	0	29	2.28	0.0000	0.0048
35	LEIN_CEREBELLUM_MARKERS	0	80	2.28	0.0000	0.0046
36	MCGARVEY_SILENCED_BY_METHYLATION_IN_COLON_CANCER	0	41	2.27	0.0000	0.0048
37	HANN_RESISTANCE_TO_BCL2_INHIBITOR_UP	0	35	2.26	0.0000	0.0051
38	HOQUE_METHYLATED_IN_CANCER	1	56	2.25	0.0000	0.0000
39	MIKKELSEN_ES_ICP_WITH_H3K27ME3	1	39	2.24	0.0000	0.0000
40	MATZUK_IMPLANTATION_AND_UTERINE	0	22	2.24	0.0011	0.0058
41	MEISSNER_NPC_HCP_WITH_H3_UNMETHYLATED	1	506	2.24	0.0000	0.0058
42	KEGG_MATURITY_ONSET_DIABETES_OF_THE_YOUNG	0	25	2.23	0.0000	0.0063
43	RIZ_ERYTHROID_DIFFERENTIATION_HBZ	0	41	2.23	0.0000	0.0001
44	LOPES_METHYLATED_IN_COLON_CANCER_UP	0	27	2.22	0.0000	0.0067
45	CERIBELLI_PROMOTERS_INACTIVE_AND_BOUND_BY_NFY	0	33	2.18	0.0000	0.0001
46	REACTOME_VOLTAGE_GATED_POTASSIUM_CHANNELS	0	43	2.15	0.0000	0.0148
47	BEGUM_TARGETS_OF_PAX3_FOXO1_FUSION_DN	0	44	2.15	0.0000	0.0002
48	HALMOS_CEBPA_TARGETS_DN	0	44	2.14	0.0000	0.0161
49	VALK_AML_WITH_FLT3_ITD	0	39	2.14	0.0000	0.0002
50	NIKOLSKY_BREAST_CANCER_20Q12_Q13_AMPLICON	0	136	2.14	0.0000	0.0003

Supplemental Table 2. (D) Top 50 GSEA hits for H3K27me3 ChIP-seq target genes in LAN-1 cells. PRC2 related gene sets are significantly over-represented in the collection of GSEA hits (odds-ratios = 9.5, $P < 0.001$ according to the two-tailed Fisher exact test).

Rank	Gene Set	PRC2 Complex	Size	NES	P	FDR
1	MEISSNER_NPC_HCP_WITH_H3K27ME3	1	79	2.03	0.0000	0.0000
2	MEISSNER_BRAIN_HCP_WITH_H3K27ME3	1	262	1.99	0.0000	0.0000
3	MIKKELSEN_NPC_HCP_WITH_H3K27ME3	1	333	1.92	0.0000	0.0003
4	MIKKELSEN_IPS_WITH_HCP_H3K27ME3	1	100	1.88	0.0000	0.0004
5	NIKOLSKY_BREAST_CANCER_5P15_AMPLICON	0	26	1.87	0.0000	0.0000
6	LI_WILMS_TUMOR	0	26	1.85	0.0000	0.0011
7	MEISSNER_NPC_HCP_WITH_H3K4ME2_AND_H3K27ME3	1	338	1.85	0.0000	0.0009
8	BENPORATH_PRC2_TARGETS	1	617	1.82	0.0000	0.0000
9	KEGG_MATURITY_ONSET_DIABETES_OF_THE_YOUNG	0	25	1.80	0.0000	0.0035
10	MIKKELSEN_MCV6_HCP_WITH_H3K27ME3	1	419	1.80	0.0000	0.0039
11	SCHLESINGER_METHYLATED_DE_NOVO_IN_CANCER	0	86	1.78	0.0000	0.0000
12	MIKKELSEN_MEF_HCP_WITH_H3K27ME3	1	568	1.78	0.0000	0.0061
13	KEGG_HEDGEHOG_SIGNALING_PATHWAY	0	56	1.78	0.0000	0.0060
14	REACTOME_REGULATION_OF_BETA_CELL_DEVELOPMENT	0	30	1.77	0.0000	0.0000
15	RORIE_TARGETS_OF_EWSR1_FLI1_FUSION_UP	0	27	1.77	0.0000	0.0000
16	CERIBELLI_PROMOTERS_INACTIVE_AND_BOUND_BY_NFY	0	33	1.74	0.0000	0.0163
17	LOPES_METHYLATED_IN_COLON_CANCER_UP	0	27	1.74	0.0000	0.0001
18	MARTENS_TRETINOIN_RESPONSE_UP	0	804	1.72	0.0000	0.0261
19	BEGUM_TARGETS_OF_PAX3_FOXO1_FUSION_DN	0	44	1.72	0.0000	0.0002
20	BENPORATH_SUZ12_TARGETS	1	987	1.71	0.0000	0.0002
21	FUKUSHIMA_TNFSF11_TARGETS	0	15	1.70	0.0011	0.0420
22	WATANABE_COLON_CANCER_MSI_VS_MSS_UP	0	26	1.70	0.0000	0.0003
23	ZHENG_RESPONSE_TO_ARSENITE_UP	0	18	1.69	0.0000	0.0002
24	THEODOROU_MAMMARY_TUMORIGENESIS	0	28	1.69	0.0000	0.0003
25	RIZ_ERYTHROID_DIFFERENTIATION_APOBEC2	0	24	1.69	0.0000	0.0004
26	SHIN_B_CELL_LYMPHOMA_CLUSTER_5	0	16	1.69	0.0000	0.0003
27	VALK_AML_WITH_FLT3_ITD	0	39	1.69	0.0000	0.0452
28	REACTOME_NA_CL_DEPENDENT_NEUROTRANSMITTER_TRANSPORTERS	0	17	1.69	0.0010	0.0005
29	KEGG_BASAL_CELL_CARCINOMA	0	55	1.68	0.0000	0.0513
30	MAHADEVAN_IMATINIB_RESISTANCE_DN	0	20	1.68	0.0020	0.0005
31	MATZUK_IMPLANTATION_AND_UTERINE	0	22	1.68	0.0000	0.0536
32	VANDESLUIS_COMMD1_TARGETS_GROUP_4_DN	0	15	1.68	0.0011	0.0526
33	WANG_THOC1_TARGETS_DN	0	19	1.67	0.0000	0.0540
34	RIZ_ERYTHROID_DIFFERENTIATION_12HR	0	42	1.67	0.0000	0.0007
35	REACTOME_ACTIVATED_POINT_MUTANTS_OF_FGFR2	0	16	1.66	0.0021	0.0669
36	LOPES_METHYLATED_IN_COLON_CANCER_DN	0	28	1.66	0.0000	0.0005
37	HALMOS_CEBPA_TARGETS_DN	0	44	1.66	0.0000	0.0005
38	RIZ_ERYTHROID_DIFFERENTIATION_HBZ	0	41	1.66	0.0000	0.0008
39	REACTOME_CLASS_B_2_SECRETIN_FAMILY_RECEPTORS	0	87	1.65	0.0000	0.0010
40	MEISSNER_BRAIN_HCP_WITH_H3K4ME2_AND_H3K27ME3	1	56	1.65	0.0000	0.0813
41	MIKKELSEN_NPC_HCP_WITH_H3K4ME3_AND_H3K27ME3	1	204	1.65	0.0000	0.0792
42	LU_TUMOR_ANGIOGENESIS_UP	0	25	1.65	0.0020	0.0776
43	REACTOME_REGULATION_OF_GENE_EXPRESSION_IN_BETA_CELLS	0	20	1.64	0.0021	0.0012
44	KORKOLA_CORRELATED_WITH_POU5F1	0	34	1.64	0.0010	0.0894
45	ALONSO_METASTASIS_DN	0	23	1.63	0.0020	0.0928
46	PARK_TRETINOIN_RESPONSE_AND_PML_RARA_FUSION	0	29	1.63	0.0000	0.0924
47	HANN_RESISTANCE_TO_BCL2_INHIBITOR_UP	0	35	1.63	0.0000	0.0008
48	MIKKELSEN_MCV6_LCP_WITH_H3K27ME3	1	27	1.62	0.0010	0.1012
49	FIGUEROA_AML_METHYLATION_CLUSTER_5_DN	0	47	1.62	0.0000	0.1020
50	RIZ_ERYTHROID_DIFFERENTIATION_6HR	0	40	1.62	0.0000	0.0016

Supplemental Table 3. Custom neuroblastoma PRC2 signatures consisting of the top 300 EZH2 and H3K27me3 ChIP-seq target genes in Kelly and LAN-1 cell lines. Shown in table are the EZH2 and H3K27me3 promoter relative binding signal in Kelly and LAN-1 cells. Genes were ranked in decreasing order based on the promoter binding signal in the highlighted ranking score column. The high level for the relative occupancy signal in the promoter regions was estimated based on the cut-off 1.5 for the ratio of the AUC ChIP-seq signal of the mark vs the AUC signal of the input.

(A) Custom neuroblastoma PRC2 signature consisting of the top 300 EZH2 ChIP-seq target genes in Kelly cells.

#	Gene	Kelly rel AUC EZH2 (ranking score)	Kelly rel AUC H3K27me3	LAN-1 rel AUC EZH2	LAN-1 rel AUC H3K27me3
1	<i>NFATC1</i>	32.51	23.21	8.52	11.65
2	<i>PAX2</i>	18.04	13.13	9.27	11.36
3	<i>PDGFA</i>	17.82	12.54	6.60	9.41
4	<i>LBX1</i>	17.76	10.41	5.29	8.45
5	<i>NKX1-1</i>	17.14	8.88	2.30	3.80
6	<i>SOX8</i>	16.45	12.54	5.57	11.05
7	<i>PRDM12</i>	15.81	8.51	5.55	6.50
8	<i>SIGIRR</i>	13.33	18.72	1.50	2.04
9	<i>LHX5</i>	12.77	10.54	5.23	7.65
10	<i>ZIC1</i>	12.60	10.24	0.88	0.39
11	<i>FOXL2</i>	12.53	10.62	4.23	6.50
12	<i>EN2</i>	12.41	10.34	6.53	9.53
13	<i>SORCS3</i>	12.35	11.54	3.49	6.60
14	<i>HOXC12</i>	12.26	10.61	4.52	7.43
15	<i>LMX1B</i>	12.23	10.09	6.93	9.23
16	<i>FOXF1</i>	12.13	7.53	5.56	8.73
17	<i>GATA4</i>	12.04	10.44	3.35	5.17
18	<i>FOXF2</i>	12.04	7.84	4.29	6.86
19	<i>HES4</i>	11.41	10.22	1.18	0.49
20	<i>IRX1</i>	11.30	7.80	3.52	7.59
21	<i>ZIC2</i>	11.22	7.69	6.31	9.76
22	<i>TBX15</i>	10.94	8.77	3.14	6.40
23	<i>EVX1</i>	10.74	9.50	3.28	7.78
24	<i>OLIG2</i>	10.30	9.01	4.33	8.13
25	<i>GBX2</i>	10.23	9.71	1.19	1.74
26	<i>IRX2</i>	10.20	7.85	3.54	6.33
27	<i>HOXB8</i>	10.05	7.42	8.66	12.41
28	<i>BARX1</i>	10.02	6.81	2.71	5.38
29	<i>EMX1</i>	9.97	8.39	5.55	8.53
30	<i>NKX2-2</i>	9.70	7.01	5.16	9.46
31	<i>GATA6</i>	9.63	7.77	4.69	8.26
32	<i>MN1</i>	9.51	7.56	6.66	12.22
33	<i>TFAP2C</i>	9.41	7.83	2.67	5.29
34	<i>OTX2</i>	9.36	8.40	2.81	5.81
35	<i>LHX2</i>	9.36	8.05	3.08	5.21
36	<i>EGR3</i>	9.29	8.00	2.30	3.47
37	<i>FLT4</i>	9.28	12.36	2.97	7.02
38	<i>ATHL1</i>	9.17	12.57	1.56	1.63
39	<i>SOX21</i>	9.15	9.13	2.51	5.47
40	<i>HOXB7</i>	8.92	7.41	7.55	12.16
41	<i>NKX2-5</i>	8.84	7.82	3.05	5.01
42	<i>SOX3</i>	8.83	6.40	3.18	5.20
43	<i>SIM2</i>	8.78	6.87	3.54	5.86
44	<i>PRDM16</i>	8.72	7.89	8.90	15.23
45	<i>ALX4</i>	8.59	8.11	3.48	7.03
46	<i>VENTX</i>	8.56	8.51	5.50	11.58
47	<i>OVOL1</i>	8.56	7.78	2.62	6.07
48	<i>ZIC5</i>	8.54	7.21	3.91	7.16
49	<i>PAX7</i>	8.40	7.11	5.88	8.93
50	<i>BNC1</i>	8.38	7.42	2.35	3.49
51	<i>TNFRSF18</i>	8.31	10.59	2.88	7.59
52	<i>GATA5</i>	8.28	7.51	4.87	9.10
53	<i>SALL3</i>	8.15	8.20	1.79	4.52
54	<i>NKX2-3</i>	8.14	7.07	5.10	9.02
55	<i>SOX14</i>	8.04	8.74	2.79	5.51
56	<i>FOXB1</i>	8.04	8.62	2.70	6.34
57	<i>HOXA6</i>	8.04	7.37	3.08	6.71
58	<i>HOXA5</i>	8.04	7.37	3.08	6.71
59	<i>HOXA7</i>	8.04	7.37	3.08	6.71
60	<i>PRDM13</i>	7.89	8.12	2.00	3.95
61	<i>ZIC4</i>	7.82	7.84	0.89	0.58
62	<i>HOXA11</i>	7.81	8.34	4.68	9.05
63	<i>PPL</i>	7.71	9.56	2.13	5.44
64	<i>DMRTA2</i>	7.70	7.32	1.51	3.30
65	<i>GCGR</i>	7.69	7.45	1.23	3.03
66	<i>KLF2</i>	7.66	8.67	2.82	5.26

#	Gene	Kelly rel AUC EZH2 (ranking score)	Kelly rel AUC H3K27me3	LAN-1 rel AUC EZH2	LAN-1 rel AUC H3K27me3
67	<i>IRX4</i>	7.61	8.30	6.13	10.81
68	<i>NKX2-8</i>	7.59	7.92	3.05	7.71
69	<i>SLC32A1</i>	7.47	9.07	2.24	5.10
70	<i>LHX1</i>	7.46	8.95	5.24	7.60
71	<i>TBX1</i>	7.40	7.56	5.43	9.21
72	<i>UTF1</i>	7.39	8.17	2.56	6.89
73	<i>EBF2</i>	7.34	8.07	4.17	8.26
74	<i>NOTCH1</i>	7.30	5.72	5.71	11.09
75	<i>GPR123</i>	7.18	8.41	3.10	5.83
76	<i>HOXB9</i>	7.13	7.04	4.66	8.97
77	<i>SHH</i>	7.02	7.95	4.44	7.17
78	<i>INHBB</i>	6.99	7.35	5.49	8.34
79	<i>CBFA2T3</i>	6.95	8.67	4.14	10.05
80	<i>HOXB6</i>	6.94	7.83	4.51	9.53
81	<i>HOXB5</i>	6.94	7.83	4.51	9.53
82	<i>BARX2</i>	6.94	6.93	3.52	5.40
83	<i>LHX6</i>	6.90	7.47	2.69	4.31
84	<i>CACNA1H</i>	6.89	7.06	1.75	2.00
85	<i>FOXC2</i>	6.81	6.05	2.35	5.54
86	<i>FIBCD1</i>	6.78	9.20	5.36	11.43
87	<i>ONECUT1</i>	6.77	7.06	1.84	4.11
88	<i>DMRT3</i>	6.77	7.01	3.36	8.10
89	<i>TPSG1</i>	6.75	6.30	1.86	1.40
90	<i>PRDM14</i>	6.72	7.58	1.70	1.96
91	<i>SLC24A4</i>	6.64	9.46	2.18	5.48
92	<i>RREB1</i>	6.63	5.92	2.33	4.45
93	<i>HOXB4</i>	6.61	7.13	2.95	5.82
94	<i>THPO</i>	6.57	8.06	2.02	2.76
95	<i>TTLL10</i>	6.57	6.47	2.62	5.85
96	<i>FOXA1</i>	6.56	6.96	1.37	2.21
97	<i>EFNA2</i>	6.51	8.34	1.27	1.50
98	<i>FOXP2</i>	6.49	6.79	2.95	4.56
99	<i>NEUROD2</i>	6.45	6.48	6.29	9.43
100	<i>CXCL16</i>	6.44	10.12	3.15	7.32
101	<i>TLX1</i>	6.43	6.76	3.29	6.68
102	<i>MSX1</i>	6.42	6.87	2.69	4.67
103	<i>COMP</i>	6.40	7.23	3.43	5.72
104	<i>CHRD</i>	6.37	7.82	2.22	2.94
105	<i>ESPN</i>	6.37	7.44	2.99	6.65
106	<i>GAD2</i>	6.23	7.11	2.79	6.86
107	<i>PAX3</i>	6.23	6.80	3.34	6.17
108	<i>AJAP1</i>	6.22	8.11	3.91	8.24
109	<i>LHX4</i>	6.22	5.80	2.08	3.66
110	<i>ZMYND15</i>	6.18	9.62	3.15	7.36
111	<i>GAD1</i>	6.18	7.14	2.02	5.26
112	<i>LMX1A</i>	6.17	5.86	2.23	4.89
113	<i>FGFRL1</i>	6.15	8.12	1.69	2.00
114	<i>NR2E1</i>	6.13	6.13	2.45	5.08
115	<i>CDX2</i>	6.12	5.20	11.43	19.24
116	<i>C1ORF94</i>	6.11	9.61	2.77	5.73
117	<i>MUC5B</i>	6.04	8.93	3.85	9.44
118	<i>OVOL2</i>	6.03	6.56	2.42	5.27
119	<i>DRD4</i>	6.02	6.10	1.38	0.59
120	<i>OTP</i>	6.02	6.02	2.48	5.32
121	<i>EN1</i>	5.94	5.66	3.19	6.39
122	<i>HES2</i>	5.92	6.57	3.95	8.22
123	<i>RELN</i>	5.90	9.95	1.72	3.82
124	<i>PRKCZ</i>	5.89	7.47	3.29	7.65
125	<i>NPTX1</i>	5.89	6.01	6.66	10.93
126	<i>KLHDC7B</i>	5.88	6.71	1.71	2.95
127	<i>SLC30A3</i>	5.84	7.27	1.25	0.63
128	<i>POU4F3</i>	5.84	7.03	2.42	4.85
129	<i>COL12A1</i>	5.81	7.17	0.81	1.07
130	<i>GSC</i>	5.81	6.41	2.56	4.98
131	<i>ICAM5</i>	5.80	8.51	1.33	0.54
132	<i>HBB</i>	5.79	2.15	2.06	1.55
133	<i>NTN1</i>	5.78	5.89	2.09	5.38
134	<i>DGKQ</i>	5.77	7.79	1.26	0.74
135	<i>GPC4</i>	5.77	7.36	2.91	6.04
136	<i>TFAP2A</i>	5.75	5.83	3.45	6.21
137	<i>FZD10</i>	5.72	6.68	2.64	6.25
138	<i>HOXC13</i>	5.67	7.55	1.93	5.08
139	<i>HTRA1</i>	5.67	7.30	2.40	4.04
140	<i>HOXC11</i>	5.67	5.50	3.26	5.74
141	<i>PAX9</i>	5.67	5.27	4.15	6.77
142	<i>ATP2A3</i>	5.66	7.38	2.13	5.91

#	Gene	Kelly rel AUC EZH2 (ranking score)	Kelly rel AUC H3K27me3	LAN-1 rel AUC EZH2	LAN-1 rel AUC H3K27me3
143	<i>OLIG3</i>	5.62	5.29	2.88	7.35
144	<i>RASSF7</i>	5.55	6.14	2.50	4.68
145	<i>DSP</i>	5.53	5.78	3.27	5.91
146	<i>ITGB2</i>	5.47	8.13	3.50	8.17
147	<i>GABRD</i>	5.45	6.21	4.40	10.95
148	<i>DLX4</i>	5.43	6.36	2.61	6.21
149	<i>EMX2OS</i>	5.41	5.62	3.05	5.72
150	<i>GRWD1</i>	5.41	3.46	0.76	0.75
151	<i>SIX1</i>	5.40	7.25	2.66	4.73
152	<i>HOXA10</i>	5.39	6.64	2.80	6.33
153	<i>BARHL1</i>	5.38	5.73	5.29	8.60
154	<i>ATAD3C</i>	5.37	7.68	1.28	0.98
155	<i>WNT7B</i>	5.34	6.44	4.23	7.47
156	<i>HS3ST6</i>	5.33	6.64	2.23	4.82
157	<i>TPSD1</i>	5.31	6.81	1.66	1.57
158	<i>ADAM3A</i>	5.27	3.14	0.53	0.48
159	<i>HMX2</i>	5.22	6.65	3.79	6.95
160	<i>LHX3</i>	5.22	3.61	3.77	4.98
161	<i>OLIG1</i>	5.21	8.98	1.96	4.63
162	<i>FOXQ1</i>	5.21	6.59	4.25	9.51
163	<i>NFIX</i>	5.20	5.28	2.65	4.57
164	<i>FOXD2</i>	5.20	4.79	2.40	4.90
165	<i>MMP25</i>	5.18	5.95	2.74	4.96
166	<i>NOG</i>	5.15	6.75	2.74	6.11
167	<i>OSR1</i>	5.14	6.57	1.85	4.65
168	<i>FGF3</i>	5.14	4.72	3.92	7.28
169	<i>CSMD2</i>	5.11	8.14	2.74	5.74
170	<i>TCF21</i>	5.10	9.71	1.84	4.65
171	<i>FOXL1</i>	5.10	7.18	1.88	5.11
172	<i>NEUROG3</i>	5.08	6.19	3.22	6.91
173	<i>SIX6</i>	5.08	4.86	2.53	4.39
174	<i>NRK</i>	5.04	7.20	1.04	1.75
175	<i>FOXE1</i>	5.03	6.18	1.13	2.84
176	<i>ACSS1</i>	5.01	6.90	1.88	3.88
177	<i>SIM1</i>	5.01	5.82	1.34	3.10
178	<i>SLC4A11</i>	5.01	5.62	1.97	3.05
179	<i>PTRF</i>	5.00	6.52	3.08	5.68
180	<i>PPAP2C</i>	4.98	7.77	1.91	4.34
181	<i>WTIP</i>	4.98	5.11	1.29	0.55
182	<i>MAF</i>	4.97	6.50	2.05	5.02
183	<i>HOXA13</i>	4.96	5.46	2.15	5.17
184	<i>ITGB4</i>	4.94	8.19	2.05	5.52
185	<i>CRLF1</i>	4.93	5.45	2.29	4.78
186	<i>SP8</i>	4.90	5.50	6.33	11.39
187	<i>GUCY2D</i>	4.88	5.64	1.45	3.94
188	<i>PRDM6</i>	4.87	6.81	2.25	4.10
189	<i>T</i>	4.85	5.25	1.93	4.51
190	<i>FEZF2</i>	4.82	5.55	3.51	6.40
191	<i>FAM110C</i>	4.81	7.04	1.90	3.44
192	<i>IGF2BP2</i>	4.81	6.92	1.67	3.60
193	<i>SCN4B</i>	4.78	8.17	1.95	5.22
194	<i>GRIN3B</i>	4.78	6.07	1.61	3.06
195	<i>SMARCA2</i>	4.78	5.41	1.76	2.20
196	<i>ALDH1A2</i>	4.77	8.75	1.29	1.97
197	<i>IHH</i>	4.76	5.31	1.49	2.76
198	<i>KCNA1</i>	4.76	4.64	2.44	4.45
199	<i>FOXD3</i>	4.75	5.43	4.14	7.56
200	<i>SOX17</i>	4.74	5.11	1.66	4.03
201	<i>ICOSLG</i>	4.74	4.56	3.57	8.03
202	<i>TWIST2</i>	4.73	4.78	1.66	3.88
203	<i>FAM83H</i>	4.72	6.27	2.36	3.78
204	<i>SCO2</i>	4.71	4.93	1.32	1.30
205	<i>CYP26A1</i>	4.68	5.70	2.77	6.30
206	<i>HOXA2</i>	4.68	4.71	3.84	7.46
207	<i>LONRF3</i>	4.63	5.97	1.59	3.04
208	<i>NRN1</i>	4.63	5.48	1.50	3.30
209	<i>KRTAP10-12</i>	4.58	7.05	2.06	4.25
210	<i>C21ORF90</i>	4.58	7.05	2.06	4.25
211	<i>KRTAP10-11</i>	4.58	7.05	2.06	4.25
212	<i>MUC2</i>	4.58	6.12	2.27	6.64
213	<i>WNT1</i>	4.54	5.06	4.12	8.96
214	<i>BMP4</i>	4.53	5.65	1.35	2.33
215	<i>KISS1R</i>	4.52	4.93	2.14	3.89
216	<i>RIPK4</i>	4.51	7.77	2.22	5.85
217	<i>SLITRK2</i>	4.48	7.13	2.35	7.34
218	<i>HEY2</i>	4.48	5.81	1.68	3.64

#	Gene	Kelly rel AUC EZH2 (ranking score)	Kelly rel AUC H3K27me3	LAN-1 rel AUC EZH2	LAN-1 rel AUC H3K27me3
219	SLC1A1	4.47	7.16	2.12	4.99
220	BMP6	4.46	5.44	2.88	5.72
221	ATP8A2	4.45	5.99	3.18	8.23
222	LOC401463	4.45	5.58	1.01	2.50
223	HOXB3	4.42	5.69	2.82	6.31
224	HOXB2	4.42	5.69	2.82	6.31
225	TFAP2E	4.42	5.22	1.19	0.58
226	SSTR5	4.39	3.92	1.69	2.07
227	RAX	4.38	7.16	0.70	0.67
228	IRF4	4.36	5.31	1.89	4.79
229	ACHE	4.35	4.17	2.55	3.26
230	FOXE3	4.34	5.63	1.31	3.57
231	TP73	4.32	3.33	0.82	0.41
232	MATK	4.31	5.59	1.43	3.75
233	FAM43B	4.30	5.90	1.22	0.40
234	PFKL	4.30	5.54	1.61	2.45
235	PAX1	4.29	5.65	3.62	7.48
236	SCT	4.29	5.42	1.33	0.68
237	HOXC10	4.28	5.17	5.37	10.33
238	PAPLN	4.26	6.54	2.05	2.32
239	GRTP1	4.26	6.41	1.05	1.07
240	NPR3	4.26	5.92	0.93	1.06
241	TBX5	4.26	4.34	3.10	6.09
242	BACE2	4.22	7.57	2.44	6.38
243	PRRX1	4.22	6.31	2.41	4.27
244	DLX2	4.22	5.65	1.71	2.64
245	MT1G	4.21	6.39	1.97	5.74
246	GADD45B	4.21	5.96	1.07	1.37
247	ICAM4	4.20	5.62	1.13	0.57
248	GJB2	4.20	5.41	1.83	4.53
249	PHLDA2	4.19	3.95	2.52	5.94
250	PCSK6	4.18	5.30	1.19	1.87
251	FBLN5	4.17	7.83	1.55	2.75
252	THBD	4.16	6.61	1.35	2.91
253	PFKFB3	4.16	5.83	1.59	0.87
254	NKD2	4.16	4.38	2.73	6.11
255	MYO5B	4.14	7.40	3.30	7.61
256	MAD2L2	4.14	6.19	1.69	2.27
257	GPR50	4.12	6.02	1.03	1.29
258	RGL3	4.12	5.83	1.67	2.51
259	GRIN2C	4.12	4.10	2.09	3.50
260	CACNG2	4.11	5.84	1.57	4.34
261	PIK3CD	4.10	5.87	1.51	3.01
262	ZNF92	4.10	3.63	2.15	2.66
263	BCL2L11	4.10	3.20	1.33	1.29
264	MRGPRX3	4.08	8.67	1.09	1.53
265	NR5A1	4.08	3.31	2.11	3.69
266	GLI3	4.06	5.52	3.02	7.17
267	WNT7A	4.05	4.43	2.51	5.13
268	FAM20A	4.04	6.52	1.17	2.38
269	SLC16A6	4.04	6.52	1.17	2.38
270	WIP1	4.04	6.52	1.17	2.38
271	NTSR1	4.03	5.10	1.89	4.55
272	ROBO3	4.01	7.66	1.46	5.18
273	CDC42EP5	4.01	6.61	2.36	4.96
274	MT1M	4.01	5.43	2.69	6.93
275	HMHA1	4.01	5.16	2.80	5.96
276	SNAPC2	4.01	3.32	1.59	0.87
277	PDGFRA	4.00	4.27	1.07	1.31
278	SLC22A18AS	3.98	3.26	2.89	6.41
279	HOXA1	3.97	5.21	2.57	5.60
280	HOXB13	3.97	5.13	4.07	8.80
281	MUC6	3.96	6.09	2.84	5.90
282	HS3ST3B1	3.96	4.61	1.93	3.25
283	MGC12916	3.96	4.61	1.93	3.25
284	HTR2C	3.95	7.93	1.58	2.74
285	DUSP8	3.94	6.54	3.76	4.88
286	ADRA1A	3.94	6.19	1.02	1.36
287	PTPRT	3.93	4.97	2.17	3.99
288	PPP2R2C	3.92	5.93	2.43	5.46
289	NEUROG1	3.92	5.35	0.85	1.30
290	FOSL1	3.91	5.41	2.50	5.35
291	KCNK4	3.91	3.91	2.40	3.58
292	BAD	3.90	3.34	2.40	3.03
293	GF11	3.89	5.38	2.28	4.26
294	SVEP1	3.88	8.02	0.60	0.40

#	Gene	Kelly rel AUC EZH2 (ranking score)	Kelly rel AUC H3K27me3	LAN-1 rel AUC EZH2	LAN-1 rel AUC H3K27me3
295	<i>BAIAP3</i>	3.88	7.16	1.56	2.90
296	<i>DLX3</i>	3.88	5.68	3.13	6.67
297	<i>HBM</i>	3.86	6.74	3.26	8.62
298	<i>CACNA1E</i>	3.86	5.71	1.82	4.82
299	<i>MMEL1</i>	3.84	6.59	2.77	6.20
300	<i>CRIM1</i>	3.83	4.87	1.29	2.58

Supplemental Table 3. (B) Custom neuroblastoma PRC2 signature consisting of the top 300 H3K27me3 ChIP-seq target genes in Kelly cells.

#	Gene	Kelly rel AUC H3K27me3 (ranking score)	Kelly rel AUC EZH2	LAN-1 rel AUC H3K27me3	LAN-1 rel AUC EZH2
1	<i>NFATC1</i>	23.21	32.51	11.65	8.52
2	<i>SIGIRR</i>	18.72	13.33	2.04	1.50
3	<i>PAX2</i>	13.13	18.04	11.36	9.27
4	<i>ATHL1</i>	12.57	9.17	1.63	1.56
5	<i>PDGFA</i>	12.54	17.82	9.41	6.60
6	<i>SOX8</i>	12.54	16.45	11.05	5.57
7	<i>FLT4</i>	12.36	9.28	7.02	2.97
8	<i>SORCS3</i>	11.54	12.35	6.60	3.49
9	<i>FOXL2</i>	10.62	12.53	6.50	4.23
10	<i>HOXC12</i>	10.61	12.26	7.43	4.52
11	<i>TNFRSF18</i>	10.59	8.31	7.59	2.88
12	<i>LHX5</i>	10.54	12.77	7.65	5.23
13	<i>GATA4</i>	10.44	12.04	5.17	3.35
14	<i>LBX1</i>	10.41	17.76	8.45	5.29
15	<i>EN2</i>	10.34	12.41	9.53	6.53
16	<i>ZIC1</i>	10.24	12.60	0.39	0.88
17	<i>HES4</i>	10.22	11.41	0.49	1.18
18	<i>CXCL16</i>	10.12	6.44	7.32	3.15
19	<i>LMX1B</i>	10.09	12.23	9.23	6.93
20	<i>RELN</i>	9.95	5.90	3.82	1.72
21	<i>GBX2</i>	9.71	10.23	1.74	1.19
22	<i>TCF21</i>	9.71	5.10	4.65	1.84
23	<i>ZMYND15</i>	9.62	6.18	7.36	3.15
24	<i>C1ORF94</i>	9.61	6.11	5.73	2.77
25	<i>PPL</i>	9.56	7.71	5.44	2.13
26	<i>EVX1</i>	9.50	10.74	7.78	3.28
27	<i>SLC24A4</i>	9.46	6.64	5.48	2.18
28	<i>FIBCD1</i>	9.20	6.78	11.43	5.36
29	<i>SOX21</i>	9.13	9.15	5.47	2.51
30	<i>SLC32A1</i>	9.07	7.47	5.10	2.24
31	<i>OLIG2</i>	9.01	10.30	8.13	4.33
32	<i>ZFYVE28</i>	9.01	3.56	5.62	2.95
33	<i>OLIG1</i>	8.98	5.21	4.63	1.96
34	<i>LHX1</i>	8.95	7.46	7.60	5.24
35	<i>MUC5B</i>	8.93	6.04	9.44	3.85
36	<i>KLK6</i>	8.93	3.80	4.82	2.37
37	<i>NKX1-1</i>	8.88	17.14	3.80	2.30
38	<i>TBX15</i>	8.77	10.94	6.40	3.14
39	<i>ALDH1A2</i>	8.75	4.77	1.97	1.29
40	<i>SOX14</i>	8.74	8.04	5.51	2.79
41	<i>KLF2</i>	8.67	7.66	5.26	2.82
42	<i>CBFA2T3</i>	8.67	6.95	10.05	4.14
43	<i>MRGPRX3</i>	8.67	4.08	1.53	1.09
44	<i>FOXB1</i>	8.62	8.04	6.34	2.70
45	<i>PRDM12</i>	8.51	15.81	6.50	5.55
46	<i>VENTX</i>	8.51	8.56	11.58	5.50
47	<i>ICAM5</i>	8.51	5.80	0.54	1.33
48	<i>GPR123</i>	8.41	7.18	5.83	3.10
49	<i>OTX2</i>	8.40	9.36	5.81	2.81
50	<i>EMX1</i>	8.39	9.97	8.53	5.55
51	<i>HOXA11</i>	8.34	7.81	9.05	4.68
52	<i>EFNA2</i>	8.34	6.51	1.50	1.27
53	<i>IRX4</i>	8.30	7.61	10.81	6.13
54	<i>SALL3</i>	8.20	8.15	4.52	1.79
55	<i>ITGB4</i>	8.19	4.94	5.52	2.05
56	<i>UTF1</i>	8.17	7.39	6.89	2.56
57	<i>SCN4B</i>	8.17	4.78	5.22	1.95
58	<i>CSMD2</i>	8.14	5.11	5.74	2.74
59	<i>ITGB2</i>	8.13	5.47	8.17	3.50
60	<i>PRDM13</i>	8.12	7.89	3.95	2.00
61	<i>FGFRL1</i>	8.12	6.15	2.00	1.69
62	<i>ALX4</i>	8.11	8.59	7.03	3.48
63	<i>AJAP1</i>	8.11	6.22	8.24	3.91
64	<i>EBF2</i>	8.07	7.34	8.26	4.17
65	<i>LOC284379</i>	8.07	2.84	5.71	1.53
66	<i>THPO</i>	8.06	6.57	2.76	2.02
67	<i>LHX2</i>	8.05	9.36	5.21	3.08
68	<i>SVEP1</i>	8.02	3.88	0.40	0.60
69	<i>EGR3</i>	8.00	9.29	3.47	2.30
70	<i>SHH</i>	7.95	7.02	7.17	4.44
71	<i>HTR2C</i>	7.93	3.95	2.74	1.58
72	<i>NKX2-8</i>	7.92	7.59	7.71	3.05
73	<i>PRDM16</i>	7.89	8.72	15.23	8.90

#	Gene	Kelly rel AUC H3K27me3 (ranking score)	Kelly rel AUC EZH2	LAN-1 rel AUC H3K27me3	LAN-1 rel AUC EZH2
74	<i>IRX2</i>	7.85	10.20	6.33	3.54
75	<i>FOXF2</i>	7.84	12.04	6.86	4.29
76	<i>ZIC4</i>	7.84	7.82	0.58	0.89
77	<i>TFAP2C</i>	7.83	9.41	5.29	2.67
78	<i>HOXB6</i>	7.83	6.94	9.53	4.51
79	<i>HOXB5</i>	7.83	6.94	9.53	4.51
80	<i>FBLN5</i>	7.83	4.17	2.75	1.55
81	<i>NKX2-5</i>	7.82	8.84	5.01	3.05
82	<i>CHRD</i>	7.82	6.37	2.94	2.22
83	<i>IRX1</i>	7.80	11.30	7.59	3.52
84	<i>DGKQ</i>	7.79	5.77	0.74	1.26
85	<i>OVOL1</i>	7.78	8.56	6.07	2.62
86	<i>GATA6</i>	7.77	9.63	8.26	4.69
87	<i>PPAP2C</i>	7.77	4.98	4.34	1.91
88	<i>RIPK4</i>	7.77	4.51	5.85	2.22
89	<i>ZIC2</i>	7.69	11.22	9.76	6.31
90	<i>ATAD3C</i>	7.68	5.37	0.98	1.28
91	<i>ROBO3</i>	7.66	4.01	5.18	1.46
92	<i>PRDM14</i>	7.58	6.72	1.96	1.70
93	<i>BACE2</i>	7.57	4.22	6.38	2.44
94	<i>MN1</i>	7.56	9.51	12.22	6.66
95	<i>TBX1</i>	7.56	7.40	9.21	5.43
96	<i>HOXC13</i>	7.55	5.67	5.08	1.93
97	<i>FOXF1</i>	7.53	12.13	8.73	5.56
98	<i>GATA5</i>	7.51	8.28	9.10	4.87
99	<i>LHX6</i>	7.47	6.90	4.31	2.69
100	<i>PRKCZ</i>	7.47	5.89	7.65	3.29
101	<i>KRT85</i>	7.46	3.50	3.01	1.36
102	<i>GCGR</i>	7.45	7.69	3.03	1.23
103	<i>ESPN</i>	7.44	6.37	6.65	2.99
104	<i>HOXB8</i>	7.42	10.05	12.41	8.66
105	<i>BNC1</i>	7.42	8.38	3.49	2.35
106	<i>HOXB7</i>	7.41	8.92	12.16	7.55
107	<i>MYO5B</i>	7.40	4.14	7.61	3.30
108	<i>ATP2A3</i>	7.38	5.66	5.91	2.13
109	<i>HOXA6</i>	7.37	8.04	6.71	3.08
110	<i>HOXA5</i>	7.37	8.04	6.71	3.08
111	<i>HOXA7</i>	7.37	8.04	6.71	3.08
112	<i>GPC4</i>	7.36	5.77	6.04	2.91
113	<i>INHBB</i>	7.35	6.99	8.34	5.49
114	<i>DMRTA2</i>	7.32	7.70	3.30	1.51
115	<i>HTRA1</i>	7.30	5.67	4.04	2.40
116	<i>KIRREL</i>	7.30	3.03	2.98	1.41
117	<i>SLC30A3</i>	7.27	5.84	0.63	1.25
118	<i>SIX1</i>	7.25	5.40	4.73	2.66
119	<i>COMP</i>	7.23	6.40	5.72	3.43
120	<i>ZIC5</i>	7.21	8.54	7.16	3.91
121	<i>NRK</i>	7.20	5.04	1.75	1.04
122	<i>FOXL1</i>	7.18	5.10	5.11	1.88
123	<i>COL12A1</i>	7.17	5.81	1.07	0.81
124	<i>SLC1A1</i>	7.16	4.47	4.99	2.12
125	<i>RAX</i>	7.16	4.38	0.67	0.70
126	<i>BAIAP3</i>	7.16	3.88	2.90	1.56
127	<i>GAD1</i>	7.14	6.18	5.26	2.02
128	<i>HOXB4</i>	7.13	6.61	5.82	2.95
129	<i>SLITRK2</i>	7.13	4.48	7.34	2.35
130	<i>PAX7</i>	7.11	8.40	8.93	5.88
131	<i>GAD2</i>	7.11	6.23	6.86	2.79
132	<i>PVALB</i>	7.10	3.03	5.90	2.48
133	<i>NKX2-3</i>	7.07	8.14	9.02	5.10
134	<i>CACNA1H</i>	7.06	6.89	2.00	1.75
135	<i>ONECUT1</i>	7.06	6.77	4.11	1.84
136	<i>KRTAP10-12</i>	7.05	4.58	4.25	2.06
137	<i>C21ORF90</i>	7.05	4.58	4.25	2.06
138	<i>KRTAP10-11</i>	7.05	4.58	4.25	2.06
139	<i>PDPN</i>	7.05	3.12	4.31	1.60
140	<i>SLC6A20</i>	7.05	2.87	2.27	1.47
141	<i>HOXB9</i>	7.04	7.13	8.97	4.66
142	<i>FAM110C</i>	7.04	4.81	3.44	1.90
143	<i>POU4F3</i>	7.03	5.84	4.85	2.42
144	<i>NKX2-2</i>	7.01	9.70	9.46	5.16
145	<i>DMRT3</i>	7.01	6.77	8.10	3.36
146	<i>NFE2L3</i>	7.01	3.56	1.06	1.24
147	<i>CD1D</i>	6.99	2.90	5.29	2.24
148	<i>IL27</i>	6.99	2.18	1.86	1.41
149	<i>FOXA1</i>	6.96	6.56	2.21	1.37

#	Gene	Kelly rel AUC H3K27me3 (ranking score)	Kelly rel AUC EZH2	LAN-1 rel AUC H3K27me3	LAN-1 rel AUC EZH2
150	<i>BARX2</i>	6.93	6.94	5.40	3.52
151	<i>IGF2BP2</i>	6.92	4.81	3.60	1.67
152	<i>DFNB31</i>	6.92	3.37	2.14	0.94
153	<i>ACSS1</i>	6.90	5.01	3.88	1.88
154	<i>SIM2</i>	6.87	8.78	5.86	3.54
155	<i>MSX1</i>	6.87	6.42	4.67	2.69
156	<i>BARX1</i>	6.81	10.02	5.38	2.71
157	<i>TPSD1</i>	6.81	5.31	1.57	1.66
158	<i>PRDM6</i>	6.81	4.87	4.10	2.25
159	<i>PAX3</i>	6.80	6.23	6.17	3.34
160	<i>FOXP2</i>	6.79	6.49	4.56	2.95
161	<i>TCF15</i>	6.79	3.26	2.39	1.42
162	<i>TLX1</i>	6.76	6.43	6.68	3.29
163	<i>NOG</i>	6.75	5.15	6.11	2.74
164	<i>HBM</i>	6.74	3.86	8.62	3.26
165	<i>XKR4</i>	6.72	3.49	3.23	1.39
166	<i>KLHDC7B</i>	6.71	5.88	2.95	1.71
167	<i>FZD10</i>	6.68	5.72	6.25	2.64
168	<i>HMX2</i>	6.65	5.22	6.95	3.79
169	<i>HOXA10</i>	6.64	5.39	6.33	2.80
170	<i>HS3ST6</i>	6.64	5.33	4.82	2.23
171	<i>GPR78</i>	6.64	3.04	3.66	1.44
172	<i>VSIG2</i>	6.63	2.69	2.59	1.35
173	<i>SERPINA9</i>	6.63	2.54	2.12	1.10
174	<i>SCNN1G</i>	6.63	2.49	3.72	1.68
175	<i>THBD</i>	6.61	4.16	2.91	1.35
176	<i>CDC42EP5</i>	6.61	4.01	4.96	2.36
177	<i>FOXQ1</i>	6.59	5.21	9.51	4.25
178	<i>MMEL1</i>	6.59	3.84	6.20	2.77
179	<i>HES2</i>	6.57	5.92	8.22	3.95
180	<i>OSR1</i>	6.57	5.14	4.65	1.85
181	<i>OVOL2</i>	6.56	6.03	5.27	2.42
182	<i>PAPLN</i>	6.54	4.26	2.32	2.05
183	<i>DUSP8</i>	6.54	3.94	4.88	3.76
184	<i>PTRF</i>	6.52	5.00	5.68	3.08
185	<i>FAM20A</i>	6.52	4.04	2.38	1.17
186	<i>SLC16A6</i>	6.52	4.04	2.38	1.17
187	<i>WIP1</i>	6.52	4.04	2.38	1.17
188	<i>MAF</i>	6.50	4.97	5.02	2.05
189	<i>PPP1R1A</i>	6.49	2.81	4.18	1.79
190	<i>NEUROD2</i>	6.48	6.45	9.43	6.29
191	<i>TMPRSS2</i>	6.48	3.55	3.37	1.59
192	<i>TLL10</i>	6.47	6.57	5.85	2.62
193	<i>WNT7B</i>	6.44	5.34	7.47	4.23
194	<i>AIRE</i>	6.43	3.55	3.17	1.71
195	<i>GSC</i>	6.41	5.81	4.98	2.56
196	<i>GRTP1</i>	6.41	4.26	1.07	1.05
197	<i>GALP</i>	6.41	3.38	1.58	0.80
198	<i>RIPK3</i>	6.41	3.10	4.32	1.61
199	<i>SOX3</i>	6.40	8.83	5.20	3.18
200	<i>ATP10A</i>	6.40	3.81	4.31	1.60
201	<i>MT1G</i>	6.39	4.21	5.74	1.97
202	<i>DLX4</i>	6.36	5.43	6.21	2.61
203	<i>CYP46A1</i>	6.34	3.15	1.88	1.36
204	<i>VGLL2</i>	6.33	3.82	2.52	0.79
205	<i>PRRX1</i>	6.31	4.22	4.27	2.41
206	<i>TPSG1</i>	6.30	6.75	1.40	1.86
207	<i>MSLN</i>	6.29	3.72	4.73	1.72
208	<i>FAM83H</i>	6.27	4.72	3.78	2.36
209	<i>PTHLH</i>	6.26	3.05	3.36	1.70
210	<i>IQGAP2</i>	6.26	2.35	1.57	1.14
211	<i>KRT5</i>	6.23	2.70	3.45	1.32
212	<i>RDH8</i>	6.22	3.64	4.38	1.51
213	<i>GABRD</i>	6.21	5.45	10.95	4.40
214	<i>ADAMTS8</i>	6.21	2.99	2.36	1.41
215	<i>GNGT2</i>	6.21	2.88	5.79	2.46
216	<i>NEUROG3</i>	6.19	5.08	6.91	3.22
217	<i>MAD2L2</i>	6.19	4.14	2.27	1.69
218	<i>ADRA1A</i>	6.19	3.94	1.36	1.02
219	<i>MRGPRX4</i>	6.19	2.14	2.39	1.19
220	<i>FOXE1</i>	6.18	5.03	2.84	1.13
221	<i>USP51</i>	6.18	2.16	0.65	1.07
222	<i>TREML4</i>	6.18	2.07	3.65	1.34
223	<i>CALCR</i>	6.17	3.34	1.40	1.26
224	<i>SYCN</i>	6.17	3.24	3.65	1.42
225	<i>SLC26A1</i>	6.17	3.20	3.33	1.69

#	Gene	Kelly rel AUC H3K27me3 (ranking score)	Kelly rel AUC EZH2	LAN-1 rel AUC H3K27me3	LAN-1 rel AUC EZH2
226	<i>NKX3-1</i>	6.16	3.10	1.01	1.02
227	<i>TKTL1</i>	6.15	2.87	0.73	0.89
228	<i>RASSF7</i>	6.14	5.55	4.68	2.50
229	<i>NR2E1</i>	6.13	6.13	5.08	2.45
230	<i>MUC2</i>	6.12	4.58	6.64	2.27
231	<i>KLK10</i>	6.11	3.60	4.32	2.03
232	<i>VDR</i>	6.11	2.20	2.91	0.93
233	<i>DRD4</i>	6.10	6.02	0.59	1.38
234	<i>PAX8</i>	6.10	3.72	3.18	1.67
235	<i>MUC6</i>	6.09	3.96	5.90	2.84
236	<i>DNMT3L</i>	6.09	2.83	3.11	1.37
237	<i>HCK</i>	6.08	3.02	2.75	1.07
238	<i>GRIN3B</i>	6.07	4.78	3.06	1.61
239	<i>IL22RA1</i>	6.07	2.28	5.40	2.15
240	<i>NRGN</i>	6.06	2.96	1.91	1.41
241	<i>FOXC2</i>	6.05	6.81	5.54	2.35
242	<i>KCNT1</i>	6.05	3.46	10.73	4.40
243	<i>LOC442028</i>	6.04	2.60	2.38	0.71
244	<i>PIGR</i>	6.04	1.89	4.93	2.24
245	<i>OTP</i>	6.02	6.02	5.32	2.48
246	<i>GPR50</i>	6.02	4.12	1.29	1.03
247	<i>NPTX1</i>	6.01	5.89	10.93	6.66
248	<i>SLC5A5</i>	6.01	3.41	2.28	1.18
249	<i>ATP12A</i>	6.00	3.00	4.69	1.84
250	<i>NHSL1</i>	6.00	2.73	0.37	0.62
251	<i>ATP8A2</i>	5.99	4.45	8.23	3.18
252	<i>CACNG6</i>	5.99	3.51	4.15	2.53
253	<i>CYP2A6</i>	5.99	2.37	3.32	1.17
254	<i>TMCO4</i>	5.98	3.40	3.77	1.55
255	<i>LONRF3</i>	5.97	4.63	3.04	1.59
256	<i>PRSS22</i>	5.97	3.21	4.53	2.05
257	<i>GADD45B</i>	5.96	4.21	1.37	1.07
258	<i>COL5A3</i>	5.96	3.34	4.81	1.64
259	<i>ACRC</i>	5.96	2.52	0.65	0.78
260	<i>GJB1</i>	5.96	2.52	0.65	0.78
261	<i>ITGB1BP2</i>	5.96	2.52	0.65	0.78
262	<i>TAF1</i>	5.96	2.52	0.65	0.78
263	<i>OGT</i>	5.96	2.52	0.65	0.78
264	<i>NONO</i>	5.96	2.52	0.65	0.78
265	<i>MMP25</i>	5.95	5.18	4.96	2.74
266	<i>FFAR2</i>	5.95	2.78	3.73	1.54
267	<i>PPP2R2C</i>	5.93	3.92	5.46	2.43
268	<i>RREB1</i>	5.92	6.63	4.45	2.33
269	<i>NPR3</i>	5.92	4.26	1.06	0.93
270	<i>UST</i>	5.92	3.76	1.41	0.81
271	<i>ACOXL</i>	5.92	3.76	2.77	0.93
272	<i>FAM43B</i>	5.90	4.30	0.40	1.22
273	<i>SFRP2</i>	5.90	3.67	2.08	1.48
274	<i>NTN1</i>	5.89	5.78	5.38	2.09
275	<i>PIK3CD</i>	5.87	4.10	3.01	1.51
276	<i>CNR2</i>	5.87	2.51	2.82	1.72
277	<i>LMX1A</i>	5.86	6.17	4.89	2.23
278	<i>GRP</i>	5.86	2.30	1.71	1.67
279	<i>CACNG2</i>	5.84	4.11	4.34	1.57
280	<i>TFAP2A</i>	5.83	5.75	6.21	3.45
281	<i>PFKFB3</i>	5.83	4.16	0.87	1.59
282	<i>RGL3</i>	5.83	4.12	2.51	1.67
283	<i>MLXIPL</i>	5.83	3.15	4.13	1.48
284	<i>SIM1</i>	5.82	5.01	3.10	1.34
285	<i>HEY2</i>	5.81	4.48	3.64	1.68
286	<i>LHX4</i>	5.80	6.22	3.66	2.08
287	<i>FAM3B</i>	5.79	2.98	6.64	2.49
288	<i>DSP</i>	5.78	5.53	5.91	3.27
289	<i>TMEM30B</i>	5.78	2.95	1.56	1.22
290	<i>FXYP7</i>	5.78	2.91	2.45	1.18
291	<i>TCP10L</i>	5.77	3.71	2.67	1.50
292	<i>IL1RL2</i>	5.76	3.12	2.57	1.04
293	<i>NOTCH2</i>	5.74	3.51	2.46	1.69
294	<i>KLK11</i>	5.74	2.36	5.36	2.24
295	<i>CST9</i>	5.74	2.16	2.68	1.15
296	<i>BARHL1</i>	5.73	5.38	8.60	5.29
297	<i>ATP8B1</i>	5.73	3.09	1.58	0.91
298	<i>NOTCH1</i>	5.72	7.30	11.09	5.71
299	<i>CACNA1E</i>	5.71	3.86	4.82	1.82
300	<i>NR5A2</i>	5.71	3.14	3.98	1.94

Supplemental Table 3. (C) Custom neuroblastoma PRC2 signature consisting of the top 300 EZH2 ChIP-seq target genes in LAN-1 cells.

#	Gene	LAN-1 rel AUC EZH2 (ranking score)	LAN-1 rel AUC H3K27me3	Kelly rel AUC EZH2	Kelly rel AUC H3K27me3
1	<i>CDX2</i>	11.43	19.24	6.12	5.20
2	<i>PAX2</i>	9.27	11.36	18.04	13.13
3	<i>PRDM16</i>	8.90	15.23	8.72	7.89
4	<i>HOXB8</i>	8.66	12.41	10.05	7.42
5	<i>NFATC1</i>	8.52	11.65	32.51	23.21
6	<i>TMEM132E</i>	7.84	13.22	0.94	0.27
7	<i>HOXB7</i>	7.55	12.16	8.92	7.41
8	<i>EBF3</i>	7.49	11.34	3.11	4.15
9	<i>LMX1B</i>	6.93	9.23	12.23	10.09
10	<i>HOXC9</i>	6.85	10.57	0.95	0.63
11	<i>SERPINA2</i>	6.66	16.44	1.36	4.41
12	<i>MN1</i>	6.66	12.22	9.51	7.56
13	<i>NPTX1</i>	6.66	10.93	5.89	6.01
14	<i>PDGFA</i>	6.60	9.41	17.82	12.54
15	<i>EN2</i>	6.53	9.53	12.41	10.34
16	<i>SP8</i>	6.33	11.39	4.90	5.50
17	<i>ZIC2</i>	6.31	9.76	11.22	7.69
18	<i>NEUROD2</i>	6.29	9.43	6.45	6.48
19	<i>IRX4</i>	6.13	10.81	7.61	8.30
20	<i>PAX7</i>	5.88	8.93	8.40	7.11
21	<i>NOTCH1</i>	5.71	11.09	7.30	5.72
22	<i>SOX8</i>	5.57	11.05	16.45	12.54
23	<i>FOXF1</i>	5.56	8.73	12.13	7.53
24	<i>EMX1</i>	5.55	8.53	9.97	8.39
25	<i>PRDM12</i>	5.55	6.50	15.81	8.51
26	<i>KLK12</i>	5.50	12.51	2.39	5.49
27	<i>VENTX</i>	5.50	11.58	8.56	8.51
28	<i>INHBB</i>	5.49	8.34	6.99	7.35
29	<i>TBX1</i>	5.43	9.21	7.40	7.56
30	<i>ZNF469</i>	5.42	12.27	1.07	0.75
31	<i>HOXC10</i>	5.37	10.33	4.28	5.17
32	<i>FIBCD1</i>	5.36	11.43	6.78	9.20
33	<i>BARHL1</i>	5.29	8.60	5.38	5.73
34	<i>LBX1</i>	5.29	8.45	17.76	10.41
35	<i>LHX1</i>	5.24	7.60	7.46	8.95
36	<i>LHX5</i>	5.23	7.65	12.77	10.54
37	<i>NKX2-2</i>	5.16	9.46	9.70	7.01
38	<i>NKX2-3</i>	5.10	9.02	8.14	7.07
39	<i>CDH4</i>	4.99	8.46	1.37	1.04
40	<i>GATA5</i>	4.87	9.10	8.28	7.51
41	<i>PDGFB</i>	4.84	7.90	3.69	3.76
42	<i>GATA6</i>	4.69	8.26	9.63	7.77
43	<i>HOXA11</i>	4.68	9.05	7.81	8.34
44	<i>HOXB9</i>	4.66	8.97	7.13	7.04
45	<i>HOXC12</i>	4.52	7.43	12.26	10.61
46	<i>HOXB6</i>	4.51	9.53	6.94	7.83
47	<i>HOXB5</i>	4.51	9.53	6.94	7.83
48	<i>CBX4</i>	4.50	5.24	3.71	2.98
49	<i>SHH</i>	4.44	7.17	7.02	7.95
50	<i>CLCNKB</i>	4.41	9.42	0.70	0.23
51	<i>GABRD</i>	4.40	10.95	5.45	6.21
52	<i>KCNT1</i>	4.40	10.73	3.46	6.05
53	<i>OLIG2</i>	4.33	8.13	10.30	9.01
54	<i>GRIK3</i>	4.31	6.58	0.86	0.34
55	<i>FOXF2</i>	4.29	6.86	12.04	7.84
56	<i>TTYH1</i>	4.27	8.53	2.97	5.03
57	<i>KIAA0125</i>	4.26	10.03	1.67	0.97
58	<i>HIC1</i>	4.26	5.13	3.00	3.96
59	<i>FOXQ1</i>	4.25	9.51	5.21	6.59
60	<i>NUDT14</i>	4.23	10.15	1.52	1.97
61	<i>WNT7B</i>	4.23	7.47	5.34	6.44
62	<i>FOXL2</i>	4.23	6.50	12.53	10.62
63	<i>CDH15</i>	4.22	10.54	2.88	4.81
64	<i>EBF2</i>	4.17	8.26	7.34	8.07
65	<i>PKNOX2</i>	4.16	9.10	1.40	0.92
66	<i>PAX9</i>	4.15	6.77	5.67	5.27
67	<i>CBFA2T3</i>	4.14	10.05	6.95	8.67
68	<i>FOXD3</i>	4.14	7.56	4.75	5.43
69	<i>MADCAM1</i>	4.13	6.45	3.64	4.11
70	<i>WNT1</i>	4.12	8.96	4.54	5.06
71	<i>SOHLH1</i>	4.08	9.91	3.47	5.48
72	<i>HOXB13</i>	4.07	8.80	3.97	5.13
73	<i>SLC9A3</i>	4.05	8.47	3.60	4.52

#	Gene	LAN-1 rel AUC EZH2 (ranking score)	LAN-1 rel AUC H3K27me3	Kelly rel AUC EZH2	Kelly rel AUC H3K27me3
74	<i>BAHCC1</i>	4.02	6.37	1.20	0.39
75	<i>SOX18</i>	3.98	7.65	3.42	2.69
76	<i>HES2</i>	3.95	8.22	5.92	6.57
77	<i>CYP26B1</i>	3.95	6.69	3.22	3.81
78	<i>COL18A1</i>	3.94	7.79	2.07	1.54
79	<i>FGF3</i>	3.92	7.28	5.14	4.72
80	<i>AJAP1</i>	3.91	8.24	6.22	8.11
81	<i>ZIC5</i>	3.91	7.16	8.54	7.21
82	<i>KLHDC7A</i>	3.86	8.71	0.70	0.22
83	<i>MUC5B</i>	3.85	9.44	6.04	8.93
84	<i>HOXA2</i>	3.84	7.46	4.68	4.71
85	<i>HMX2</i>	3.79	6.95	5.22	6.65
86	<i>LHX3</i>	3.77	4.98	5.22	3.61
87	<i>DUSP8</i>	3.76	4.88	3.94	6.54
88	<i>KCNK9</i>	3.72	5.60	2.69	2.66
89	<i>SDK2</i>	3.70	8.36	1.35	1.34
90	<i>CDKN1C</i>	3.70	6.60	2.03	2.21
91	<i>WIZ</i>	3.69	2.08	1.31	1.50
92	<i>RUNX1</i>	3.67	7.49	1.90	4.04
93	<i>POU3F3</i>	3.63	7.20	3.82	3.87
94	<i>PAX1</i>	3.62	7.48	4.29	5.65
95	<i>IRS4</i>	3.62	6.51	3.31	4.81
96	<i>MAGEA11</i>	3.60	6.89	0.81	2.18
97	<i>ICOSLG</i>	3.57	8.03	4.74	4.56
98	<i>DAAM2</i>	3.54	7.98	0.83	0.71
99	<i>IRX2</i>	3.54	6.33	10.20	7.85
100	<i>SIM2</i>	3.54	5.86	8.78	6.87
101	<i>IRX1</i>	3.52	7.59	11.30	7.80
102	<i>BARX2</i>	3.52	5.40	6.94	6.93
103	<i>ARC</i>	3.51	8.25	1.24	0.13
104	<i>FEZF2</i>	3.51	6.40	4.82	5.55
105	<i>ITGB2</i>	3.50	8.17	5.47	8.13
106	<i>ITPR3</i>	3.49	7.83	2.61	3.90
107	<i>SORCS3</i>	3.49	6.60	12.35	11.54
108	<i>COL13A1</i>	3.48	8.46	0.94	1.39
109	<i>ALX4</i>	3.48	7.03	8.59	8.11
110	<i>NCKIPSD</i>	3.48	1.68	0.84	0.17
111	<i>JAG2</i>	3.47	9.45	0.98	0.22
112	<i>TAL1</i>	3.46	6.49	3.62	3.44
113	<i>TFAP2A</i>	3.45	6.21	5.75	5.83
114	<i>COMP</i>	3.43	5.72	6.40	7.23
115	<i>TPPP</i>	3.41	1.49	1.85	0.43
116	<i>DMRT3</i>	3.36	8.10	6.77	7.01
117	<i>GATA4</i>	3.35	5.17	12.04	10.44
118	<i>HSPB7</i>	3.34	7.55	0.90	0.42
119	<i>PAX3</i>	3.34	6.17	6.23	6.80
120	<i>FLT1</i>	3.33	7.03	3.55	4.22
121	<i>NKX6-1</i>	3.32	7.17	1.21	0.79
122	<i>MYO5B</i>	3.30	7.61	4.14	7.40
123	<i>PRKCZ</i>	3.29	7.65	5.89	7.47
124	<i>NTF3</i>	3.29	7.23	2.45	3.69
125	<i>TLX1</i>	3.29	6.68	6.43	6.76
126	<i>EVX1</i>	3.28	7.78	10.74	9.50
127	<i>DSP</i>	3.27	5.91	5.53	5.78
128	<i>HBM</i>	3.26	8.62	3.86	6.74
129	<i>HOXC11</i>	3.26	5.74	5.67	5.50
130	<i>NEUROG3</i>	3.22	6.91	5.08	6.19
131	<i>VMO1</i>	3.22	4.75	2.37	4.02
132	<i>ACTRT2</i>	3.21	9.03	2.88	5.14
133	<i>CHST1</i>	3.21	7.33	0.91	0.97
134	<i>ADSSL1</i>	3.21	2.44	3.61	1.87
135	<i>EN1</i>	3.19	6.39	5.94	5.66
136	<i>ATP8A2</i>	3.18	8.23	4.45	5.99
137	<i>PLCH2</i>	3.18	7.48	1.10	0.36
138	<i>CABP7</i>	3.18	6.08	2.10	1.80
139	<i>NETO1</i>	3.18	5.92	0.89	0.41
140	<i>SOX3</i>	3.18	5.20	8.83	6.40
141	<i>SLC22A18</i>	3.16	4.51	2.09	2.20
142	<i>ZMYND15</i>	3.15	7.36	6.18	9.62
143	<i>CXCL16</i>	3.15	7.32	6.44	10.12
144	<i>NTNG2</i>	3.14	7.77	1.11	1.01
145	<i>TBX15</i>	3.14	6.40	10.94	8.77
146	<i>DLX3</i>	3.13	6.67	3.88	5.68
147	<i>SFMBT2</i>	3.11	6.59	3.10	4.49
148	<i>GPR101</i>	3.11	6.05	3.80	5.63
149	<i>LSP1</i>	3.10	7.06	0.65	0.21

#	Gene	LAN-1 rel AUC EZH2 (ranking score)	LAN-1 rel AUC H3K27me3	Kelly rel AUC EZH2	Kelly rel AUC H3K27me3
150	TBX5	3.10	6.09	4.26	4.34
151	GPR123	3.10	5.83	7.18	8.41
152	NEU2	3.09	6.82	1.62	3.26
153	HOXA6	3.08	6.71	8.04	7.37
154	HOXA5	3.08	6.71	8.04	7.37
155	HOXA7	3.08	6.71	8.04	7.37
156	GALNT9	3.08	6.61	3.46	4.51
157	PTRF	3.08	5.68	5.00	6.52
158	LHX2	3.08	5.21	9.36	8.05
159	KRT35	3.07	7.05	0.73	0.34
160	METRNL	3.07	3.89	2.09	2.00
161	NKX2-8	3.05	7.71	7.59	7.92
162	EMX2OS	3.05	5.72	5.41	5.62
163	COL20A1	3.05	5.48	1.85	2.35
164	NKX2-5	3.05	5.01	8.84	7.82
165	BCL11B	3.03	5.57	1.42	1.16
166	GLI3	3.02	7.17	4.06	5.52
167	HOXC8	3.01	6.43	0.95	0.26
168	FSCN2	3.00	6.90	2.77	3.40
169	TNNI2	2.99	7.27	2.36	1.00
170	ESPN	2.99	6.65	6.37	7.44
171	CYP24A1	2.99	6.11	1.88	3.55
172	FLT4	2.97	7.02	9.28	12.36
173	KCNK16	2.96	7.11	0.73	0.78
174	APOC3	2.96	1.32	0.96	0.28
175	HOXB4	2.95	5.82	6.61	7.13
176	ZFYVE28	2.95	5.62	3.56	9.01
177	LOC284930	2.95	4.89	0.72	1.15
178	FOXP2	2.95	4.56	6.49	6.79
179	CPNE9	2.95	2.12	1.30	1.15
180	CEACAM21	2.94	9.33	1.97	4.36
181	EGFL7	2.92	8.03	1.54	1.27
182	CD300C	2.91	6.96	0.75	0.43
183	GPC4	2.91	6.04	5.77	7.36
184	KIR2DS4	2.91	4.54	2.15	5.14
185	PACS2	2.91	2.02	1.30	0.54
186	BTBD6	2.91	2.02	1.30	0.54
187	KNDC1	2.90	8.44	3.05	5.69
188	VGFB	2.90	2.66	1.05	1.14
189	SMAD7	2.90	0.95	1.07	0.35
190	SLC22A18AS	2.89	6.41	3.98	3.26
191	WNT10A	2.89	6.38	1.07	0.70
192	OTOS	2.89	5.40	2.41	4.28
193	TNFRSF18	2.88	7.59	8.31	10.59
194	OLIG3	2.88	7.35	5.62	5.29
195	BMP6	2.88	5.72	4.46	5.44
196	GDF10	2.86	6.87	0.79	0.79
197	LIF	2.85	7.74	0.72	0.41
198	AGPAT2	2.85	6.53	1.13	0.50
199	COL15A1	2.85	5.76	2.44	4.27
200	ABTB1	2.85	1.98	0.75	0.29
201	MUC6	2.84	5.90	3.96	6.09
202	ST14	2.83	1.00	2.46	2.72
203	HOXB3	2.82	6.31	4.42	5.69
204	HOXB2	2.82	6.31	4.42	5.69
205	KLF2	2.82	5.26	7.66	8.67
206	FLNA	2.82	1.97	1.35	1.06
207	FMNL1	2.81	6.76	1.41	1.73
208	SLC8A3	2.81	6.54	1.01	0.60
209	CDH22	2.81	6.11	1.12	1.10
210	OTX2	2.81	5.81	9.36	8.40
211	SIGLEC9	2.80	8.14	2.31	5.12
212	EPHA2	2.80	6.86	0.79	0.52
213	HOXA10	2.80	6.33	5.39	6.64
214	GPRC5C	2.80	6.11	1.17	0.57
215	HMHA1	2.80	5.96	4.01	5.16
216	PMF1	2.80	2.26	2.07	0.69
217	GAD2	2.79	6.86	6.23	7.11
218	RASSF5	2.79	6.59	1.98	3.13
219	SOX14	2.79	5.51	8.04	8.74
220	KCNAB2	2.79	1.19	0.72	0.21
221	EPHA8	2.78	6.90	1.21	0.70
222	ETV4	2.78	6.68	1.63	2.51
223	WNT3	2.78	5.56	1.25	1.27
224	C1ORF159	2.78	4.50	3.32	3.10
225	CYP26A1	2.77	6.30	4.68	5.70

#	Gene	LAN-1 rel AUC EZH2 (ranking score)	LAN-1 rel AUC H3K27me3	Kelly rel AUC EZH2	Kelly rel AUC H3K27me3
226	<i>MMEL1</i>	2.77	6.20	3.84	6.59
227	<i>BAI1</i>	2.77	6.02	0.95	0.19
228	<i>C1ORF94</i>	2.77	5.73	6.11	9.61
229	<i>FGF9</i>	2.77	5.51	0.84	0.90
230	<i>KCND3</i>	2.76	5.82	1.56	2.43
231	<i>SLC24A3</i>	2.76	5.65	2.61	4.32
232	<i>CARD10</i>	2.75	6.60	2.39	2.76
233	<i>NOG</i>	2.74	6.11	5.15	6.75
234	<i>CSMD2</i>	2.74	5.74	5.11	8.14
235	<i>MMP25</i>	2.74	4.96	5.18	5.95
236	<i>NKD2</i>	2.73	6.11	4.16	4.38
237	<i>DSCAML1</i>	2.71	6.18	1.50	1.98
238	<i>BARX1</i>	2.71	5.38	10.02	6.81
239	<i>GPR26</i>	2.71	5.19	0.80	0.66
240	<i>FOXB1</i>	2.70	6.34	8.04	8.62
241	<i>ZBTB7A</i>	2.70	2.30	1.43	1.72
242	<i>MT1M</i>	2.69	6.93	4.01	5.43
243	<i>MSX1</i>	2.69	4.67	6.42	6.87
244	<i>LHX6</i>	2.69	4.31	6.90	7.47
245	<i>CLEC11A</i>	2.69	3.76	1.25	0.13
246	<i>LMO1</i>	2.68	5.82	0.89	0.21
247	<i>PITPNM3</i>	2.68	5.61	0.99	1.85
248	<i>FLI1</i>	2.67	6.99	2.62	5.01
249	<i>DMRT1</i>	2.67	6.43	3.60	4.89
250	<i>GALR2</i>	2.67	5.49	3.28	3.12
251	<i>TFAP2C</i>	2.67	5.29	9.41	7.83
252	<i>SLC30A2</i>	2.67	5.27	2.89	4.33
253	<i>HTR5A</i>	2.66	6.35	2.50	5.16
254	<i>SLC17A7</i>	2.66	5.71	1.85	3.17
255	<i>SIX1</i>	2.66	4.73	5.40	7.25
256	<i>NOTUM</i>	2.66	3.60	3.52	2.86
257	<i>CHST7</i>	2.66	2.67	0.87	1.61
258	<i>KCNG2</i>	2.66	2.30	2.35	4.27
259	<i>DGKG</i>	2.65	5.88	1.93	3.38
260	<i>GLIS3</i>	2.65	5.03	3.37	3.31
261	<i>NFIX</i>	2.65	4.57	5.20	5.28
262	<i>SP6</i>	2.64	7.86	1.99	3.90
263	<i>FZD10</i>	2.64	6.25	5.72	6.68
264	<i>WFDC1</i>	2.63	7.14	3.00	5.52
265	<i>ELN</i>	2.63	5.82	1.24	0.37
266	<i>HAMP</i>	2.63	5.32	1.17	2.36
267	<i>PTPRE</i>	2.63	5.25	1.29	0.88
268	<i>NR2F1</i>	2.63	4.95	0.59	0.53
269	<i>CORO2B</i>	2.62	6.28	1.14	1.15
270	<i>OVOL1</i>	2.62	6.07	8.56	7.78
271	<i>TTLL10</i>	2.62	5.85	6.57	6.47
272	<i>CACNA1A</i>	2.62	5.81	2.94	4.23
273	<i>PLXDC2</i>	2.62	4.54	0.87	0.71
274	<i>SOX13</i>	2.61	6.43	3.72	4.80
275	<i>DLX4</i>	2.61	6.21	5.43	6.36
276	<i>C3ORF22</i>	2.61	2.67	0.84	0.64
277	<i>MYH7</i>	2.60	6.84	1.27	1.93
278	<i>UMODL1</i>	2.60	6.78	1.67	2.44
279	<i>C21ORF128</i>	2.60	6.78	1.67	2.44
280	<i>CTSD</i>	2.60	4.26	1.10	0.37
281	<i>MAPK15</i>	2.59	4.58	2.12	5.02
282	<i>COL5A1</i>	2.58	7.59	0.91	0.82
283	<i>UNC93B1</i>	2.58	5.95	1.59	1.65
284	<i>CACNA1S</i>	2.58	5.62	0.94	0.69
285	<i>ARHGEF16</i>	2.58	5.12	1.66	2.58
286	<i>SLFN5</i>	2.58	5.11	2.35	4.77
287	<i>MAG</i>	2.57	7.04	2.12	4.04
288	<i>HOXA1</i>	2.57	5.60	3.97	5.21
289	<i>ETNK2</i>	2.57	3.71	1.55	2.58
290	<i>UTF1</i>	2.56	6.89	7.39	8.17
291	<i>GSC</i>	2.56	4.98	5.81	6.41
292	<i>HSPA12A</i>	2.56	4.21	1.67	1.36
293	<i>CALML6</i>	2.56	3.44	1.51	2.85
294	<i>SLC6A18</i>	2.55	7.39	1.72	2.18
295	<i>HOXD11</i>	2.55	6.12	1.35	1.78
296	<i>KRTAP5-9</i>	2.55	3.65	0.94	2.50
297	<i>ACHE</i>	2.55	3.26	4.35	4.17
298	<i>RILP</i>	2.55	1.23	1.18	0.33
299	<i>PFKP</i>	2.54	4.24	1.24	1.55
300	<i>HIPK4</i>	2.54	2.56	1.11	2.34

Supplemental Table 3. (D) Custom neuroblastoma PRC2 signature consisting of the top 300 H3K27me3 ChIP-seq target genes in LAN-1 cells.

#	Gene	LAN-1 rel AUC H3K27me3 (ranking score)	LAN-1 rel AUC EZH2	Kelly rel AUC H3K27me3	Kelly rel AUC EZH2
1	<i>CDX2</i>	19.24	11.43	5.20	6.12
2	<i>SERPINA2</i>	16.44	6.66	4.41	1.36
3	<i>PRDM16</i>	15.23	8.90	7.89	8.72
4	<i>TMEM132E</i>	13.22	7.84	0.27	0.94
5	<i>KLK12</i>	12.51	5.50	5.49	2.39
6	<i>HOXB8</i>	12.41	8.66	7.42	10.05
7	<i>ZNF469</i>	12.27	5.42	0.75	1.07
8	<i>MN1</i>	12.22	6.66	7.56	9.51
9	<i>HOXB7</i>	12.16	7.55	7.41	8.92
10	<i>NFATC1</i>	11.65	8.52	23.21	32.51
11	<i>VENTX</i>	11.58	5.50	8.51	8.56
12	<i>FIBCD1</i>	11.43	5.36	9.20	6.78
13	<i>SP8</i>	11.39	6.33	5.50	4.90
14	<i>PAX2</i>	11.36	9.27	13.13	18.04
15	<i>EBF3</i>	11.34	7.49	4.15	3.11
16	<i>NOTCH1</i>	11.09	5.71	5.72	7.30
17	<i>SOX8</i>	11.05	5.57	12.54	16.45
18	<i>GABRD</i>	10.95	4.40	6.21	5.45
19	<i>NPTX1</i>	10.93	6.66	6.01	5.89
20	<i>IRX4</i>	10.81	6.13	8.30	7.61
21	<i>KCNT1</i>	10.73	4.40	6.05	3.46
22	<i>HOXC9</i>	10.57	6.85	0.63	0.95
23	<i>CDH15</i>	10.54	4.22	4.81	2.88
24	<i>HOXC10</i>	10.33	5.37	5.17	4.28
25	<i>NUDT14</i>	10.15	4.23	1.97	1.52
26	<i>CBFA2T3</i>	10.05	4.14	8.67	6.95
27	<i>KIAA0125</i>	10.03	4.26	0.97	1.67
28	<i>SOHLH1</i>	9.91	4.08	5.48	3.47
29	<i>ZIC2</i>	9.76	6.31	7.69	11.22
30	<i>EN2</i>	9.53	6.53	10.34	12.41
31	<i>HOXB6</i>	9.53	4.51	7.83	6.94
32	<i>HOXB5</i>	9.53	4.51	7.83	6.94
33	<i>FOXQ1</i>	9.51	4.25	6.59	5.21
34	<i>NKX2-2</i>	9.46	5.16	7.01	9.70
35	<i>JAG2</i>	9.45	3.47	0.22	0.98
36	<i>MUC5B</i>	9.44	3.85	8.93	6.04
37	<i>NEUROD2</i>	9.43	6.29	6.48	6.45
38	<i>CLCNKB</i>	9.42	4.41	0.23	0.70
39	<i>PDGFA</i>	9.41	6.60	12.54	17.82
40	<i>CEACAM21</i>	9.33	2.94	4.36	1.97
41	<i>LMX1B</i>	9.23	6.93	10.09	12.23
42	<i>TBX1</i>	9.21	5.43	7.56	7.40
43	<i>GATA5</i>	9.10	4.87	7.51	8.28
44	<i>PKNOX2</i>	9.10	4.16	0.92	1.40
45	<i>HOXA11</i>	9.05	4.68	8.34	7.81
46	<i>ACTRT2</i>	9.03	3.21	5.14	2.88
47	<i>NKX2-3</i>	9.02	5.10	7.07	8.14
48	<i>HOXB9</i>	8.97	4.66	7.04	7.13
49	<i>WNT1</i>	8.96	4.12	5.06	4.54
50	<i>PAX7</i>	8.93	5.88	7.11	8.40
51	<i>HOXB13</i>	8.80	4.07	5.13	3.97
52	<i>FOXF1</i>	8.73	5.56	7.53	12.13
53	<i>KLHDC7A</i>	8.71	3.86	0.22	0.70
54	<i>HBM</i>	8.62	3.26	6.74	3.86
55	<i>BARHL1</i>	8.60	5.29	5.73	5.38
56	<i>EMX1</i>	8.53	5.55	8.39	9.97
57	<i>TTYH1</i>	8.53	4.27	5.03	2.97
58	<i>SLC9A3</i>	8.47	4.05	4.52	3.60
59	<i>CDH4</i>	8.46	4.99	1.04	1.37
60	<i>COL13A1</i>	8.46	3.48	1.39	0.94
61	<i>LBX1</i>	8.45	5.29	10.41	17.76
62	<i>KNDC1</i>	8.44	2.90	5.69	3.05
63	<i>SDK2</i>	8.36	3.70	1.34	1.35
64	<i>INHBB</i>	8.34	5.49	7.35	6.99
65	<i>GATA6</i>	8.26	4.69	7.77	9.63
66	<i>EBF2</i>	8.26	4.17	8.07	7.34
67	<i>ARC</i>	8.25	3.51	0.13	1.24
68	<i>AJAP1</i>	8.24	3.91	8.11	6.22
69	<i>ATP8A2</i>	8.23	3.18	5.99	4.45
70	<i>HES2</i>	8.22	3.95	6.57	5.92
71	<i>ITGB2</i>	8.17	3.50	8.13	5.47
72	<i>SIGLEC9</i>	8.14	2.80	5.12	2.31
73	<i>OLIG2</i>	8.13	4.33	9.01	10.30

#	Gene	LAN-1 rel AUC H3K27me3 (ranking score)	LAN-1 rel AUC EZH2	Kelly rel AUC H3K27me3	Kelly rel AUC EZH2
74	<i>DMRT3</i>	8.10	3.36	7.01	6.77
75	<i>ICOSLG</i>	8.03	3.57	4.56	4.74
76	<i>EGFL7</i>	8.03	2.92	1.27	1.54
77	<i>DAAM2</i>	7.98	3.54	0.71	0.83
78	<i>PDGFB</i>	7.90	4.84	3.76	3.69
79	<i>SP6</i>	7.86	2.64	3.90	1.99
80	<i>ITPR3</i>	7.83	3.49	3.90	2.61
81	<i>COL18A1</i>	7.79	3.94	1.54	2.07
82	<i>EVX1</i>	7.78	3.28	9.50	10.74
83	<i>NTNG2</i>	7.77	3.14	1.01	1.11
84	<i>LCN6</i>	7.76	2.42	0.85	0.91
85	<i>LIF</i>	7.74	2.85	0.41	0.72
86	<i>NKX2-8</i>	7.71	3.05	7.92	7.59
87	<i>LHX5</i>	7.65	5.23	10.54	12.77
88	<i>PRKCZ</i>	7.65	3.29	7.47	5.89
89	<i>SOX18</i>	7.65	3.98	2.69	3.42
90	<i>SLC38A3</i>	7.64	2.47	0.65	0.87
91	<i>MYO5B</i>	7.61	3.30	7.40	4.14
92	<i>LHX1</i>	7.60	5.24	8.95	7.46
93	<i>IRX1</i>	7.59	3.52	7.80	11.30
94	<i>TNFRSF18</i>	7.59	2.88	10.59	8.31
95	<i>COL5A1</i>	7.59	2.58	0.82	0.91
96	<i>FOXD3</i>	7.56	4.14	5.43	4.75
97	<i>HSPB7</i>	7.55	3.34	0.42	0.90
98	<i>RUNX1</i>	7.49	3.67	4.04	1.90
99	<i>PAX1</i>	7.48	3.62	5.65	4.29
100	<i>PLCH2</i>	7.48	3.18	0.36	1.10
101	<i>WNT7B</i>	7.47	4.23	6.44	5.34
102	<i>HOXA2</i>	7.46	3.84	4.71	4.68
103	<i>HOXC12</i>	7.43	4.52	10.61	12.26
104	<i>SLC6A18</i>	7.39	2.55	2.18	1.72
105	<i>ZMYND15</i>	7.36	3.15	9.62	6.18
106	<i>OLIG3</i>	7.35	2.88	5.29	5.62
107	<i>SLITRK2</i>	7.34	2.35	7.13	4.48
108	<i>C20ORF166</i>	7.33	2.41	2.12	1.37
109	<i>CHST1</i>	7.33	3.21	0.97	0.91
110	<i>CXCL16</i>	7.32	3.15	10.12	6.44
111	<i>FGF3</i>	7.28	3.92	4.72	5.14
112	<i>TNNI2</i>	7.27	2.99	1.00	2.36
113	<i>NTF3</i>	7.23	3.29	3.69	2.45
114	<i>POU3F3</i>	7.20	3.63	3.87	3.82
115	<i>SHH</i>	7.17	4.44	7.95	7.02
116	<i>GLI3</i>	7.17	3.02	5.52	4.06
117	<i>NKX6-1</i>	7.17	3.32	0.79	1.21
118	<i>ZIC5</i>	7.16	3.91	7.21	8.54
119	<i>WFDC1</i>	7.14	2.63	5.52	3.00
120	<i>KCNK16</i>	7.11	2.96	0.78	0.73
121	<i>KCNQ1OT1</i>	7.07	2.47	0.38	0.56
122	<i>LSP1</i>	7.06	3.10	0.21	0.65
123	<i>KRT35</i>	7.05	3.07	0.34	0.73
124	<i>MAG</i>	7.04	2.57	4.04	2.12
125	<i>ALX4</i>	7.03	3.48	8.11	8.59
126	<i>FLT1</i>	7.03	3.33	4.22	3.55
127	<i>FLT4</i>	7.02	2.97	12.36	9.28
128	<i>FLI1</i>	6.99	2.67	5.01	2.62
129	<i>CD300C</i>	6.96	2.91	0.43	0.75
130	<i>HMX2</i>	6.95	3.79	6.65	5.22
131	<i>MT1M</i>	6.93	2.69	5.43	4.01
132	<i>NEUROG3</i>	6.91	3.22	6.19	5.08
133	<i>FSCN2</i>	6.90	3.00	3.40	2.77
134	<i>EPHA8</i>	6.90	2.78	0.70	1.21
135	<i>UTF1</i>	6.89	2.56	8.17	7.39
136	<i>MAGEA11</i>	6.89	3.60	2.18	0.81
137	<i>HAS1</i>	6.87	2.15	4.46	2.36
138	<i>GDF10</i>	6.87	2.86	0.79	0.79
139	<i>FOXF2</i>	6.86	4.29	7.84	12.04
140	<i>GAD2</i>	6.86	2.79	7.11	6.23
141	<i>EPHA2</i>	6.86	2.80	0.52	0.79
142	<i>MYH7</i>	6.84	2.60	1.93	1.27
143	<i>NEU2</i>	6.82	3.09	3.26	1.62
144	<i>CYP11B2</i>	6.78	2.34	5.59	2.82
145	<i>UMODL1</i>	6.78	2.60	2.44	1.67
146	<i>C21ORF128</i>	6.78	2.60	2.44	1.67
147	<i>PAX9</i>	6.77	4.15	5.27	5.67
148	<i>FMNL1</i>	6.76	2.81	1.73	1.41
149	<i>CLEC10A</i>	6.75	2.02	3.49	1.61

#	Gene	LAN-1 rel AUC H3K27me3 (ranking score)	LAN-1 rel AUC EZH2	Kelly rel AUC H3K27me3	Kelly rel AUC EZH2
150	<i>CHRNA4</i>	6.72	2.30	3.34	1.93
151	<i>HOXA6</i>	6.71	3.08	7.37	8.04
152	<i>HOXA5</i>	6.71	3.08	7.37	8.04
153	<i>HOXA7</i>	6.71	3.08	7.37	8.04
154	<i>CYP26B1</i>	6.69	3.95	3.81	3.22
155	<i>TLX1</i>	6.68	3.29	6.76	6.43
156	<i>ETV4</i>	6.68	2.78	2.51	1.63
157	<i>DLX3</i>	6.67	3.13	5.68	3.88
158	<i>ESPN</i>	6.65	2.99	7.44	6.37
159	<i>MUC2</i>	6.64	2.27	6.12	4.58
160	<i>FAM3B</i>	6.64	2.49	5.79	2.98
161	<i>GALNT9</i>	6.61	3.08	4.51	3.46
162	<i>CCRL2</i>	6.61	2.24	3.25	1.39
163	<i>SORCS3</i>	6.60	3.49	11.54	12.35
164	<i>CARD10</i>	6.60	2.75	2.76	2.39
165	<i>CDKN1C</i>	6.60	3.70	2.21	2.03
166	<i>LCN1</i>	6.60	2.11	4.40	2.01
167	<i>SFMBT2</i>	6.59	3.11	4.49	3.10
168	<i>RASSF5</i>	6.59	2.79	3.13	1.98
169	<i>LOC400043</i>	6.58	2.43	0.44	1.04
170	<i>GRIK3</i>	6.58	4.31	0.34	0.86
171	<i>HOXC5</i>	6.56	2.26	0.32	0.71
172	<i>HOXC4</i>	6.56	2.26	0.32	0.71
173	<i>HOXC6</i>	6.56	2.26	0.32	0.71
174	<i>SLC8A3</i>	6.54	2.81	0.60	1.01
175	<i>FGF17</i>	6.54	2.24	0.91	0.72
176	<i>AGPAT2</i>	6.53	2.85	0.50	1.13
177	<i>IRS4</i>	6.51	3.62	4.81	3.31
178	<i>PRDM12</i>	6.50	5.55	8.51	15.81
179	<i>FOXL2</i>	6.50	4.23	10.62	12.53
180	<i>TAL1</i>	6.49	3.46	3.44	3.62
181	<i>C9ORF62</i>	6.46	2.36	0.45	0.88
182	<i>MADCAM1</i>	6.45	4.13	4.11	3.64
183	<i>SOX13</i>	6.43	2.61	4.80	3.72
184	<i>DMRT1</i>	6.43	2.67	4.89	3.60
185	<i>HOXC8</i>	6.43	3.01	0.26	0.95
186	<i>SLC22A18AS</i>	6.41	2.89	3.26	3.98
187	<i>TBX15</i>	6.40	3.14	8.77	10.94
188	<i>FEZF2</i>	6.40	3.51	5.55	4.82
189	<i>EN1</i>	6.39	3.19	5.66	5.94
190	<i>IRF8</i>	6.39	2.22	4.30	2.76
191	<i>PDYN</i>	6.39	2.31	3.77	1.50
192	<i>BACE2</i>	6.38	2.44	7.57	4.22
193	<i>WNT10A</i>	6.38	2.89	0.70	1.07
194	<i>BAHCC1</i>	6.37	4.02	0.39	1.20
195	<i>HTR5A</i>	6.35	2.66	5.16	2.50
196	<i>FOXB1</i>	6.34	2.70	8.62	8.04
197	<i>FXVD5</i>	6.34	2.32	5.54	2.79
198	<i>IRX2</i>	6.33	3.54	7.85	10.20
199	<i>HOXA10</i>	6.33	2.80	6.64	5.39
200	<i>PTPN3</i>	6.33	2.11	2.64	1.84
201	<i>HOXB3</i>	6.31	2.82	5.69	4.42
202	<i>HOXB2</i>	6.31	2.82	5.69	4.42
203	<i>CYP26A1</i>	6.30	2.77	5.70	4.68
204	<i>CORO2B</i>	6.28	2.62	1.15	1.14
205	<i>FZD10</i>	6.25	2.64	6.68	5.72
206	<i>ZBTB7C</i>	6.23	2.42	1.52	1.23
207	<i>TFAP2A</i>	6.21	3.45	5.83	5.75
208	<i>DLX4</i>	6.21	2.61	6.36	5.43
209	<i>MMEL1</i>	6.20	2.77	6.59	3.84
210	<i>USH1G</i>	6.20	2.34	5.69	3.56
211	<i>KLK2</i>	6.20	2.21	1.17	0.96
212	<i>DSCAML1</i>	6.18	2.71	1.98	1.50
213	<i>PAX3</i>	6.17	3.34	6.80	6.23
214	<i>LOC200772</i>	6.17	2.27	0.31	0.98
215	<i>MUC12</i>	6.14	2.52	4.14	2.05
216	<i>HOXD11</i>	6.12	2.55	1.78	1.35
217	<i>HS3ST4</i>	6.12	2.20	0.85	0.72
218	<i>NOG</i>	6.11	2.74	6.75	5.15
219	<i>NKD2</i>	6.11	2.73	4.38	4.16
220	<i>CYP24A1</i>	6.11	2.99	3.55	1.88
221	<i>GPRC5C</i>	6.11	2.80	0.57	1.17
222	<i>CDH22</i>	6.11	2.81	1.10	1.12
223	<i>TBX5</i>	6.09	3.10	4.34	4.26
224	<i>CABP7</i>	6.08	3.18	1.80	2.10
225	<i>OVOL1</i>	6.07	2.62	7.78	8.56

#	Gene	LAN-1 rel AUC H3K27me3 (ranking score)	LAN-1 rel AUC EZH2	Kelly rel AUC H3K27me3	Kelly rel AUC EZH2
226	<i>GPR101</i>	6.05	3.11	5.63	3.80
227	<i>GPC4</i>	6.04	2.91	7.36	5.77
228	<i>TFF1</i>	6.04	2.04	2.34	1.07
229	<i>BAI1</i>	6.02	2.77	0.19	0.95
230	<i>HMHA1</i>	5.96	2.80	5.16	4.01
231	<i>UNC93B1</i>	5.95	2.58	1.65	1.59
232	<i>PHLDA2</i>	5.94	2.52	3.95	4.19
233	<i>KLK13</i>	5.93	2.22	4.58	1.73
234	<i>ALOX15</i>	5.92	2.49	4.49	2.82
235	<i>NETO1</i>	5.92	3.18	0.41	0.89
236	<i>ATP2A3</i>	5.91	2.13	7.38	5.66
237	<i>DSP</i>	5.91	3.27	5.78	5.53
238	<i>MUC6</i>	5.90	2.84	6.09	3.96
239	<i>PVALB</i>	5.90	2.48	7.10	3.03
240	<i>DGKG</i>	5.88	2.65	3.38	1.93
241	<i>SIM2</i>	5.86	3.54	6.87	8.78
242	<i>TLL10</i>	5.85	2.62	6.47	6.57
243	<i>RIPK4</i>	5.85	2.22	7.77	4.51
244	<i>CD22</i>	5.84	2.25	3.73	1.32
245	<i>FLJ12825</i>	5.84	2.06	0.25	0.72
246	<i>GPR123</i>	5.83	3.10	8.41	7.18
247	<i>HOXB4</i>	5.82	2.95	7.13	6.61
248	<i>KCND3</i>	5.82	2.76	2.43	1.56
249	<i>ELN</i>	5.82	2.63	0.37	1.24
250	<i>GPR20</i>	5.82	2.14	0.38	0.94
251	<i>LMO1</i>	5.82	2.68	0.21	0.89
252	<i>OTX2</i>	5.81	2.81	8.40	9.36
253	<i>CACNA1A</i>	5.81	2.62	4.23	2.94
254	<i>GNGT2</i>	5.79	2.46	6.21	2.88
255	<i>CCK</i>	5.78	2.17	3.85	2.80
256	<i>SLC13A5</i>	5.77	2.14	3.32	1.53
257	<i>TINAGL1</i>	5.77	2.35	0.37	1.12
258	<i>COL15A1</i>	5.76	2.85	4.27	2.44
259	<i>HOXC11</i>	5.74	3.26	5.50	5.67
260	<i>CSMD2</i>	5.74	2.74	8.14	5.11
261	<i>MT1G</i>	5.74	1.97	6.39	4.21
262	<i>FGF4</i>	5.74	2.42	2.80	2.60
263	<i>TMPRSS6</i>	5.74	1.90	0.61	0.79
264	<i>C1ORF94</i>	5.73	2.77	9.61	6.11
265	<i>COMP</i>	5.72	3.43	7.23	6.40
266	<i>EMX2OS</i>	5.72	3.05	5.62	5.41
267	<i>BMP6</i>	5.72	2.88	5.44	4.46
268	<i>ZIC3</i>	5.72	2.21	0.69	0.94
269	<i>SLC22A3</i>	5.71	2.35	4.41	3.49
270	<i>LOC284379</i>	5.71	1.53	8.07	2.84
271	<i>SLC17A7</i>	5.71	2.66	3.17	1.85
272	<i>SIRPA</i>	5.71	2.36	0.42	0.89
273	<i>CLDN9</i>	5.69	2.33	3.95	1.90
274	<i>PTRF</i>	5.68	3.08	6.52	5.00
275	<i>WNT2</i>	5.67	2.48	5.52	3.24
276	<i>SLC24A3</i>	5.65	2.76	4.32	2.61
277	<i>KCNJ5</i>	5.63	2.30	0.42	0.74
278	<i>ZFYVE28</i>	5.62	2.95	9.01	3.56
279	<i>CACNA1S</i>	5.62	2.58	0.69	0.94
280	<i>KRT13</i>	5.62	1.92	0.34	0.76
281	<i>ALPI</i>	5.61	2.07	2.78	1.31
282	<i>PITPNM3</i>	5.61	2.68	1.85	0.99
283	<i>HOXA1</i>	5.60	2.57	5.21	3.97
284	<i>VSX1</i>	5.60	2.45	3.81	2.71
285	<i>KCNK9</i>	5.60	3.72	2.66	2.69
286	<i>FGF6</i>	5.57	1.75	4.21	1.76
287	<i>BCL11B</i>	5.57	3.03	1.16	1.42
288	<i>CACNA2D3</i>	5.57	2.50	0.46	0.73
289	<i>SKAP1</i>	5.56	1.62	4.00	1.77
290	<i>WNT3</i>	5.56	2.78	1.27	1.25
291	<i>CYP11B1</i>	5.55	1.96	3.05	1.57
292	<i>CACNA2D2</i>	5.55	2.45	0.68	1.10
293	<i>TMEM115</i>	5.55	2.45	0.68	1.10
294	<i>FOXC2</i>	5.54	2.35	6.05	6.81
295	<i>SMOC2</i>	5.53	2.27	3.88	2.31
296	<i>ITGB4</i>	5.52	2.05	8.19	4.94
297	<i>SOX14</i>	5.51	2.79	8.74	8.04
298	<i>BTBD11</i>	5.51	2.41	4.06	2.31
299	<i>PPP1R1B</i>	5.51	2.36	3.32	2.09
300	<i>FGF9</i>	5.51	2.77	0.90	0.84

Supplemental Table 4. Top 60 significant GSEA hits for EZH2 and H3K27me3 ChIP-seq target genes in Kelly and LAN-1 cells using the MSigDB v5.1 c5 collection of 25 Gene Ontology (GO) gene sets related to biological processes. For each gene set hit the table shows if the gene set is related to any of the 15 Neural Development signatures available in the MSigDB c5 collection (1= yes, 0=no), the size of the gene set, the GSEA normalized enrichment score (NES), *P* and false discovery rate (FDR). The significance cut-offs were 0.05 for *P* and 0.25 for FDR. The top 60 gene set hits are ranked in decreasing order based on the NES.

(A) Top 60 GSEA hits for EZH2 ChIP-seq target genes in Kelly cells. Neural Development related gene sets are significantly over-represented in the collection of GSEA hits (odds-ratios = 51.03, *P* < 0.001, according to the two-tailed Fisher exact test).

Rank	Gene Set	Neural Development	Size	NES	<i>P</i>	FDR
1	NEURON_DIFFERENTIATION	1	70	1.82	0.0000	0.1167
2	GENERATION_OF_NEURONS	1	76	1.76	0.0000	0.1721
3	NEURON_DEVELOPMENT	1	57	1.75	0.0000	0.1206
4	AXONOGENESIS	1	40	1.75	0.0013	0.0918
5	AXON_GUIDANCE	1	20	1.75	0.0014	0.0754
6	NEUROGENESIS	1	85	1.70	0.0000	0.1267
7	POSITIVE_REGULATION_OF_CELL_DIFFERENTIATION	0	20	1.68	0.0042	0.1369
8	NEURITE_DEVELOPMENT	1	49	1.67	0.0013	0.1495
9	CELLULAR_MORPHOGENESIS_DURING_DIFFERENTIATION	0	46	1.66	0.0000	0.1403
10	HEART_DEVELOPMENT	0	32	1.66	0.0068	0.1326
11	REGULATION_OF_BODY_FLUID_LEVELS	0	38	1.62	0.0066	0.2159
12	NERVOUS_SYSTEM_DEVELOPMENT	0	348	1.58	0.0000	0.3089
13	REGULATION_OF_ANATOMICAL_STRUCTURE_MORPHOGENESIS	0	24	1.57	0.0182	0.3008
15	CELL_CELL_SIGNALING	0	292	1.51	0.0010	0.4733
16	REGULATION_OF_CELL_DIFFERENTIATION	0	48	1.51	0.0183	0.4455
17	ANATOMICAL_STRUCTURE_MORPHOGENESIS	0	302	1.51	0.0000	0.4273
18	EXTRACELLULAR_STRUCTURE_ORGANIZATION_AND_BIOGENESIS	0	30	1.50	0.0240	0.4442
20	B_CELL_ACTIVATION	0	16	1.47	0.0476	0.5145
21	BLOOD_COAGULATION	0	28	1.47	0.0418	0.5062
22	ANATOMICAL_STRUCTURE_DEVELOPMENT	0	829	1.47	0.0000	0.4952
23	BRAIN_DEVELOPMENT	1	45	1.46	0.0393	0.4949
24	SYSTEM_DEVELOPMENT	0	706	1.45	0.0000	0.5227
25	CENTRAL_NERVOUS_SYSTEM_DEVELOPMENT	0	107	1.45	0.0151	0.5296
26	TISSUE_DEVELOPMENT	0	93	1.44	0.0233	0.5109
27	PROTEIN_OLIGOMERIZATION	0	32	1.44	0.0501	0.5167
28	REGULATION_OF_ACTION_POTENTIAL	0	16	1.43	0.0603	0.5252
29	TUBE_DEVELOPMENT	0	15	1.43	0.0755	0.5241
30	COAGULATION	0	29	1.43	0.0510	0.5125
31	HUMORAL_IMMUNE_RESPONSE	0	19	1.43	0.0801	0.4969
32	SULFUR_COMPOUND_BIOSYNTHETIC_PROCESS	0	18	1.43	0.0508	0.4868
33	REGULATION_OF_HEART_CONTRACTION	0	21	1.42	0.0655	0.4787
34	CELL_CELL_ADHESION	0	64	1.42	0.0369	0.4749
35	ADENYLATE_CYCLASE_ACTIVATION	0	15	1.42	0.0854	0.4786
36	MULTICELLULAR_ORGANISMAL_DEVELOPMENT	0	857	1.42	0.0000	0.4744
37	PROTEOGLYCAN_METABOLIC_PROCESS	0	19	1.41	0.0922	0.4960
38	SKELETAL_DEVELOPMENT	0	83	1.40	0.0244	0.5066
39	EMBRYONIC_DEVELOPMENT	0	46	1.40	0.0459	0.5057
40	SYNAPTIC_TRANSMISSION	0	144	1.39	0.0209	0.5058
41	G_PROTEIN_SIGNALING_ADENYLATE_CYCLASE_ACTIVATING_PATHWAY	0	17	1.39	0.0938	0.4999
42	POTASSIUM_ION_TRANSPORT	0	49	1.39	0.0462	0.5050
43	TRANSMISSION_OF_NERVE_IMPULSE	0	158	1.38	0.0132	0.5073
44	ORGAN_DEVELOPMENT	0	445	1.38	0.0000	0.4994
45	RESPONSE_TO_EXTERNAL_STIMULUS	0	202	1.38	0.0075	0.5024
46	REGULATION_OF_RAS_PROTEIN_SIGNAL_TRANSDUCTION	0	17	1.38	0.0844	0.4986
47	RECEPTOR_MEDIATED_ENDOCYTOSIS	0	30	1.38	0.0727	0.4887
48	POSITIVE_REGULATION_OF_RESPONSE_TO_STIMULUS	0	28	1.38	0.0856	0.4850
49	ANION_TRANSPORT	0	22	1.37	0.0924	0.4845
50	SYNAPSE_ORGANIZATION_AND_BIOGENESIS	0	22	1.37	0.0952	0.4949
51	ACTIN_POLYMERIZATION_AND_OR_DEPOLYMERIZATION	0	22	1.35	0.1029	0.5372
53	CELL_MIGRATION	0	78	1.35	0.0585	0.5391
54	PROTEIN_POLYMERIZATION	0	18	1.34	0.1196	0.5672
55	NEUROLOGICAL_SYSTEM_PROCESS	1	293	1.33	0.0125	0.5795
56	MESODERM_DEVELOPMENT	0	15	1.33	0.1245	0.5707
57	EMBRYONIC_MORPHOGENESIS	0	15	1.33	0.1393	0.5658
58	METAL_ION_TRANSPORT	0	98	1.33	0.0596	0.5590
59	CATION_TRANSPORT	0	121	1.33	0.0454	0.5527
60	HEMOSTASIS	0	32	1.33	0.1148	0.5495
61	MEISSNER_NPC_HCP_WITH_H3K4ME3_AND_H3K27ME3	1	139	2.21	0.0000	0.0242
62	YAO_TEMPORAL_RESPONSE_TO_PROGESTERONE_CLUSTER_4	0	15	2.20	0.0000	0.0286
63	MEISSNER_NPC_HCP_WITH_H3_UNMETHYLATED	1	505	2.19	0.0000	0.0301

Supplemental Table 4. (B) Top 60 GSEA hits for EZH2 ChIP-seq target genes in LAN-1 cells. Neural Development related gene sets are significantly over-represented in the collection of GSEA hits (odds-ratios = 39.73, $P < 0.001$, according to the two-tailed Fisher exact test).

Rank	Gene Set	Neural Development	Size	NES	P	FDR
1	SKELETAL_DEVELOPMENT	0	83	1.87	0.0000	0.1256
2	ION_TRANSPORT	0	150	1.82	0.0000	0.1276
3	ANION_TRANSPORT	0	22	1.81	0.0017	0.0899
4	NEURON_DIFFERENTIATION	1	70	1.78	0.0000	0.1125
5	GENERATION_OF_NEURONS	1	76	1.77	0.0000	0.1053
6	SYSTEM_DEVELOPMENT	0	706	1.76	0.0000	0.0948
7	MONOVALENT_INORGANIC_CATION_TRANSPORT	0	78	1.75	0.0000	0.0878
8	NEURON_DEVELOPMENT	1	57	1.73	0.0000	0.1125
9	POTASSIUM_ION_TRANSPORT	0	49	1.72	0.0016	0.1116
10	ANATOMICAL_STRUCTURE_DEVELOPMENT	0	829	1.72	0.0000	0.1019
11	NEURITE_DEVELOPMENT	1	49	1.71	0.0000	0.0936
12	REGULATION_OF_HEART_CONTRACTION	0	21	1.71	0.0072	0.0942
13	ORGAN_DEVELOPMENT	0	445	1.71	0.0000	0.0876
14	MULTICELLULAR_ORGANISMAL_DEVELOPMENT	0	857	1.70	0.0000	0.0860
15	NERVOUS_SYSTEM_DEVELOPMENT	0	348	1.70	0.0000	0.0852
16	LIPID_TRANSPORT	0	21	1.69	0.0114	0.0836
17	METAL_ION_TRANSPORT	0	98	1.64	0.0015	0.1565
18	CATION_TRANSPORT	0	121	1.61	0.0029	0.2012
19	NEUROGENESIS	1	85	1.60	0.0015	0.2087
20	ECTODERM_DEVELOPMENT	0	54	1.59	0.0093	0.2001
21	MUSCLE_DEVELOPMENT	0	83	1.59	0.0031	0.2038
22	EPIDERMIS_DEVELOPMENT	0	47	1.55	0.0227	0.2680
23	SYSTEM_PROCESS	0	440	1.55	0.0000	0.2598
24	HUMORAL_IMMUNE_RESPONSE	0	19	1.55	0.0297	0.2621
25	CELLULAR_MORPHOGENESIS_DURING_DIFFERENTIATION	0	46	1.54	0.0182	0.2590
26	RESPONSE_TO_EXTERNAL_STIMULUS	0	202	1.52	0.0027	0.2952
27	AXONOGENESIS	1	40	1.51	0.0190	0.3104
28	INSULIN_RECEPTOR_SIGNALING_PATHWAY	0	18	1.51	0.0374	0.3019
29	TRANSMEMBRANE_RECEPTOR_PROTEIN_TYROSINE_KINASE_SIGN	0	74	1.51	0.0201	0.3050
30	CELL_CELL_SIGNALING	0	292	1.50	0.0013	0.3118
31	NEUROLOGICAL_SYSTEM_PROCESS	1	293	1.50	0.0000	0.3042
32	ORGAN_MORPHOGENESIS	0	112	1.49	0.0124	0.3167
33	ANATOMICAL_STRUCTURE_MORPHOGENESIS	0	302	1.49	0.0013	0.3083
34	TISSUE_DEVELOPMENT	0	93	1.48	0.0118	0.3359
35	WOUND_HEALING	0	36	1.47	0.0378	0.3569
36	RESPONSE_TO_NUTRIENT	0	16	1.46	0.0673	0.3492
37	PROTEOGLYCAN_METABOLIC_PROCESS	0	19	1.46	0.0506	0.3408
38	REGULATION_OF_G_PROTEIN_COUPLED_RECEPTOR_PROTEIN_SIG	0	22	1.46	0.0565	0.3467
39	SULFUR_METABOLIC_PROCESS	0	36	1.46	0.0571	0.3412
40	RESPONSE_TO_CHEMICAL_STIMULUS	0	232	1.46	0.0054	0.3336
41	SYNAPTIC_TRANSMISSION	0	144	1.45	0.0099	0.3425
42	HEART_DEVELOPMENT	0	32	1.45	0.0570	0.3401
43	BLOOD_COAGULATION	0	28	1.45	0.0600	0.3365
44	DEVELOPMENTAL_MATURATION	0	16	1.44	0.0584	0.3450
45	PATTERN_SPECIFICATION_PROCESS	0	25	1.43	0.0637	0.3595
46	CELL_SURFACE_RECEPTOR_LINKED_SIGNAL_TRANSDUCTION_GO	0	481	1.42	0.0000	0.3716
47	TRANSMISSION_OF_NERVE_IMPULSE	0	158	1.41	0.0240	0.3921
48	SYNAPTOGENESIS	0	18	1.41	0.0829	0.4007
49	PROTEIN_AMINO_ACID_DEPHOSPHORYLATION	0	59	1.41	0.0579	0.3940
50	EXOCYTOSIS	0	20	1.40	0.0786	0.3917
51	G_PROTEIN_COUPLED_RECEPTOR_PROTEIN_SIGNALING_PATHWA	0	238	1.40	0.0067	0.3917
52	RESPONSE_TO_EXTRACELLULAR_STIMULUS	0	30	1.40	0.0759	0.3890
53	RESPONSE_TO_WOUNDING	0	116	1.39	0.0377	0.4037
54	DEPHOSPHORYLATION	0	66	1.39	0.0402	0.3965
55	SODIUM_ION_TRANSPORT	0	16	1.38	0.0904	0.4093
56	STEROID_METABOLIC_PROCESS	0	48	1.38	0.0648	0.4057
57	NEGATIVE_REGULATION_OF_MAP_KINASE_ACTIVITY	0	16	1.38	0.1082	0.4007
58	COAGULATION	0	29	1.38	0.0935	0.3954
59	HEMOSTASIS	0	32	1.37	0.0880	0.4081
60	SENSORY_PERCEPTION	0	135	1.37	0.0188	0.4154

Supplemental Table 5. The shRNA sequences and the CRISPR-Cas9 sgRNA sequences targeting *MYCN* and *EZH2* that were used in this study.

#	Designation	Clone ID	Clone Name	Target Sequence
1	shNT			CCTAAGGTTAAGTCGCCCTCGC
2	shLUC			CTTCGAAATGTCGGTTCGGTT
3	shMYCN1	TRCN0000020694	NM_005378.3-2000s1c1	GCCAGTATTAGACTGGAAGTT
4	shMYCN3	TRCN0000020696	NM_005378.3-230s1c1	CGGACGAAGATGACTTCTACT
5	shMYCN5	TRCN0000020698	NM_005378.3-919s1c1	CTGAGCGATTGATGATGAA
6	shEZH2-4	TRCN0000040073	NM_004456.3-2582s1c1	CGGAAATCTTAAACCAAGAAT
7	shEZH2-5	TRCN0000040076	NM_004456.3-324s1c1	TATTGCCTTCTCACCAGCTGC
8	sgNT			TAGCGAACGTGTCCGGCGT
9	sgEZH2-1			TTATCAGAAGGAAATTTCCG
10	sgEZH2-2			TTATGATGGGAAAGTACACG
11	sgEZH2-3			AGAAGGGACCAGTTTGTGG
12	sgEZH2-4			CTGCTGCTCTCACCGCTGAG